Calhoun: The NPS Institutional Archive

DSpace Repository

Theses and Dissertations 1. Thesis and Dissertation Collection, all items

1982

Geometry effects on triangular pitch curricular finned heat exchangers in crossflow.

Robinson, Thomas Reeder

Massachusetts Institute of Technology

http://hdl.handle.net/10945/20190

Downloaded from NPS Archive: Calhoun

Calhoun is the Naval Postgraduate School's public access digital repository for research materials and institutional publications created by the NPS community. Calhoun is named for Professor of Mathematics Guy K. Calhoun, NPS's first appointed -- and published -- scholarly author.

Dudley Knox Library / Naval Postgraduate School
411 Dyer Road / 1 University Circle
Monterey, California USA 93943

http://www.nps.edu/library

DUDLEY KNOX LIBRARY
NAVAL POSTGRADUATE SCHOOL
MONTEREY, CALIF. 93940

GEOMETRY EFFECTS ON TRIANGULAR PITCH CIRCULAR FINNED TUBE HEAT EXCHANGERS IN CROSSFLOW

by

THOMAS REEDER ROBINSON

B.S.E.E., University of Utah
(1973)

SUBMITTED TO THE DEPARTMENT OF
OCEAN ENGINEERING IN PARTIAL
FULFILLMENT OF THE
REQUIREMENTS FOR THE
DEGREES OF

OCEAN ENGINEER

and

MASTER OF SCIENCE IN
NAVAL ARCHITECTURE AND MARINE ENGINEERING

at the

MASSACHUSETTS INSTITUTE OF TECHNOLOGY

June 1982

© Thomas Reeder Robinson 1982

The author hereby grants to MIT permission to reproduce and to distribute copies of this thesis document in whole or in part.

Thesis
S6409
c.1

DUDLEY KNOX LIBRARY
NAVAL POSTGRADUATE SCHO
MONTEREY, CALIF. 93940

GEOMETRY EFFECTS ON TRIANGULAR PITCH CIRCULAR FINNED TUBE HEAT EXCHANGERS IN CROSSFLOW

by

THOMAS REEDER ROBINSON

Submitted to the Department of Ocean Engineering on May 7, 1982 in partial fulfillment of the requirements for the Degree of Ocean Engineer and Master of Science in Naval Architecture and Marine Engineering.

ABSTRACT

The traditional method of data presentation for heat exchanger surfaces does not permit comparison of individual surface types in any simple manner, nor is the published experimental data plentiful enough to conduct a meaningful study of the effect of varying geometries on surface performance. This data is most commonly presented in terms of heat transfer coefficients and friction factors referenced to the exposed area as a function of Reynolds number based on the minimum free flow area. There are six basic geometric parameters for a triangular pitch circular finned tube bank: tube diameter; tube transverse and diagonal pitch; fin height, thickness, and spacing.

Baskerville (3) developed a method of surface comparison for circular finned tube heat exchangers. Biery (4) developed a method for prediction of heat transfer for finned tube banks in crossflow. Jameson, et al., (5) developed an empirical relation for correlation of pressure drop data across triangular pitch circular finned tube banks.

The correlations for heat transfer and pressure drop for triangular pitch circular finned tube banks in crossflow are used with the comparison method to study the effect of varying geometry on surface performance. Optimal fin spacing and height are found for specific fin thicknesses, tube diameters, and tube pitch. Performance trends for the six possible geometric parameters are established.

Thesis Supervisor: Professor Warren M. Rohsenow

Title: Professor of Mechanical Engineering

ACKNOWLEDGEMENTS

I would like to extend my deepest appreciation to Commander James E. Baskerville for the use of his thesis which served as a basis for my work, and to Professor Warren M. Rohsenow for his untiring help and guidance.

I would like to thank an enduring friend, Lieutenant Commander Charlie Long (Ret), and his assistant, Sue, for the production of this thesis with his computerized printing press business "Ye Olde Scirbe" in Worcester, Massachusetts.

I would especially like to thank my wife, Mary, whose understanding, constant faith, and abiding love have been a constant support through our three years at MIT.

TABLE OF CONTENTS

PAGE

TITLE PAGE 1

ABSTRACT 2

ACKNOWLEDGEMENTS 3

TABLE OF CONTENTS 4

NOMENCLATURE 6

LIST OF FIGURES 15

LIST OF TABLES 19

I. INTRODUCTION 20

A. PURPOSE 20

B. BACKGROUND 21

II. COMPARISON METHOD 24

III. HEAT TRANSFER CORRELATIONS 41

IV. PRESSURE DROP CORRELATIONS 46

V. COMPARISON OF PERFORMANCE PARAMETER PREDICTION PROGRAM 50

VI. GEOMETRY EFFECTS ON TRIANGULAR PITCH CIRCULAR FINNED TUBE HEAT EXCHANGERS IN CROSSFLOW 57

A. GENERAL 57

B. EFFECTS OF TUBE DIAMETER AND TUBE PITCH 57

C. EFFECTS OF FIN GEOMETRY 67

D. SUMMARY, CONCLUSIONS AND RECOMMENDATIONS FOR FUTURE STUDIES 89

TABLE OF CONTENTS (Cont)

PAGE

REFERENCES 92

APPENDIX I. DERIVATION OF GEOMETRICAL RELATIONSHIPS 94

APPENDIX II. COMPARISON OF BIERY'S (4) METHOD FOR PREDICTION OF COLBURN j-MODULUS FOR GAS FLOW NORMAL TO TRIANGULAR PITCH FINNED TUBE BANKS 100

APPENDIX III. COMPARISON OF JAMESON'S CORRELATION FOR PRESSURE DROP ACROSS TRIANGULAR PITCH FINNED TUBE BANKS. 106

APPENDIX IV. PERFORMANCE PARAMETER PREDICTION PROGRAM 109

NOMENCLATURE

A	Dimensionless factor; defined by equation (22b).
a_d	Minimum free flow dimension between tubes measured diagonally between adjacent rows from base to base as if fins were not present; see Figure 3, [FT].
a_t	Minimum free flow dimension between tubes measured transversely to the direction of flow from base to base as if fins were not present; see Figure 3, [FT].
A_b	Heat transfer area of the bare base tubular surfaces; equals length times heated perimeter [FT^2].
A_c	Exchanger minimum flow area for gas: (minimum area can be transverse to flow or diagonal to flow; see Figure 3). [FT^2].
A_f	Total fin area of a tube of length L; defined by equation (A14), [FT^2].
A_F	Exchanger flow passage frontal area ignoring any enhancing surfaces; see Figure 3, [FT^2].
A_f/A_T	Ratio of fin area to total transfer area; defined by equation (A15).
A_T	Total air heat transfer surface area (same as total surface area exposed to gas crossflow), including fin surface and edges of fins [FT^2].
b	Longitudinal center-to-center tube spacing; see Figure 3, [FT].

C_D	Constant used in the computation of friction factor (f) for flow over smooth tube banks; defined by equation (32).
C_Δ	Constant required for the computation of radial fin efficiency; defined in Figure 5.
C_H	Dimensionless coefficient defined in equation (23).
C_p	Specific heat at constant pressure, [BTU/LBM-^{o}F].
C_T	Constant used in calculation of friction factor for gas flow over smooth tube banks; defined by equation (31).
D	Constant required for the computation of radial fin efficiency; defined in Figure 5.
D_E	Equivalent diameter defined by equation (20).
d_e	Equivalent diameter of a finned tube; defined by equation (A18).
D_f	Fin diameter, [FT].
D_J	Equivalent diameter of a triangular pitch finned tube bundle; defined by equation (26).
D_h	Hydraulic diameter; defined by equation (1a), [FT].
$(D_h/D_o)_\Delta$	Ratio of hydraulic diameter to the equivalent diameter for an equilateral triangular pitch infinite smooth tube bank (ETP-I-STB); defined by equation (21).
D_N	Nominal diameter; defined by equation (1b), [FT].

D_o	Tube outside diameter, [FT].
E	Factor defined by equation (20).
ETP-I-STB	Equilateral triangular pitch infinite smooth tube bank.
F	Transverse center-to-center tube spacing; see Figure 3, [FT].
f'	Friction factor predicted by the Jameson (5) correlation and based on total area (A_T); defined by equation (A23).
f	Friction factor based on total area (A_T); defined by equation (4a).
f_J	Friction factor used by Jameson (5); defined by equation (29).
F_{in}	Number of fins per inch; defined by equation (46).
f_N	Friction factor based on base area (A_b); defined by equation (4b).
f_s	Friction factor based on total area (A_T) for a smooth surface, defined by equations (31) and (32).
g_o	32.174 [LBM/LBF] [FT/SEC^2].
G_c	Mass flux based on minimum free flow area, [A_c]; defined by equation (2a), [LBM/HR-FT^2].
G_f	Dimensionless geometry factor; defined by equation (A7).
G_N	Mass flux based on free flow area, [A_F]; defined by equation (2b), [LBM/HR-FT^2].

h	Heat transfer coefficient based on total area, $[A_T]$; defined by equation (5a), $[BTU/HR-FT^2-^oF]$.
h_N	Heat transfer coefficient based on base area, $[A_b]$; defined by equation (5b), $[BTU/HR-FT^2-^oF]$.
l_k	Projected perimeter of a finned tube; defined by equation A17, [FT].
j	Colburn j-factor based on total area, $[A_T]$; defined by equation (7a).
$j_{B\&Y}$	Colburn j-factor based on outside tube diameter $[D_o]$; defined by equation (A22).
j_B	Colburn j-factor predicted by Biery's [4] method as outlined in Chapter 3.
j_N	Colburn j-factor based on base area, $[A_b]$; defined by equation (7b).
$j_{K\&L}$	Colburn j-factor based on experimental data from Kays & London [2].
j_M	Colburn j-factor based on equivalent diameter, $[d_e]$; defined by equation (A20).
j_s	Colburn j-factor based on total area, $[A_T]$, for a smooth surface, defined by equation (24).
k	Thermal conductivity $[BTU/HR-FT-^oF]$.
l	Fin height defined by r_e-r_o; for rectangular fin sheets, see Figure 5, [FT].

L	Flow length along the axis of the tubes (i.e. for the fluid inside the tubes).
m	Component of fin efficiency (η_{f-L}); defined by equation (10).
N	Number of tube rows in a tube bank.
N_{HD}	Parameter used in algorithm of Figure A4 for calculating D_h when minimum free flow area occurs in the diagonal space.
N_{HT}	Parameter used in algorithm of Figure A4 for calculating D_h when minimum free flow area occurs in the transverse space.
N_N	Parameter used in algorithm of Figure A4 for calculating nominal diameter [D_N].
N_{PR}	Symbol used in Kays and London [2] for PR.
N_R	Symbol used in Kays and London [2] for RE.
N_{ST}	Stanton Number [$h/G_c C_P$].
Nu	Nusselt number; defined by equation (6a).
Nu_N	Nusselt number; defined by equation (6b).
NTU	Number of transfer units.
η_{f-corr}	Corrected fin efficiency per Figure 5.
η_{f-L}	Fin temperature effectiveness of a longitudinal fin of rectangular profile; defined by (9).

$\Delta\eta_{corr}$	Correction factor applied to η_{f-L} (9) to permit the use of the simpler [Tanh ml]/ml equation for fin temperature effectiveness in lieu of Bessel Function type equations. See Figure 4.
η_o	Total surface temperature effectiveness, defined by (8).
P	Pumping Power, [HP].
P_c	Property constant for fin material and air properties; defined by equation (A28).
ΔP_f	Friction pressure drop, [LBF/FT^2].
Pr	Prandtl Number [$\mu C_p/K$].
q	Heat transfer rate, [BTU/HR].
RE	Reynolds number based on minimum free flow area, [A_c]; defined by equation (3a) and labeled N_R by ref [2].
RE_{D_J}	Reynolds number based on the equivalent diameter of a finned tube handle, [D_J], and the mass flux based on the minimum free flow area, [G_c]; defined by equation (28).
RE_N	Reynolds number based on free flow area, [A_F]; defined by equation (3b).
r_e	Radius of enhanced (finned) surface, [FT].
R_f	Dimensionless geometry factor; defined by equation (A5).
r_h	Hydraulic radius, equals hydraulic diameter divided by four for a round tube, [FT].

r_o	Outside radius of base tube, [FT].
S_{BF}	Ratio of spacing between fins to tube outside diameter.
T	Temperature, [^oF].
$T_{c,in}$	Cold gas inlet temperature, [$T_{c,in}$].
t_f	Ratio of fin thickness to tube outside diameter, [δ/D_o].
$T_{H,in}$	Hot fluid inlet temperature, [^oF].
V	Volume, [FT^3]
V_{os}	Volume one side; volume of the gas side of the heat exchanger on a per tube basis. [FT^3]
V_T	Total volume of heat exchanger on a per tube basis [FT^3].
W	Mass flow rate, [LBM/HR].
X,Y,Z	Principle dimensions of heat exchanger, [FT].
X_D	Ratio of diagonal tube spacing to tube outside diameter.
X_L	Ratio of longitudinal tube spacing to tube outside diameter, equals b divided by D_o.
X_{MAX}	The greater of X_T or X_D.
$(X_L)_\Delta$	Ratio of longitudinal spacing to tube outside diameter for an equilateral pitch tube bank.

$(X_T)_\Delta$	Ratio of transverse tube spacing to tube outside diameter for an equilateral triangular pitch tube bank.

Miscellaneous

α	In tube geometry, angle defined by the longitudinal centerline and the diagonal centerline; see Figure 4, [degrees].
β	Ratio of total transfer area on one side of the exchanger to total volume of the exchanger, labeled as α in reference [2], [FT^2/FT^3].
δ	Fin thickness, or average fin thickness if tapered, [FT].
μ	Viscosity, [LBM/HR-FT].
ρ	Density, [LBM/FT^3].

Subscripts

d	Diagonal
e	Enhanced surface
ETP	Equilateral triangular pitch.
MAX	The maximum value a variable may assume.
m	Heat exchanger fin material
o	Outside
os	One side
p	Predicted

REF	Reference value for indicated parameter.
s	Smoth surface
T	Total
1	Tube side; hotter fluid flowing inside smooth tubes.
2	Finned side, colder fluid flowing over finned tube banks.

LIST OF FIGURES

FIGURE	TITLE	PAGE
1	Finned tubular heat exchangers	23
2	Example of the traditional method of presenting required data and geometrical properties.	25
3	Two cases of minimum free flow area occurence and the associated geometric relations of each case.	29
4	Calculation of A_Fb/V_{OS} for cases I and II.	30
5	Computing fin efficiency of a radial fin.	31
6	Performance Parameter Curves for two hypothetical surfaces showing points used in sample comparisons.	33
7	Performance Parameter Curve for finned tubular surfaces.	34
8	Performance Parameter plot for the two surfaces used in the design example.	39
9	Deviation of Zhukauskaus (9) correlation for j factor in predicting experimentally obtained value as presented in Kays and London (2).	45
10	Deviation of derived correlation for friction factor in predicting experimentally obtained values as presented in Kays and London (2).	49
11	Comparison of predicted performance parameters with performance parameters calculated by Baskerville from Kays and London (2) experimental data.	51

LIST OF FIGURES (Cont)

FIGURE	TITLE	PAGE
12A	$(V_{os})/_{REF}/V_{os}$ versus D_o for several values of tube pitch for a bare tube surface.	61
12B	$(V_{os})_{REF}/V_{os}$ versus X_{ETP} for two values of tube diameter for a bare tube surface.	62
12C	$(V_{os})_{REF}/V_{os}$ versus X_D for a bare tube surface for several values of tube diameter and transverse tube pitch.	63
12D	$(V_{os})_{REF}/V_{os}$ versus X_T for a bare tube surface for two values of diagonal tube pitch.	64
13A	$(V_{os})_{REF}/V_{os}$ versus fin spacing for four fin thicknesses (t_f = .005, .01, .02, .04) for an enhanced tube surface with D_o = 1", X_{ETP} = 2, and $H_f = (H_f)_{MAX} = .5$	79
13B	$(V_{os})_{REF}/V_{os}$ versus fin height for four fin thicknesses (t_f = .005, .01, .02, .04) for an enhanced tube surface with D_o = 1" and X_{ETP} = 2 and with fin spacing at the optimal value found in Figure 13A for $H_f = (H_f)_{MAX} = .5$	80
13C	$(V_{os})_{REF}/V_{os}$ versus fin spacing for three fin thicknesses (t_f = .01, .02, .04) for an enhanced tube surface with D_o = .4", X_{ETP} = 2, and $H_f = (H_f)_{MAX} = .5$	81

LIST OF FIGURES (Cont)

FIGURE	TITLE	PAGE
13D	$(V_{os})_{REF}/V_{os}$ versus fin height for three fin thicknesses (t_f = .01, .02, .04) for an enhanced tube surface with D_o = .4" and X_{ETP} =2 and with fin spacing at the optimal value found in Figure 13C for $H_f = (H_f)_{MAX}$ = .5	82
13E	$(V_{os})_{REF}/V_{os}$ versus fin spacing for four fin thicknesses (t_f = .005, .01, .02, .04) for an enhanced tube surface with D_o = 1", X_{ETP} =3, $H_f = (H_f)_{MAX}$ = 1.0	83
13F	$(V_{os})_{REF}/V_{os}$ versus fin height for four fin thicknesses (t_f = .005, .01, .02, .04) for an enhanced tube surface with D_o = 1", X_{ETP} = 3 and with fin spacing at the optimal value found in Figure 13E for $H_f = (H_f)_{MAX}$ = 1.0	84
13G	$(V_{os})_{REF}/V_{os}$ versus fin spacing for three fin thicknesses (t_f = .01, .02, .04) for an enhanced tube surface with D_o = .4", X_{ETP} = 3 and $H_f = (H_f)_{MAX}$ = 1.0	85
13H	$(V_{os})_{REF}/V_{os}$ versus fin height for three fin thicknesses (t_f = .01, .02, .04) for an enhanced tube surface with D_o = .4", X_{ETP} =3, and with fin spacing at the optimal value found in Figure 13G for $H_f = (H_f)_{MAX}$ = 1.0	86

LIST OF FIGURES (Cont)

FIGURE	TITLE	PAGE
13I	$(V_{os})_{REF}/V_{os}$ versus fin thicknesses for two values of fin spacing (S_{BF} = .04, .10) for an enhanced tube surface with D_o = 1", X_{ETP} = 2, and $H_f = (H_f)_{MAX} = .5$	87
13J	$(V_{os})_{REF}/V_{os}$ versus fins per inch for two values of fin thicknesses (t_f = .01, .02) for an enhanced tube surface with D_o = 1", X_{ETP} = 2, and $H_f = (H_f)_{MAX} = .5$	88
A1	Circular finned tube with fins of rectangular profile.	95
A2	Triangular layout of a tube bank.	95
A3	Layout of a tube bank with gas flow normal to paper.	97
A4	Algorithm for prediction of performance parameters for triangular pitch circular finned tube surfaces and bare tube surfaces.	113
A5	TI-59 Calculator program for predicting performance parameters.	118
A6	Sample output generated by program listed in Figure A5.	128

LIST OF TABLES

TABLE	TITLE	PAGE
I	Definitions	26
II	Derived ratios used to convert data found in the literature to the new basis.	28
III	Finned circular tube surfaces.	36
IV	5000 SHP gas turbine plant intercooler fluid properties.	37
V	Deviation of performance parameter program of Figure A5 for volume one side in predicting experimentally obtained value as presented in Kays and London (2) and calculated by Baskerville (3).	55
VI	$(V_{os})_{REF}/V_{os}$ for various values of tube diameter and pitch for smooth tubes.	58
VII	$(V_{os})_{REF}/V_{os}$ for various values of fin thickness, fin height, and fin spacing for two tube diameters and two values of equilateral triangular pitch.	69
AI	Deviation of the Biery (4) method for Colburn j-modulus in predicting experimentally obtained value as presented in Kays and London (2).	101
AII	Deviation of the Jameson (5) correlation for friction factor in predicting experimentally obtained value as presented in Kays and London (2).	107
AIII	Data registers used for storage of parameters for program of Figure A5.	127

I. Introduction

A. Purpose

The objective of any heat exchanger comparison is to enable the designer to select that unique surface which can be termed as the most beneficial to his particular application. The comparison technique should be logical, easily implemented, and inherently accurate.

Enhanced surfaces, in the form of plate fins and finned tubes, have long been used in heat exchanger design to improve heat transfer characteristics. Many have presented methods of comparing the performance of various types of surface designs.

Soland, et al., (1) developed a method of comparison that permits performance comparisons of all the Kays and London (2) plate finned and unfinned surfaces. Baskerville (3) developed a method of comparison, using theory and principle inherent in Soland's method as a basis, that permits performance comparisons of crossflow finned tube surfaces presented in Kays and London. Biery (4) developed a method to predict heat transfer coefficients for gas flow normal to smooth and finned tubes. Jameson, et al (5) developed an empirical relation that correlates pressure drop data for circular finned tubes.

The purpose of this paper is to:

1. Employ the methods and correlations developed by Biery, Jameson, and Baskerville to predict the performance of a crossflow circular finned tube surface for any given geometry.

2. Evaluate the accuracy of the predicted performance by comparison to surfaces presented in Kays and London.
3. Use the performance predictions to evaluate the effect of varying geometry on the performance of crossflow circular finned tube surfaces.
4. Develop graphs and tables that will assist the designer in selecting the geometry of a crossflow circular finned tube surface which will be the most beneficial for his application.

B. Background

Crossflow finned tubular heat exchangers have found applications as gas turbine plant intercoolers, aircraft engine and electronic coolers, air conditioning units, and various other heat exchanger uses. These applications most often involve gas-liquid service. [See Figure 1].

The performance of a given heat exchanger in which the ratio of the heat transfer coefficients between the two working fluids is greater than about three is markedly improved by the employment of enhanced surfaces. The increased surface area inherent with the employment of fins yields a net improvement in heat transfer despite lower heat transfer coefficients.

Optimum design is often used synonomously with "lowest cost". Cost is frequently defined in terms of amortized acquisition cost, operating cost, or impact cost in terms of either weight or volume. An example of the latter might be aircraft engine component design where weight and volume are valuable quantities which can be directly equated to dollar cost.

Estimation of dollar cost of a particular heat exchanger design is difficult, primarily due to the proprietary nature of the required cost estimating relations. The term "cost" or "optimum", therefore, as used in this paper, will most generally refer to "impact cost" and will serve as a means of relative ranking of proposed surfaces specifically by required volume, pumping power and heat transfer (NTU) comparison.

FIGURE 1: Finned Tubular Heat Exchangers

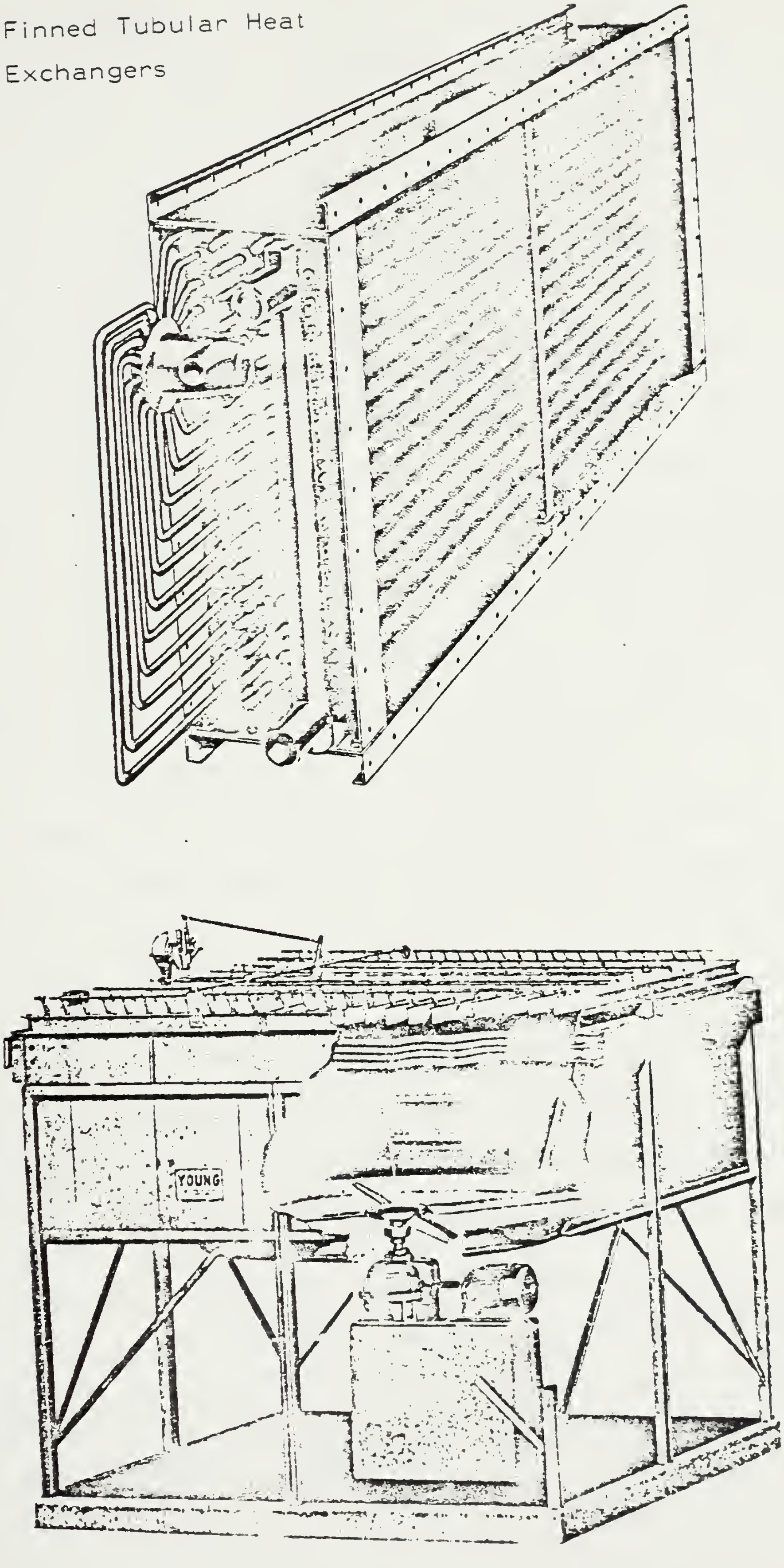

II. Comparison Method

Traditionally, data is presented in terms of heat transfer Colburn modulus, j, and friction factor, f, based on the total exposed area, A_T, as a function of Reynolds number, RE, based on minimum free flow area, A_C, and a hydraulic diameter, D_h, of the flow passage. [See Figure 2]

Baskerville's (3) comparison method converts these j and f magnitudes to new quantities j_N and f_N based on the heat transfer area of the bare base tube surface, A_b, and a Reynolds number, RE_N, which is referenced to the open flow passage area, A_F, as though fins were not present. The effect of the fins is accounted for as an increased heat flux and hence larger h for the bare base tube surface area. In order to incorporate the effect of the fins into j_N, the metal conductivity must be specified.

To convert data presented in the format of Kays and London (2) to the new basis applicable to the crossflow finned tube case, Baskerville (3) derived various ratios from basic heat transfer definitions and theory presented by Soland (1). Important assumptions are that the heat transfer resistance of the tube walls is negligible and that the controlling heat transfer resistance is assumed to be on the finned side of the heat exchanger. Comparison assumes that the flow rate, W, the hot fluid inlet temperature, $T_{h,in}$, and the cold gas inlet temperature, $T_{c,in}$, are held constant. Basic definitions are presented in Table I. Ratios for the two cases of minimum free flow area which may occur [See Figures 3 and 4] are presented in Table II. Fin efficiency is calculated per Figure 5.

FIGURE 2: Sample data plot showing traditional method of data Presentation.

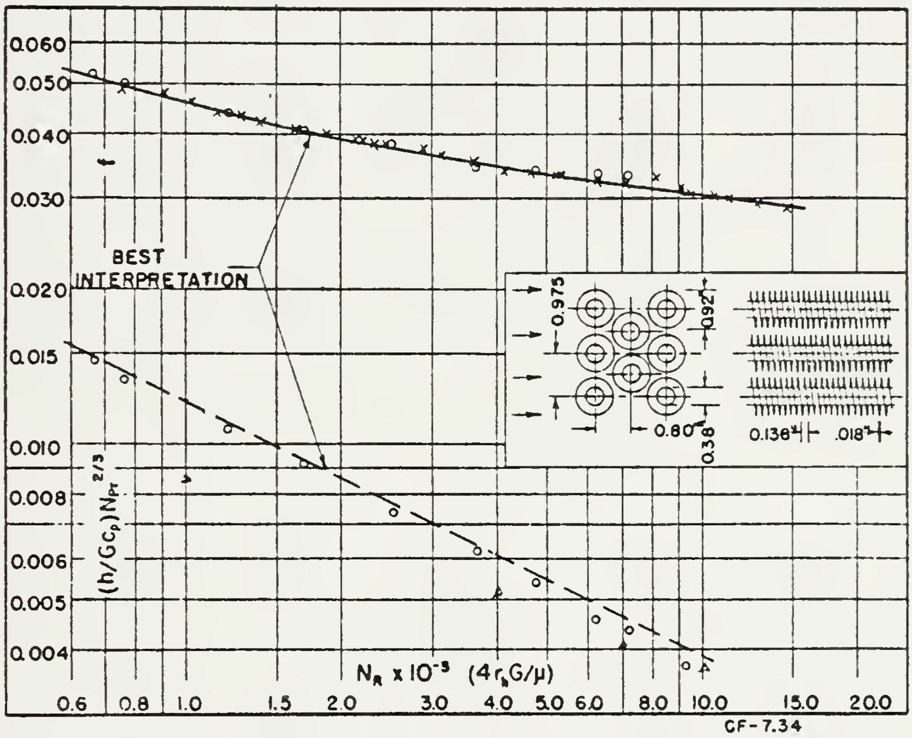

FIG. 92

FINNED CIRCULAR TUBES
SURFACE CF - 7.34

Tube outside diameter - 0.38 in.
Fin pitch - 7.34 per inch
Flow passage hydraulic diameter - $4r_h$=0.0154 ft.
Fin thickness (average)* - 0.018 in.
Free-flow area/frontal area - σ=0.538
Heat transfer area/total volume - α=140 $ft.^2/ft.^3$
Fin area/total area - 0.892

Note: Experimental uncertainty for heat transfer results possibly somewhat greater than the nominal ±5% quoted for the other surfaces because of the necessity of estimating a contact resistance in the bi-metal tubes.

* - Fins slightly tapered.

TABLE I. DEFINITIONS

QUANTITY	KAYS AND LONDON [2]	BARE TUBE
Hydraulic Diameter	$D_h = \frac{4\ A_c\ b}{A_T}$ (1a)	$D_N = \frac{4\ A_F\ b}{A_b}$ (1b)
Mass Velocity	$G_c = \frac{W}{A_c}$ (2a)	$G_N = \frac{W}{A_F}$ (2b)
Reynolds Number	$N_R = \frac{G_c\ D_h}{\mu}$ (3a)	$RE_N = \frac{G_N\ D_N}{\mu}$ (3b)
Friction Factor	$f = \frac{\Delta P_f}{\frac{4\ b}{D_h}\ \frac{G_c^2}{2\rho g_o}}$ (4a)	$f_N = \frac{\Delta P_f}{\frac{4\ b}{D_N}\ \frac{G_N^2}{2\rho g_o}}$ (4b)
Heat Transfer Coefficient	$h = \frac{[q/\eta_o\ A_T]}{\Delta T}$ (5a)	$h_N = \frac{[q/A_b]}{\Delta T}$ (5b)
Nusselt Number	$Nu = \frac{D_h\ h}{k}$ (6a)	$Nu_N = \frac{D_N\ h_N}{k}$ (6b)

TABLE I. DEFINITIONS (Continued)

QUANTITY	KAYS AND LONDON [2]	BARE TUBE
Colburn j	$j = \frac{h}{G_c \ C_p} \ (Pr)^{2/3}$ (7a)	$j_N = \frac{h_N}{G_N \ C_p} \ (Pr)^{2/3}$ (7b)
	$\eta_0 = 1 - \frac{A_f}{A_T} [1-\eta_{f-corr}]$ (8)	
	$\eta_{f-L} = \frac{\text{Tanh } ml}{ml}$ (9)**	
	$m = [(2h)/ \delta \ k_m]^{\frac{1}{2}}$ (10)	

** Use of this formula for computing fin efficiency of a radial fin is permitted as outlined in Figure 4.

TABLE II: Derived Ratios used to Convert Data Found in the Literature to the New Basis

CASE I		CASE II	
$\frac{A_b}{A_T} = \frac{\pi D_o}{\beta\ b\ F}$	(11a)	$\frac{A_b}{A_T} = \frac{\pi D_o}{\beta\ b\ F}$	(11b)
$\frac{A_F}{A_c} = \frac{4\ a_t}{\beta\ F\ D_h}$	(12a)	$\frac{A_F}{A_c} = \frac{8\ a_d}{\beta\ F\ D_h}$	(12b)
$\frac{G_N}{G_c} = \frac{A_c}{A_F} = \frac{\beta\ F\ D_h}{4\ a_t}$	(13a)	$\frac{G_N}{G_c} = \frac{\beta\ F\ D_h}{8\ a_d}$	(13b)
$\frac{RE_N}{N_R} = \frac{\beta\ b\ F}{\pi D_o}$	(14a)	$\frac{RE_N}{N_R} = \frac{\beta\ b\ F}{\pi D_o}$	(14b)
$\frac{f_N}{f} = \frac{16\ a_t^2\ D_N}{\beta^2\ F^2\ D_h^3}$	(15a)	$\frac{f_N}{f} = \frac{64\ a_d^2\ D_N}{\beta^2\ F^2\ D_h^3}$	(15b)
$\frac{j_N}{j} = \frac{\eta_o\ D_N}{D_h}$	(16a)	$\frac{j_N}{j} = \frac{\eta_o\ D_N}{D_h}$	(16b)

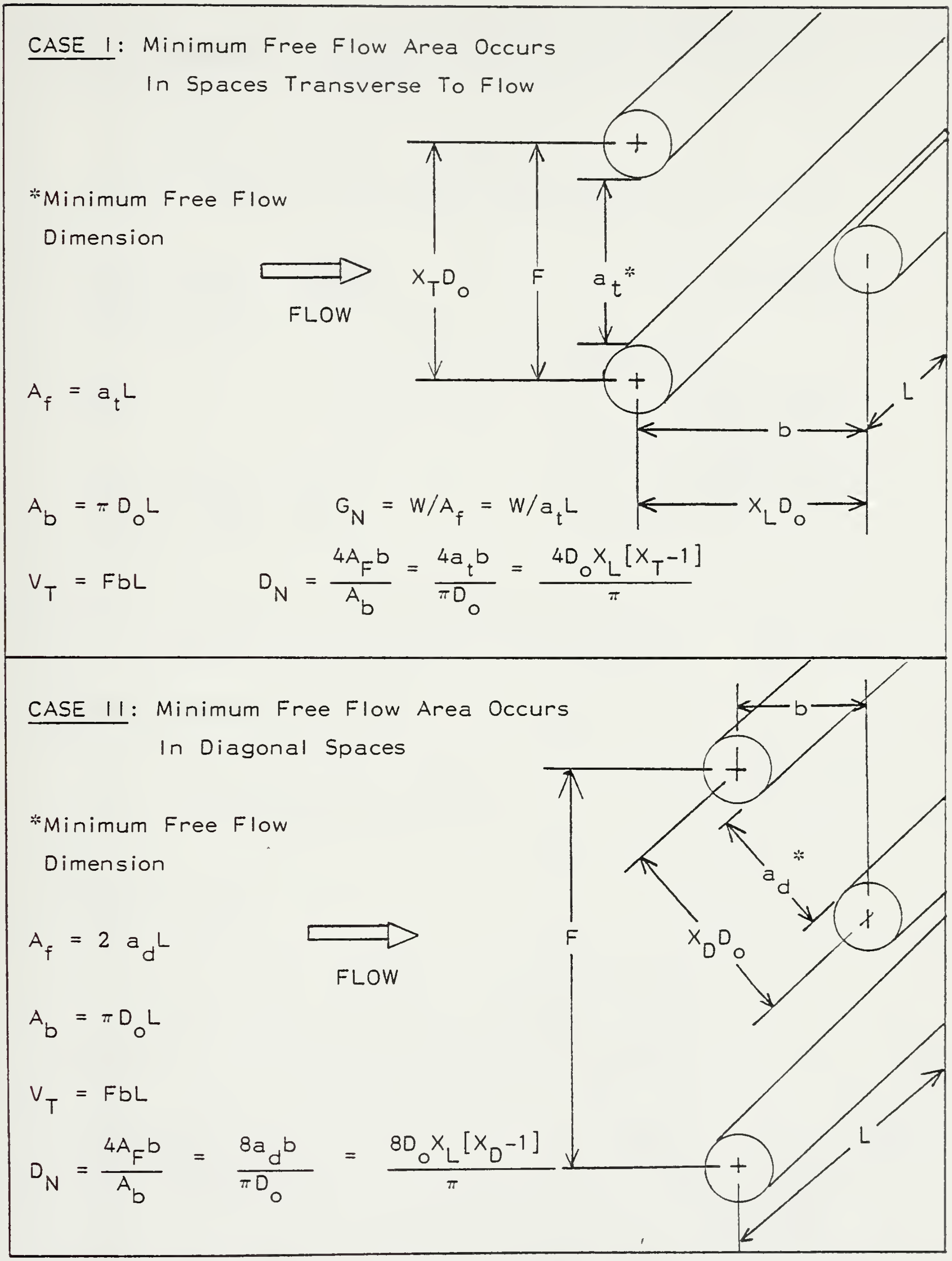
CASE I: Minimum Free Flow Area Occurs In Spaces Transverse To Flow
*Minimum Free Flow Dimension
FLOW
X_TD_o
F
a_t*
b
L
X_LD_o
$A_f = a_tL$
$A_b = \pi D_oL$
$V_T = FbL$
$G_N = W/A_f = W/a_tL$
$D_N = \frac{4A_Fb}{A_b} = \frac{4a_tb}{\pi D_o} = \frac{4D_oX_L[X_T-1]}{\pi}$
CASE II: Minimum Free Flow Area Occurs In Diagonal Spaces
*Minimum Free Flow Dimension
FLOW
b
F
a_d*
X_DD_o
L
$A_f = 2\ a_dL$
$A_b = \pi D_oL$
$V_T = FbL$
$D_N = \frac{4A_Fb}{A_b} = \frac{8a_db}{\pi D_o} = \frac{8D_oX_L[X_D-1]}{\pi}$

FIGURE 3: The Two Cases of Minimum Free Flow Area Occurence and the Associated Geometric Relations of Each Case.

CASE I: Minimum Free flow area Transverse to Flow Direction

Total Volume on one Side:

$$V_{os} = [X_T D_o]\,[X_L D_o]L - \pi D_o^2 L/4$$

L = dimension into paper along flow length of tubes.

"$A_F b$" Volume: ▨

$$A_F b = [X_T D_o - D_o]\; L\; X_L\; D_o$$

Ratio:

$$\frac{A_F b}{V_{os}} = \frac{[X_T - 1]\; X_L}{X_T X_L - \pi/4}$$

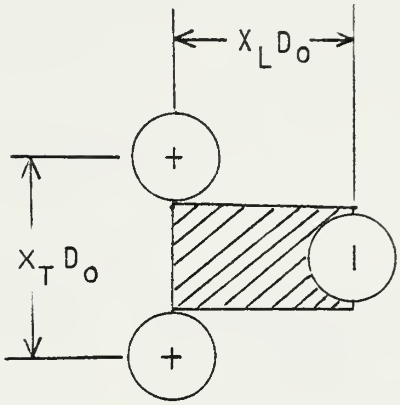

CASE II: Minimum Free Flow Area in the Diagonals

Total Volume on one Side:

$$V_{os} = \frac{[D_o^2\; X_D^2\; \sin\alpha - \pi D_o^2/4]}{2}$$

"$A_F b$" Volume:

$$A_F b = 2X_L\; D_o\; [X_D - 1]\; D_o$$

Ratio:

$$\frac{A_F b}{V_{os}} = \frac{4[X_D - 1]X_L}{X_D^2 \sin\alpha - \pi/4}$$

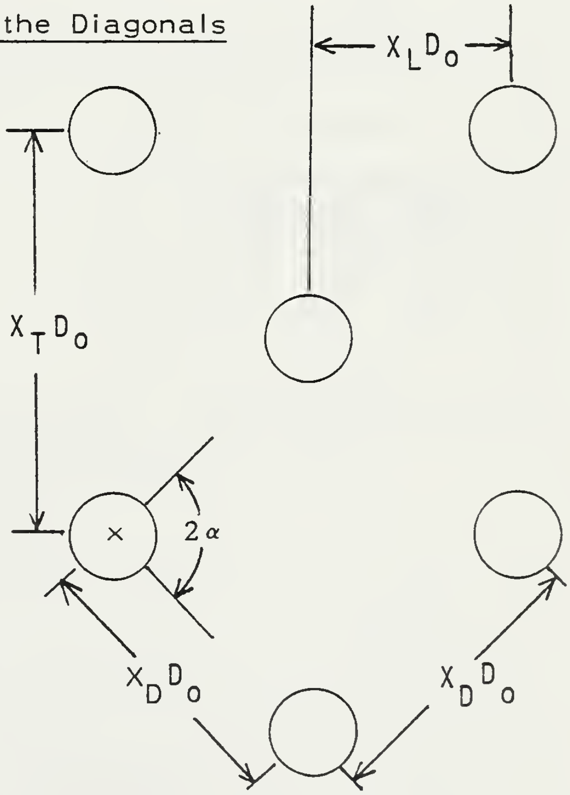

FIGURE 4: Calculation of $[A_F b]/V_{OS}$ for both Case I and II.

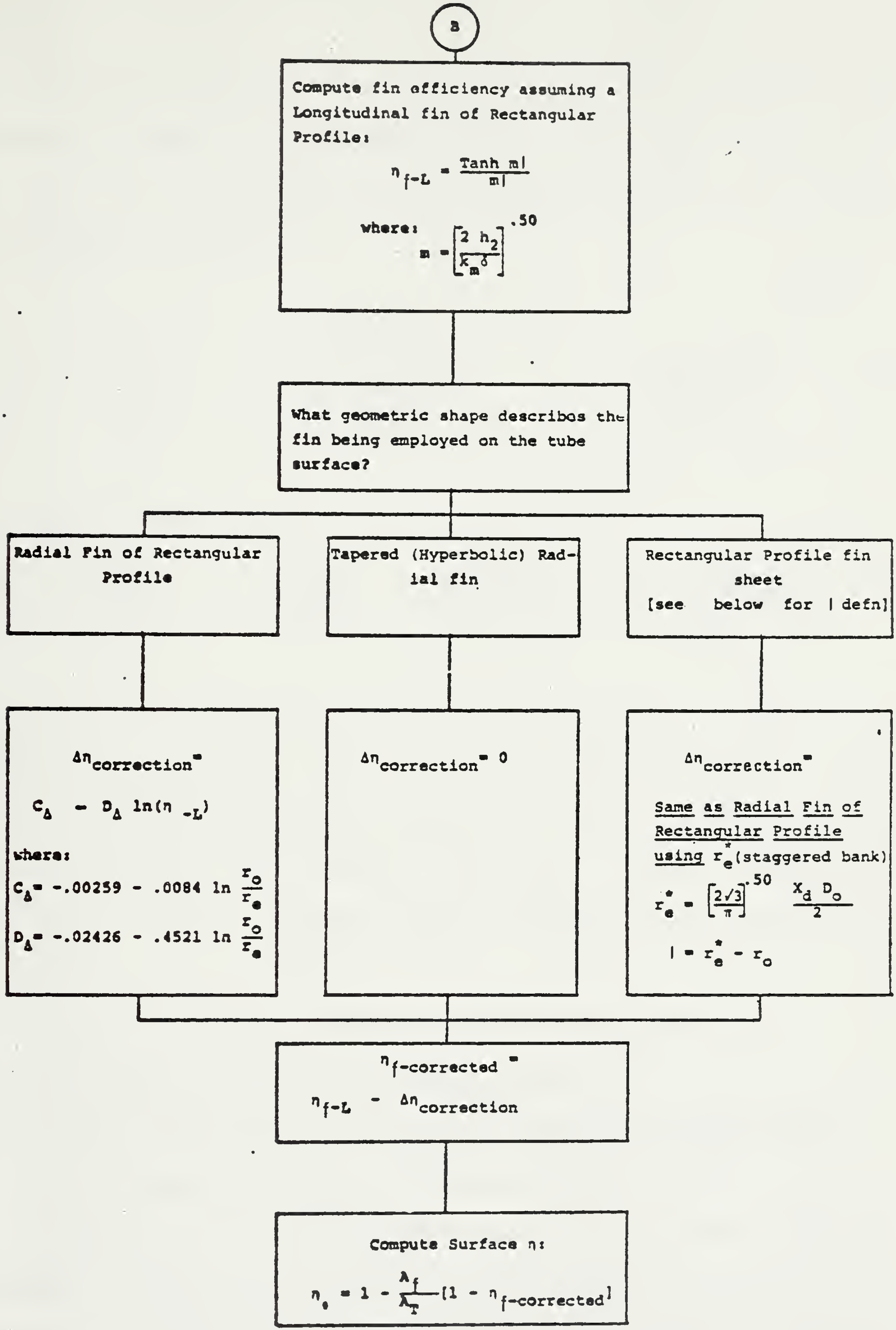
B
Compute fin efficiency assuming a Longitudinal fin of Rectangular Profile:
$\eta_{f-L} = \frac{\tanh ml}{ml}$
where: $m = \left[\frac{2 h_2}{k_m \delta}\right]^{.50}$
What geometric shape describos the fin being employed on the tube surface?
Radial Fin of Rectangular Profile
Tapered (Hyperbolic) Radial fin
Rectangular Profile fin sheet [see below for l defn]
$\Delta\eta_{correction} = C_\Delta - D_\Delta \ln(\eta_{-L})$
where:
$C_\Delta = -.00259 - .0084 \ln \frac{r_o}{r_e}$
$D_\Delta = -.02426 - .4521 \ln \frac{r_o}{r_e}$
$\Delta\eta_{correction} = 0$
$\Delta\eta_{correction} =$
Same as Radial Fin of Rectangular Profile using r_e^* (staggered bank)
$r_e^* = \left[\frac{2\sqrt{3}}{\pi}\right]^{.50} \frac{X_d D_o}{2}$
$l = r_e^* - r_o$
$\eta_{f-corrected} = \eta_{f-L} - \Delta\eta_{correction}$
Compute Surface η:
$\eta_s = 1 - \frac{A_f}{A_T}[1 - \eta_{f-corrected}]$

FIGURE 5: Computing fin efficiency of a Radial fin; Ref(3).

Further, Baskerville (3) shows that for any crossflow heat exchanger, where for the same fluid at the same temperature, μ and ρ are constant, the fluid pumping power per unit volume on one side is given by:

$$\frac{P}{V_{os}} = \frac{W \Delta P_f}{V_{os} \rho} = \frac{2 \mu^3 f_N RE_N^3 A_F b}{g_o \rho^2 D_N^4 V_{os}} \quad \alpha \quad \frac{f_N RE_N^3 A_F b}{D_N^4 V_{os}} \qquad (17)$$

And for the flow rate, W, also constant:

$$\frac{NTU}{V_{os}} = \frac{A_b h_N}{V_{os} W C_p} = \frac{4 \mu}{Pr^{2/3} W} \cdot \frac{j_N Re_N A_F b}{D_n^2 V_{os}} \quad \alpha \quad \frac{j_N Re_N A_F b}{D_n^2 V_{os}} \qquad (18)$$

Using equations (17) and (18), it is possible to construct a performance parameteter plot of NTU/V_{OS} versus P/V_{OS} from which useful performance comparisons between two heat exchangers for four different criteria are obtained. The four different comparisons, depicted in Figure 6, predict relative performance in the following categories:

Case A: Same heat exchanger shape and volume.

Case B: Same volume and pumping power.

Case C: Same pumping power and number of transfer units.

Case D: Same volume and number of transfer units.

Baskerville (3) plotted performance curves of all the finned surfaces of Kays and London (2). Figure 7 shows the resulting performance parameter plot presenting only the highest performance curve at each nominal diameter (D_N). The study considered sixteen

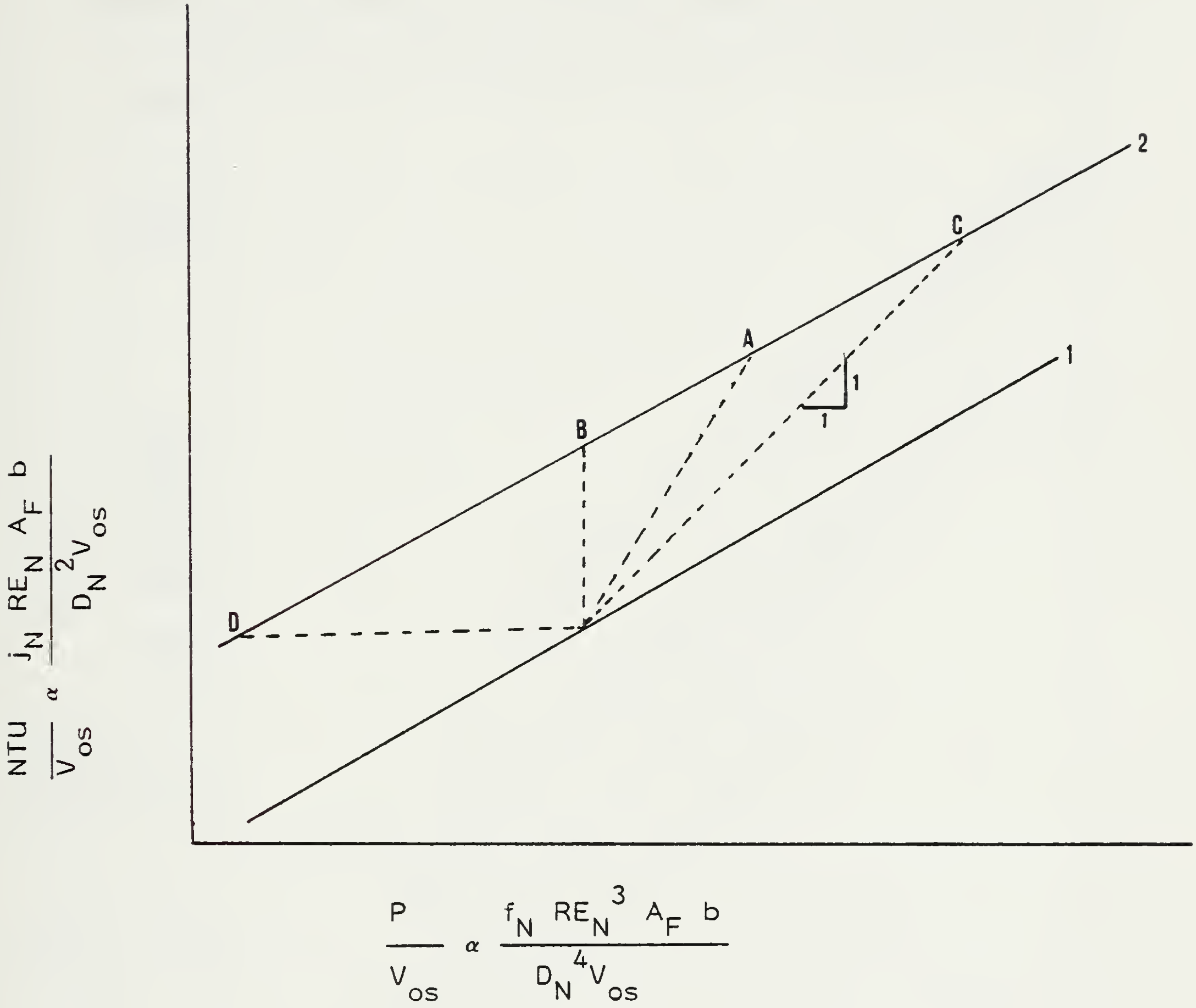

FIGURE 6: Performance Parameter Curves For Two Hypothetical Surfaces Showing Points Used in Sample Comparisons.

FIGURE 7

PERFORMANCE PARAMETER CURVE FOR FINNED TUBULAR SURFACES

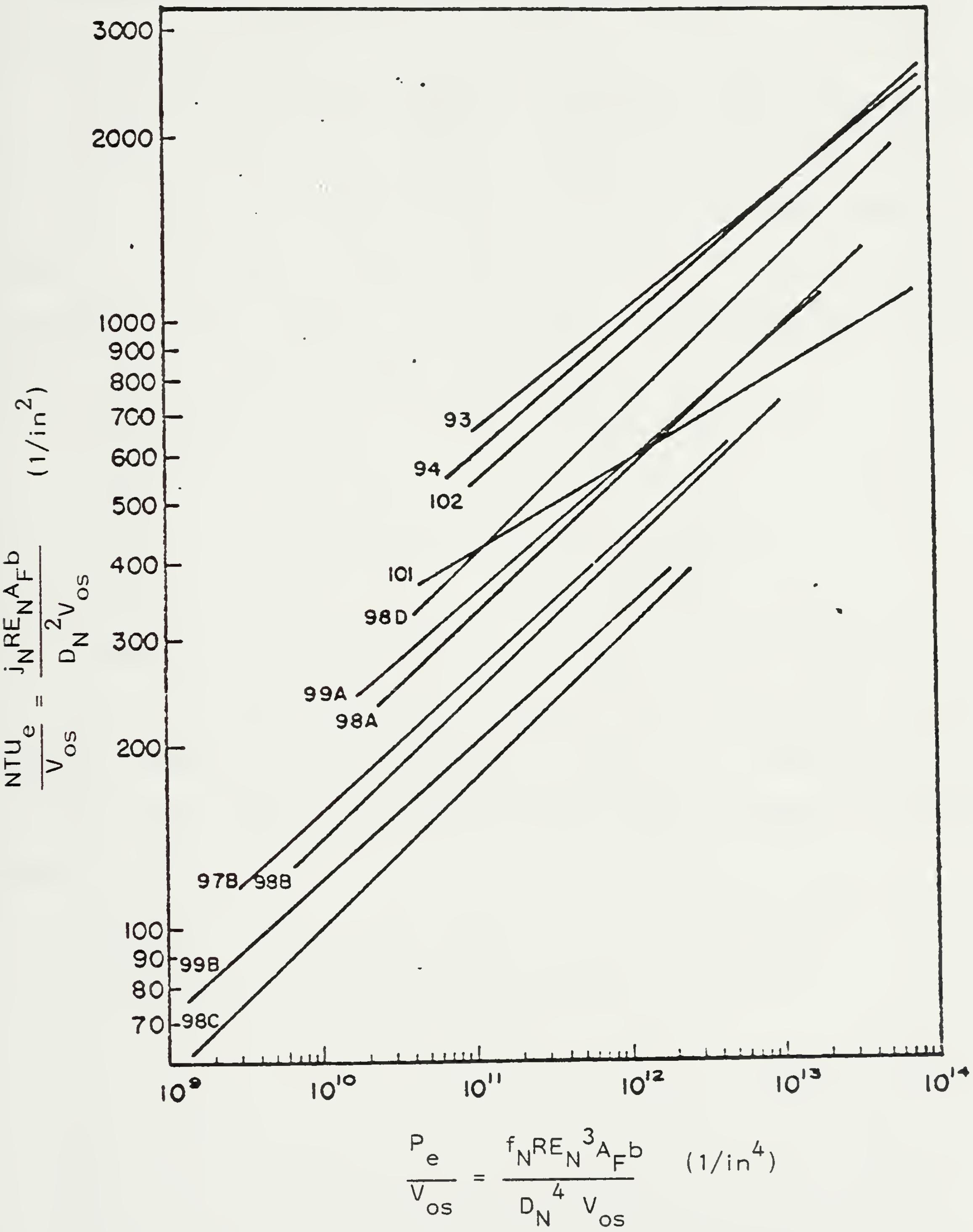

different surfaces having eleven different nominal diameters. Table III lists all of the Kays and London surfaces considered by type and surface designation in addition to the one surface supplied by the Trane Corporation.

Baskerville (3) also offered a procedure which can be used for sizing crossflow finned tubular heat exchangers. Two designs of an intercooler for a 5000 SHP gas turbine plant were undertaken using surfaces 98C and 94. Table IV lists the fluid properties assumed for both designs. The principle dimensions using surface 98C and then surface 94 were calculated to be:

Surface 98C:	Surface 94:
$X=6.43$ ft	$X=1.5$ ft
$Y=22.11$ ft	$Y=10.89$ ft
$Z=0.63$ ft	$Z=1.76$ ft
Total Volume = 105.46 ft^3	Total Volume = 28.68 ft^3

Both designs satisfy the thermodynamic and geometric constraints. However, use of surface 94 results in a 73% reduction in volume, and is seen from Figure 7 to be notably superior to surface 98C.

TABLE III

Surface Numbered in Figure 7 as:	Kays and London (2) Surface Designation.	D_o(in)	X_T	X_D	H_f	t_f	S_{BF}/t_f
92	CF - 7.34	.38	2.57	2.47	.711	.0474	6.56
93	CF - 8.72	.38	2.57	2.47	.711	.0474	5.37
94	CF - 8.72(C)	.42	2.32	2.23	.525	.0452	5.04
96	CF-7.0-5/8J	.645	1.91	2.30	.369	.0155	13.29
97A	CF-8.7-5/8J(A)	.645	1.91	2.30	.369	.0155	10.50
97B	CF-8.7-5/8J(B)	.645	2.87	2.54	.369	.0155	10.50
98A	CF-9.05-3/4J(A)	.774	2.01	2.47	.445	.0155	8.21
98B	CF-9.05-3/4J(B)	.774	2.56	2.60	.445	.0155	8.21
98C	CF-9.05-3/4J(C)	.774	3.52	2.86	.445	.0155	8.21
98D	CF-9.05-3/4J(D)	.774	3.52	2.04	.445	.0155	8.21
98E	CF-9.05-3/4J(E)	.774	2.56	2.19	.445	.0155	8.21
99A	CR-8.8-1.0J(A)	1.024	1.91	2.23	.348	.0117	8.48
99B	CF-8.8-1.0J(B)	1.024	3.01	2.51	.348	.0117	8.48
100	8.0-3/8(T)	.402	2.48	2.48	.74	.0323	8.63
101	7.75-5/8(T)	.676	2.22	2.82	.61	.0237	7.05
102	Trane Company	.391	2.56	2.86	.8427	.0205	14.59

TABLE IV

5000 SHP Gas Turbine Plant Intercooler Fluid Properties

Properties	Side I	Side II
Fluid	Water	Dry Air
W	400,000 lbm/hr	200,667 lbm/hr
T_{in}	60° F	260° F
T_{out}	82° F	80° F
P	1.554 PSI	.3060 PSI

A performance parameter plot is constructed (Figure 8) for surfaces 98C and 94 to quantitatively predict the volume savings. This comparison corresponds to Case C. From the design point of the reference heat exhchanger (surface 98C) a line of slope 1 is constructed. The intersection of this line with the surface 94 will yield the performance parameters at the design point of the new heat exchanger. The predicted volume reduction is found from the ratio of either the ordinates or abscissas of the two surfaces.

The performance parameters of the reference heat exchanger design (surface 98C) are: (See Figure 8)

$$\frac{NTU}{V_{os}} = 401.20 \ (1/in^2)$$

$$\frac{P}{V_{os}} = 2.93 \ 10^{12} \ (1/in^4)$$

The performance parameters that would result using surface 94 are: (See Figure 8)

$$\frac{NTU}{V_{os}} = 1{,}634.68 \ (1/in^2)$$

$$\frac{P}{V_{os}} = 1.19 \ 10^{13} \ (1/in^4)$$

Since pumping power and number of transfer units are the same for both surfaces it is seen that:

$$\frac{\left[\frac{NTU}{V_{os}}\right]_{98C}}{\left[\frac{NTU}{V_{os}}\right]_{94}} = \frac{\left[\frac{P}{V_{os}}\right]_{98C}}{\left[\frac{P}{V_{os}}\right]_{94}} = \frac{\left[V_{os}\right]_{94}}{\left[V_{os}\right]_{98C}} = .25$$

Therefore, a predicted volume reduction of 75% is anticipated using the comparison method proposed by Baskerville. This compares

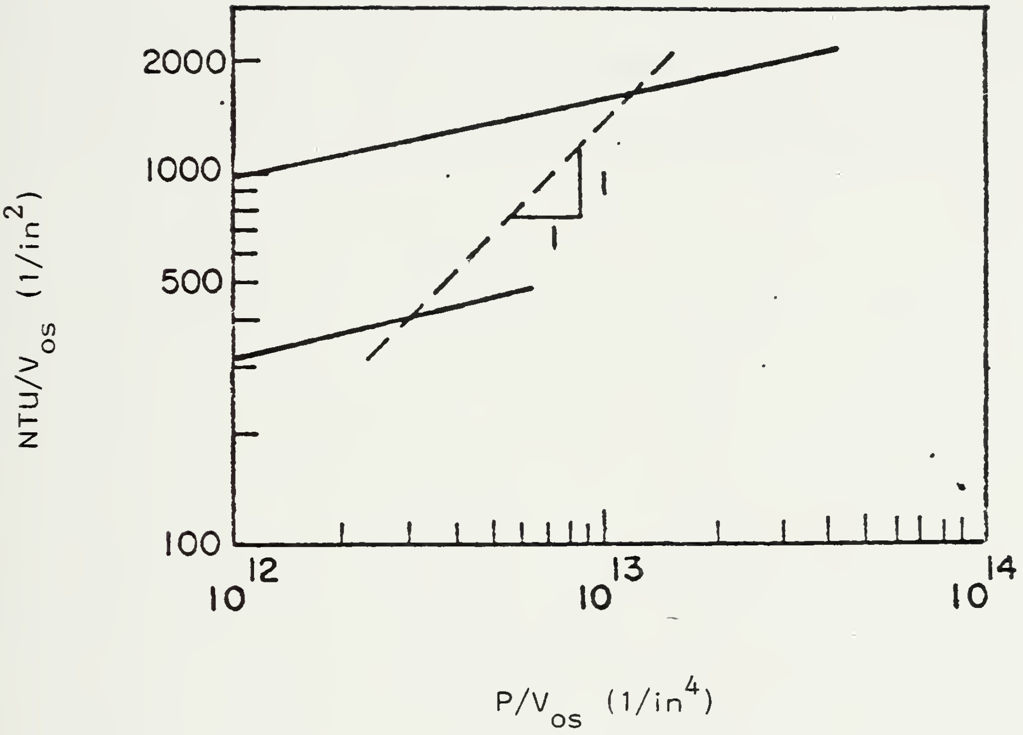

FIGURE 8

Performance Parameter Plot for the two surfaces used in the Design Example.

quite favorably with the heat exchanger design calculations made for these surfaces and therefore shows that the performance parameters for a surface allow comparison of surfaces without going through a complete heat exchanger design calculation. Where there may well be hundreds of different surfaces to be considered, such as the parametric study of geometry effects on crossflow circular finned tube heat exchangers conducted in this paper, the value of such a comparison technique cannot be overestimated.

III. Heat Transfer Correlations

Biery (4) presents a method to predict heat transfer coefficients for gas flow normal to finned tube banks with triangular pitch. A transformation from the actual tube bank to an equivalent equilateral triangular pitch infinite smooth tube bank (ETP-I-STB) is made and the heat transfer coefficient for this ETP-I-STB is that desired for the real tube bank.

The correlation for the desired heat transfer Colburn modulus, j, is given as:

$$j = N_{ST} N_{PR}^{2/3} = C_H RE^{-.4} \tag{19}$$

where RE is based upon the hydraulic diameter of Kays and London (2) and is given by:

$$D_h = 4r_h = \frac{4A_c b}{A_T} \tag{1a}$$

The minimum flow area, A_c, often will be in the transverse direction to flow. However, for tube banks with a small X_L compared to X_T, the minimum flow area may well be along the diagonal of the triangular pitched bank. Expressions for A_C and D_h are developed in Appendix I for both cases.

C_H is a function of the transverse distance between tubes, $X_T D_o$, and an equivalent diameter, D_E, given by

$$D_E = D_o + E\ (D_f - D_o) \tag{20a}$$

where for $S_{BF} D_o < .04775$ inches

$$E = 1 \tag{20b}$$

and for $.04775 \text{ inches} \leq S_{BF} D_o \leq .4 \text{ inches}$

$$E = 1.1357 - 2.842\ S_{BF} D_o \tag{20c}$$

and for $S_{BF}D_o > .4$ inches

$$E = 0 \tag{20d}$$

where $S_{BF}D_o$ is the spacing between fins in inches. Since E is equal to one for $S_{BF}D_o$ less than .04775 inches and equal to zero for $S_{BF}D_o$ greater than .4 inches, D_E has the characteristic of being equal to the fin diameter, D_f, for fins with narrow spacing and equal to the bare tube diameter, D_o, for tubes with either no fins or with fins with a wide spacing.

For an ETP-I-STB the equivalent diameter is simply the outside diameter of the tube. Therefore, the ratio of its hydraulic diameter, D_h, to the equivalent diameter is:

$$\left(\frac{D_h}{D_o}\right)_\Delta = \frac{4[(X_T)_\Delta -1]\ (X_L)_\Delta}{\pi} = \frac{4[(X_T)_\Delta -1]\ (\sqrt{3}/2)\ (X_T)_\Delta}{\pi} \tag{21}$$

where $(X_T)_\Delta$ denotes the transverse tube pitch (ratio of transverse tube spacing to tube outside diameter) for an ETP-I-STB. To transform from the actual tube bank to an equivalent ETP-I-STB, the ratio of the hydraulic diameter to the equivalent diameter $[D_h/D_E]$ is equated to the ratio of the hydraulic diameter to the equivalent diameter of the ETP-I-STB $[(D_h/D_o)_\Delta]$. $(X_T)_\Delta$ is then solved to yield:

$$(X_T)_\Delta = 1 + \frac{(4A + 1)^{\frac{1}{2}}}{2} \tag{22a}$$

where

$$A = \frac{D_h}{D_E} \quad \frac{\pi}{4\ (\sqrt{3}/2)} \tag{22b}$$

Biery found that with this transformation, C_H was a function of only $(X_T)_\Delta$ and had the property of bringing all of the various

configurations onto one curve. Correlating the data given by Kays and London (2), Jameson (5), Fraas and Ozisik (6), Mirkovic (7), and Grimeson (8) with empirical curve fitting resulted in:

$$C_H = .2818(X_T)_\Delta - .1282 - \frac{0.08263\,[1.2 - (X_T)_\Delta]}{[(X_T)_\Delta - .8924]} \qquad (23)$$

Biery's transformation and correlation for heat transfer prediction of circular finned tubes is used later in this paper to study the geometry effects on the sizing of crossflow circular finned tube heat exchangers. It should be noted that the data from which this correlation is derived is based on a limited range of tube spacing, tube diameters, fin spacing, fin thickness, and fin height. Application of this correlation beyond this limited range should be recognized as an extrapolation of the empirical data.

A study was made to compare Biery's method for prediction of heat transfer coefficients with other correlations and the data presented in Kays and London (2) for circular finned tubes. The details of this study are presented in Appendix II. In general it was found that Biery's method resulted in heat transfer coefficients that agreed with Kays and London data within 20% of the mean value with a mean 7% below the Kays and London data and a standard deviation of 8%.

Zhukauskas (9) developed a correlation for heat transfer for turbulent flow over staggered tube banks with the appropriate nominal diameter, D_N, which is also used later in this paper to study geometry effects on the sizing of crossflow circular finned tube heat exchangers. This correlation for smooth tube bank Colburn

Modulus, j_s, is given as:

$$j_s = .35\ (N_{RE})^{-0.396}\ (X_T/X_L)^{1/6}\ (D_o/D_N)^{.400} \qquad (24)$$

To justify the use of the above relation it is noted that Baskerville (3) used this relation to predict the heat transfer for crossflow over bare tube banks presented in Kays and London (2). The results showed a maximum deviation between the experimental value of j_s from Kays and London (2) and the calculated value of j_s from equation (24) of 7.5%. These results are shown in Figure 9.

FIGURE 9

Deviation of the Zhukauskas (9) correlation for forced-convection, turbulent flow over staggered tube banks in predicting experimentally obtained value of Colburn modulus [j_s] as presented in Kays and London (2).

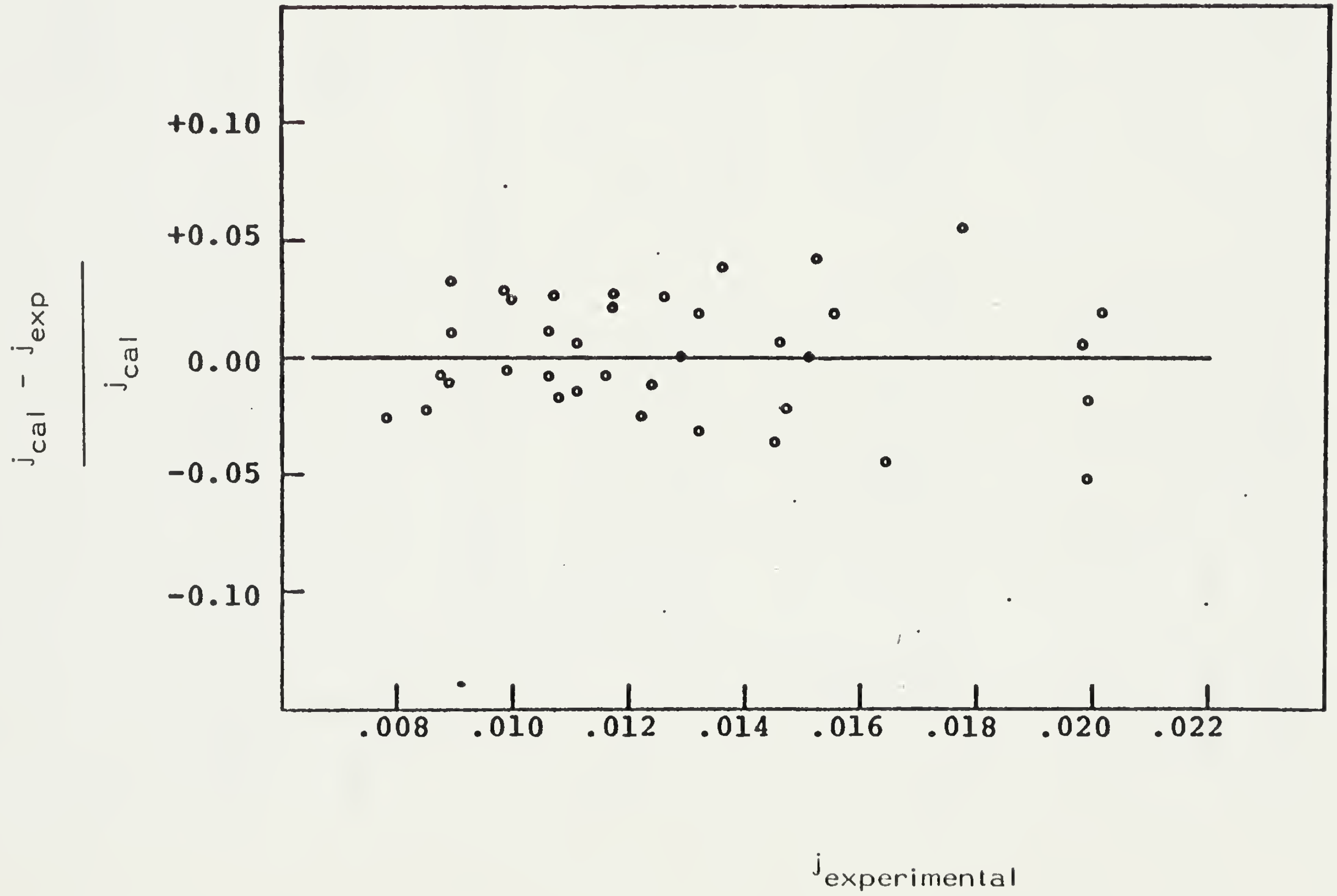

IV. Pressure Drop Correlations

In general the friction factor is a function of the Reynolds number:

$$f = C_1 RE^{C_2}, \tag{25}$$

where C_1 and C_2 are constants.

Jameson (5) developed the following empirical relation for an "equivalent diameter", D_J, of a triangular pitch finned tube bundle which correlated his data for pressure drop across tube banks in which the minimum free flow area is in the space between tubes transverse to the air flow.

$$D_j = \frac{d_e}{\left[\left[\frac{H_F}{2S_{BF}}\right]^{.4}\left(\frac{1}{2}\left[\frac{X_T D_o}{d_e} - 1\right]^{-\frac{1}{2}} + \frac{1}{2}\left[\frac{X_o D_o}{d_e} - 1\right]^{-\frac{1}{2}}\right)\right]^4} \tag{26}$$

where d_e is defined by equation (A18).

Using this expression for D_J, equation (25) becomes:

$$f_J = 1.532\ RE_{D_J}^{-.25}, \tag{27}$$

where RE_{D_J} is the Reynolds number based on D_J and G_c.

$$RE_{D_J} = \frac{G_c D_J}{\mu} \tag{28}$$

The friction factor is defined by Jameson (5) for N tube rows as follows:

$$\Delta P_f = \frac{2 f_J G_c^2 N}{\rho g_o} \tag{29}$$

This definition differs from the Kays and London (2) definition which is given by:

$$P_f = \left[\frac{fG_c^{\,2}N}{2\,\rho\, g_o}\right]\left[\frac{A_T}{A_C}\right] = \left[\frac{2fG_c^{\,2}N}{\rho\, g_o}\right]\left[\frac{X_L D_o}{D_H}\right] \qquad (30)$$

Equation (30) is the same as equation (4a), except that equation (4a) applies to a single row of tubes, where it is understood that the pressure drop is directly proportional to the number of tube rows.

To compare the friction factor used in the Jameson correlation, f_J, with the friction factor given in the data by Kays and London, the geometry factor, $(X_L D_o/D_H)$, must be included and the Reynolds number converted to a common diameter. This is done in Appendix III. In general, it was found that the Jameson correlation predicted the Kays and London data to within approximately 20% from the mean value with a mean of +7.8% and a standard deviation of 7.3%. As noted by Jameson, this correlation does not accurately predict the friction factor for finned tubes in which the minimum free flow area occurs in the diagonal of the triangular pitch tube bank. Not withstanding this difficulty, Gianolio and Cute (11) in their set of experiments for pressure-drop measurements across equilateral triangular pitch finned tubes banks in induced draft, noted the Jameson correlation compared the most favorably with their results showing a maximum deviation of only 15% compared to their data. In a study of the geometry effects on triangular pitch finned tube banks, the effect of tube pitch can be demonstrated with smooth tubes. The other geometry effects can then accurately be demonstrated by

selecting a tube pitch in which the minimum free flow area does not occur in the diagonal. Therefore, the Jameson correlation is used later to study geometry effects by predicting performance parameters for tube banks in which the minimum free flow area occurs in the spaces transverse to the air flow.

To predict the friction factor for smooth tubes, (f_S), Baskerville (3) derived the following empirical correlations based on the Kays and London (2) data for both cases of minimum free flow area.

For Case I where the minimum free flow area occurs in the spaces transverse to flow:

$$f_S = .7184\ RE^{-0.2407}\ [X_T-1]^{.703}\ [X_L]^{C_T}\ , \qquad (31)$$

where:

$$C_T = .828 - 16.596\ RE_N^{-0.4277}$$

For Case II where the minimum free flow area occurs in the diagonal spaces:

$$f_S = RE^{-0.1892}[X_D-1]^{0.703}[X_L]^{C_D}\ , \qquad (32)$$

where:

$$C_D = 130.1\ RE_N^{-\ 0.7284}$$

To justify the use of the above relations, it is noted that Baskerville used these relations to predict the actual experimental friction factor data for flow over bare tube banks as presented in Kays and London (2). The results are shown in Figure 10. The maximum deviation between the Kays and London (2) experimental value of f_S and the calculated value from either (31) or (32) is approximately 3.0% from the mean value.

FIGURE 10

Deviation of the derived correlation for forced-convection, turbulent flow over staggered tube banks in predicting experimentally obtained value friction factor $[f_s]$ as presented in Ref [2].

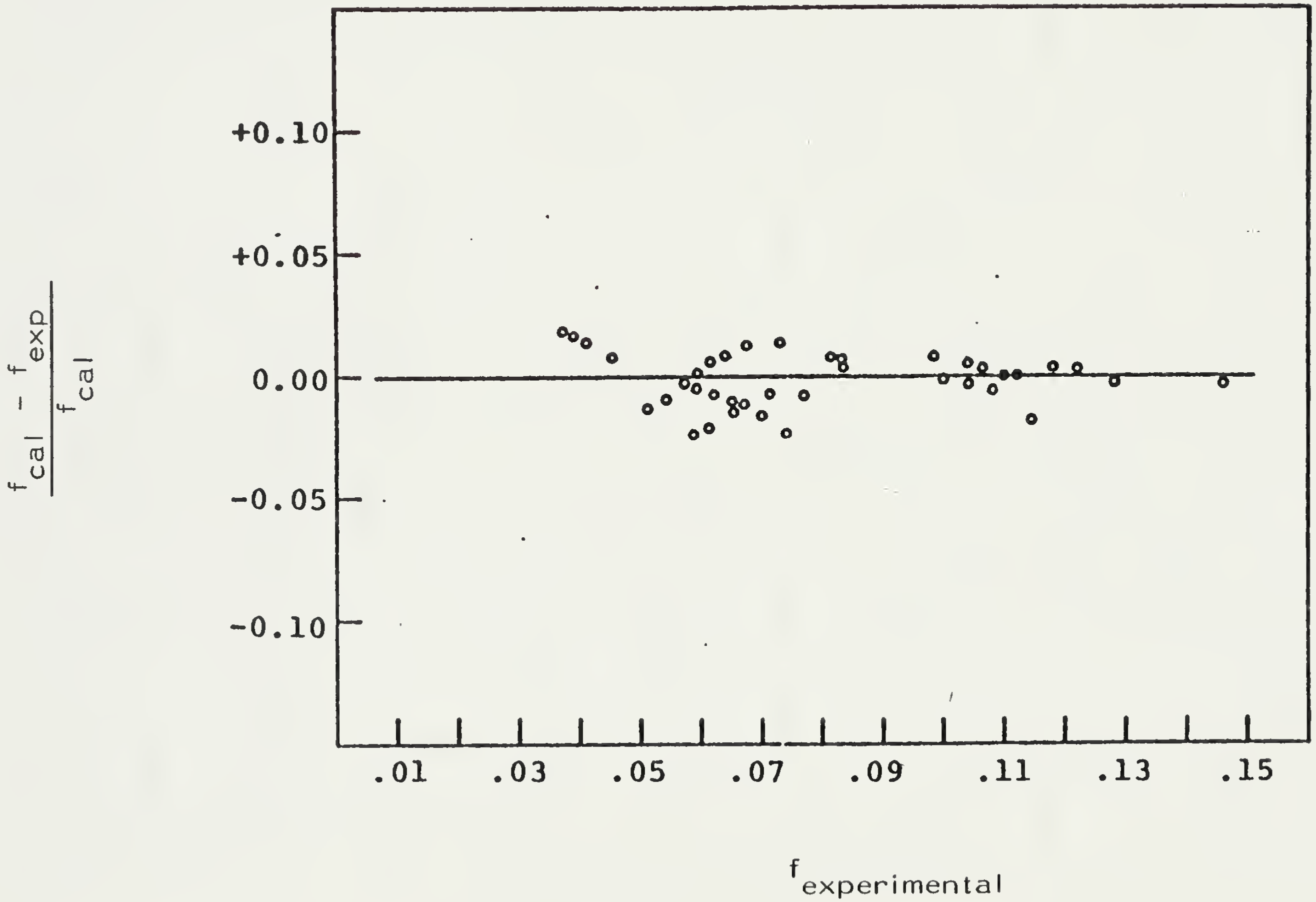

V. Comparison of Performance Parameter Prediction Program.

Appendix IV presents an algorithm and calculator program that employs the comparison method introduced in Chapter II and the heat transfer and pressure drop correlations introduced in Chapters III and IV to predict the performance parameters of a surface. This program was used to predict the performance parameters for the triangular pitch circular finned surfaces in Kays and London (2). These performance parameters were then compared to the performance parameters calculated by Baskerville (3) from the actual heat transfer and pressure drop data given in Kays and London (2) for these surfaces. The predicted performance parameters and the performance parameters calculated by Baskerville are shown graphically in Figure 11, which offers a visual comparison between the predicted performance parameters and the performance parameters generated using the Kays and London (2) experimental data. Each surface was compared on the basis of same pumping power and number of transfer units (Case C). With this comparison the ratio $(V_{os})_p/(V_{os})_e$ can be found. The percent deviation in $(V_{os})_p$ from $(V_{os})_e$ can then be found from this ratio and calculated according to equation (33).

$$\text{Percent Deviation} = \frac{(V_{os})_p - (V_{os})_e}{(V_{os})_e} \times 100\% \tag{33}$$

The average deviation of the predicted volume one side $(V_{os})_p$ from the calculated (from experimental data) volume one side $(V_{os})_e$ is given by Table V. If surfaces 93, 94, and 98D are discounted due to the difficulties already cited for these surfaces, the average deviation for the remaining surfaces is +11.7% with a standard

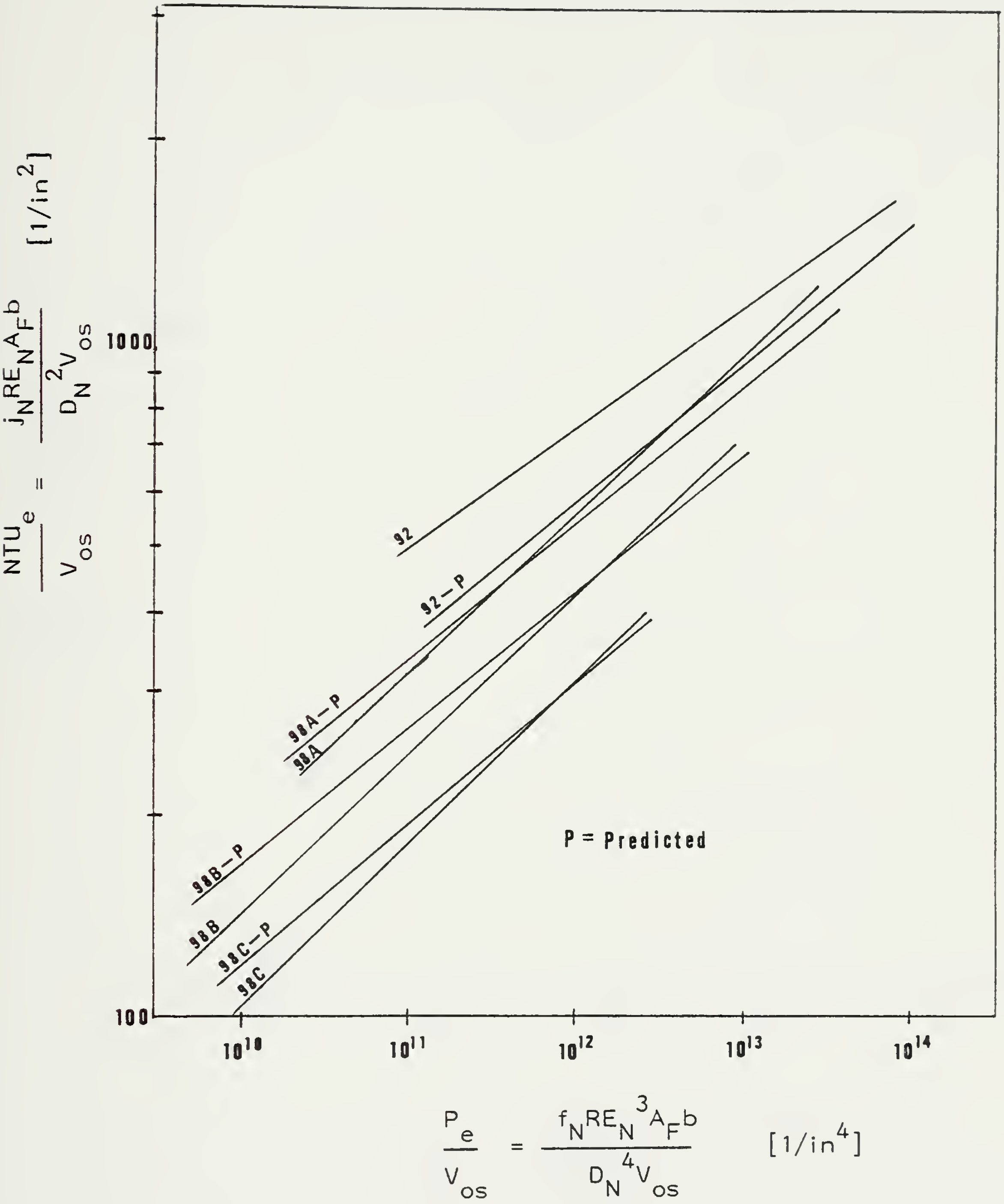

Figure 11. Comparison of predicted performance parameters with performance parameters calculated by Baskerville (3) from Kays and London (2) experimental data.

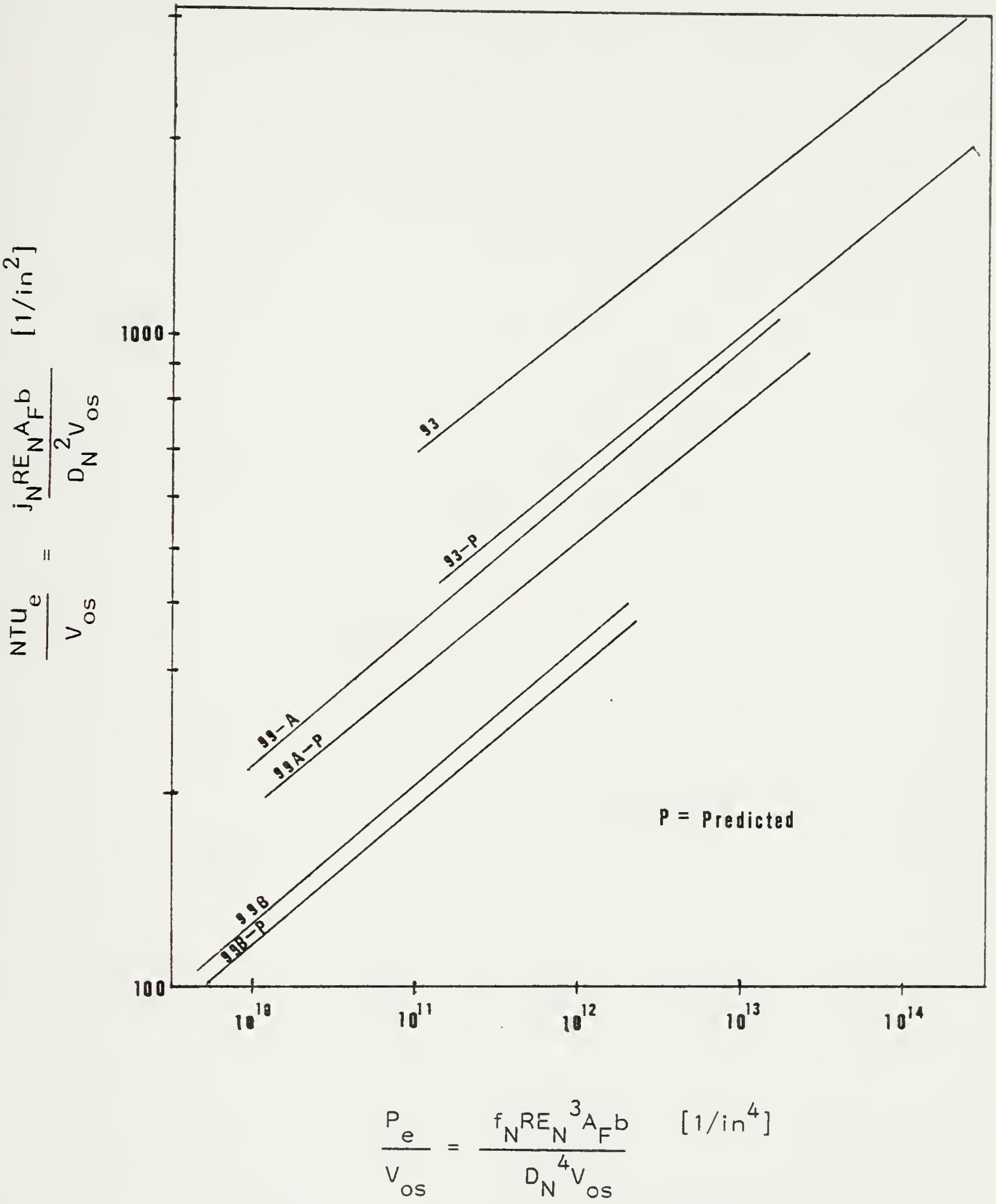

Figure 11. (Cont)

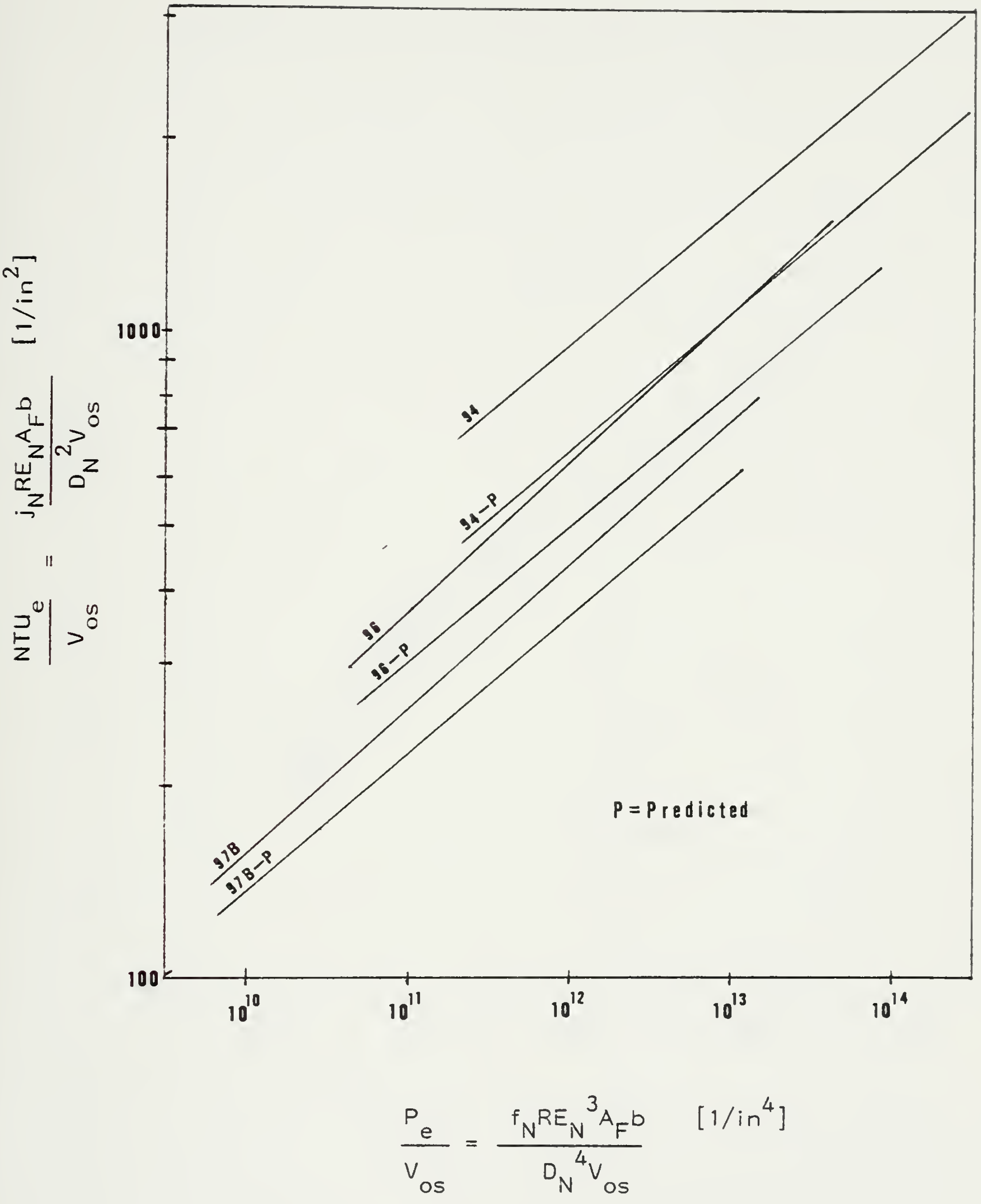

Figure 11. (Cont)

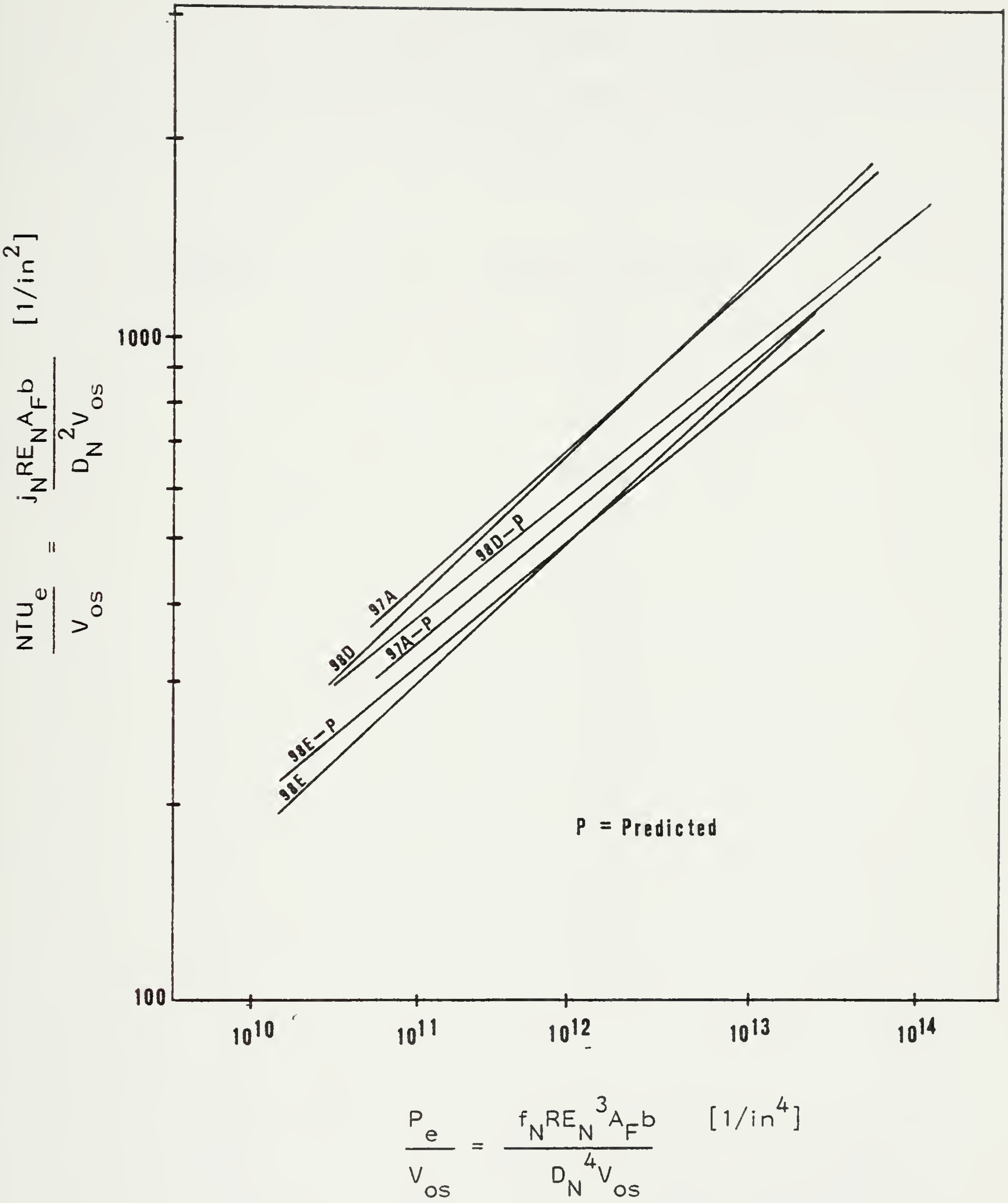

Figure 11. (Cont)

TABLE V

Deviation of performance parameter program of Figure A5 for volume one side in predicting experimentally obtained value as presented in Kays and London (2) and calculated by Baskerville (3).

Surface	Average Deviation
92	+23%
93	+86%
94	+51%
96	+24%
97A	+30%
97B	+20%
98A	+5%
98B	-6%
98C	-11%
98D	+25%
98E	-2%
99A	+24%
99B	+10%

deviation of 13.8%. This degree of accuracy should provide the correct indications in the parametric study of geometry effects on triangular pitch circular finned tubes presented in the next chapter.

VI. Geometry Effects on Triangular Pitch Circular Finned Tube Heat Exchangers in Crossflow.

A. General

A parametric study was conducted using the program of Figure A5 to determine the effect of varying tube pitch, diameter, and fin geometry on exchanger effectiveness. Copper fin material and dry air at 90° F on the enhanced surface side was assumed. Each surface was compared to a reference surface for the same pumping power and number of transfer units. This corresponds to Case C discussed in Chapter II. Therefore, the relative figure of merit for the surface in question is the ratio of the volume one side of the reference surface to the volume one side of the surface in question, $(V_{os})_{REF}/V_{os}$. With the volume of the reference surface in the numerator, this relative figure of merit can be thought of as the number of times larger (or smaller) the heat exchanger composed of the reference surface would have to be in order to have the same performance as the surface to which it is being compared. The reference surface is taken to be a bare tube surface with a one inch tube diameter and an equilateral triangular tube pitch of two. The reference surface is completely an arbitrary choice.

B. Effects of Tube Diameter and Tube Pitch

The performance parameters produced by the program of Figure A5 for smooth tubes (no enhancements) were used to study the effect of varying tube diameter and tube pitch. Table VI lists the values of $(V_{os})_{REF}/V_{os}$ which were generated for various values of tube diameter and tube pitch. These values are plotted on a log-log scale in Figure 12.

TABLE VI: $(V_{os})_{REF}/V_{os}$ for various values of tube diameter and tube pitch for smooth tubes. The reference surface is a smooth tube with a one inch tube diameter and equilateral triangular pitch of two.

A. $(V_{os})_{REF}/V_{os}$ for varied tube diameter and several tube pitches.

D_o (Inches)	$X_{ETP}=2$	$X_{ETP}=4$	$X_T=1.1$, $X_D=1.14$	$X_T=2.5$, $X_D=1.5$	$X_T=3.5$, $X_D=2.0$
.1	28.2	4.65	316	81.7*	31.0*
.3	5.74	.929	-	-	-
.5	2.74	.440	32.4	7.85*	2.99*
.75	1.52	.243	-	-	-
1.0	1.0	.159	12.02	2.86*	1.09*
2.0	.366	.0575	-	-	-
2.5	-	-	-	.755*	.288*
4.0	.134	.0208	-	-	-
5.0	-	-	-	.275*	.105*
10.0	.0354	.00545	-	-	-

B. Variation in equilateral triangular tube pitch.

X_{ETP}	$D_o=1''$	$D_o=.25$
1.1	14.5	106
1.3	4.83	35.6
1.5	2.61	19.3
2.0	1.0	7.48
3.0	.329	2.49
5.0	.0918	.705
10.0	.0172	.135

* Indicates minimum free flow area occurs in the diagonal ($2X_D < X_T+1$).

TABLE VI. (Cont)

C. Variation in diagonal tube pitch.

X_D	D_o=1", X_T=2	D_o=2.5", X_T=2	D_o=1", X_T=3	D_o=1", X_T=4	D_o=1", X_T=5
1.12	12.0*	91.2*	D.N.E.	D.N.E.	D.N.E.
1.3	6.21*	46.7*	D.N.E.	D.N.E.	D.N.E.
1.49	4.02*	30.1*	D.N.E.	D.N.E.	D.N.E.
1.51	2.08	15.4	D.N.E.	D.N.E.	D.N.E.
1.59	-	-	2.16*	D.N.E.	D.N.E.
1.75	1.36	10.2	1.64*	D.N.E.	D.N.E.
1.99	-	-	1.24*	D.N.E.	D.N.E.
2.0	1.0	7.48	-	D.N.E.	D.N.E.
2.07	-	-	-	1.00*	D.N.E.
2.25	-	-	-	.789*	D.N.E.
2.49	-	-	-	.643*	D.N.E.
2.55	-	-	-	-	.607*
2.75	-	-	-	-	.473*
2.99	-	-	-	-	.401*
3.0	.466	3.52	-	-	-
5.0	.207	1.59	-	-	-
10.0	.0746	.585	-	-	-

*Indicates minimum free flow area occurs in the diagonal ($2X_D < X_T + 1$)

D.N.E. = Does Not Exist; indicates geometry not possible for the indicated values of tube pitch.

TABLE VI. (Cont)

D. Variation in transverse tube pitch.

X_T	D_o=1", X_D=2	D_o=1", X_D=3
1.1	2.34	1.11
1.5	1.36	.653
2.0	1.0	.466
2.5	.883	.377
2.99	.914	.329
3.0	-	-
3.01	1.22*	-
3.5	1.09*	.305
3.87	1.11*	-
4.99	-	.364
5.01	-	.398*
5.5	-	.385*
5.91	-	.417*

* Indicates minimum free flow area occurs in the diagonal ($2X_D < X_T + 1$)

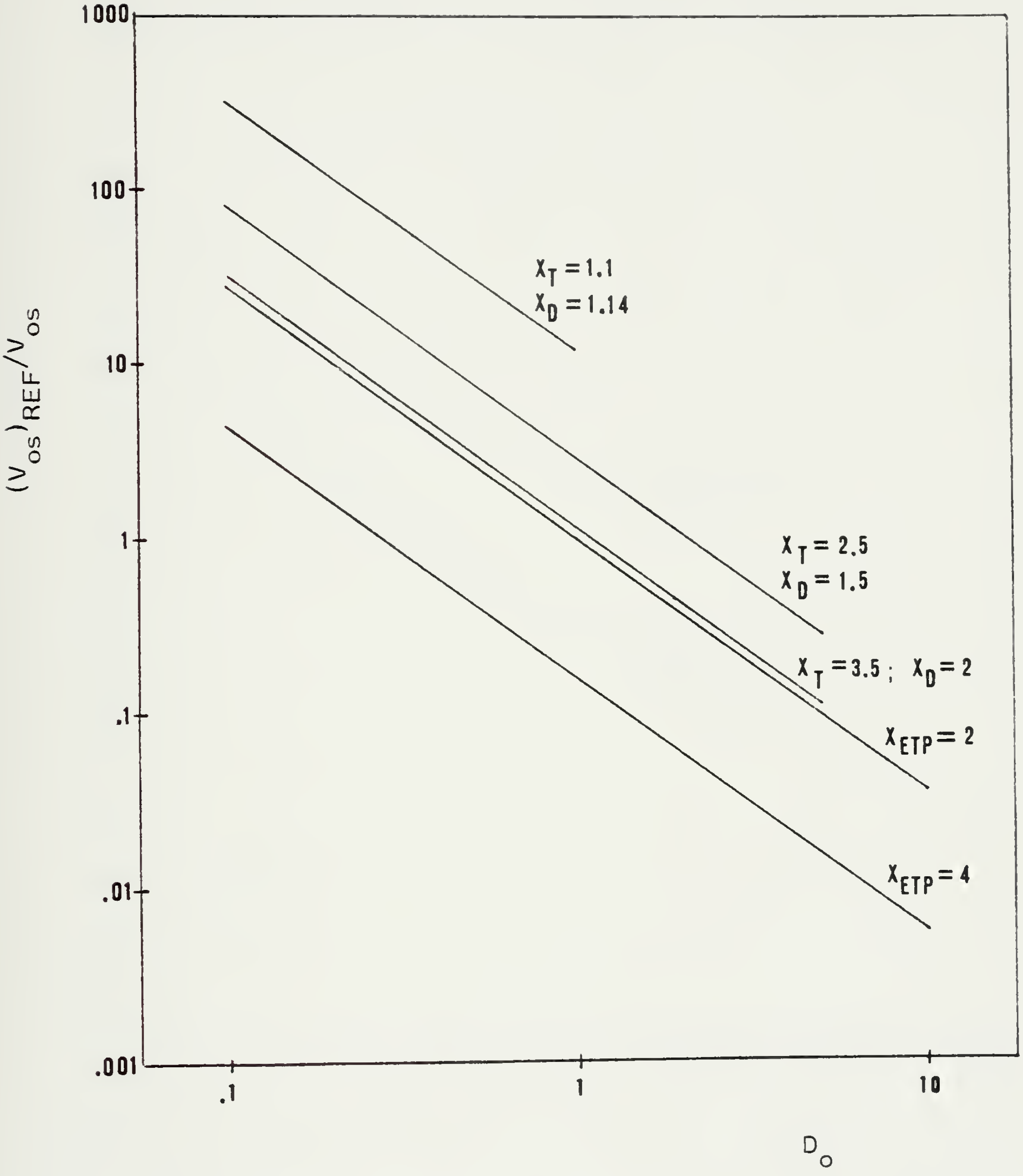

Figure 12A. $(V_{os})_{REF}/V_{os}$ versus D_o for several values of tube pitch for a bare tube surface.

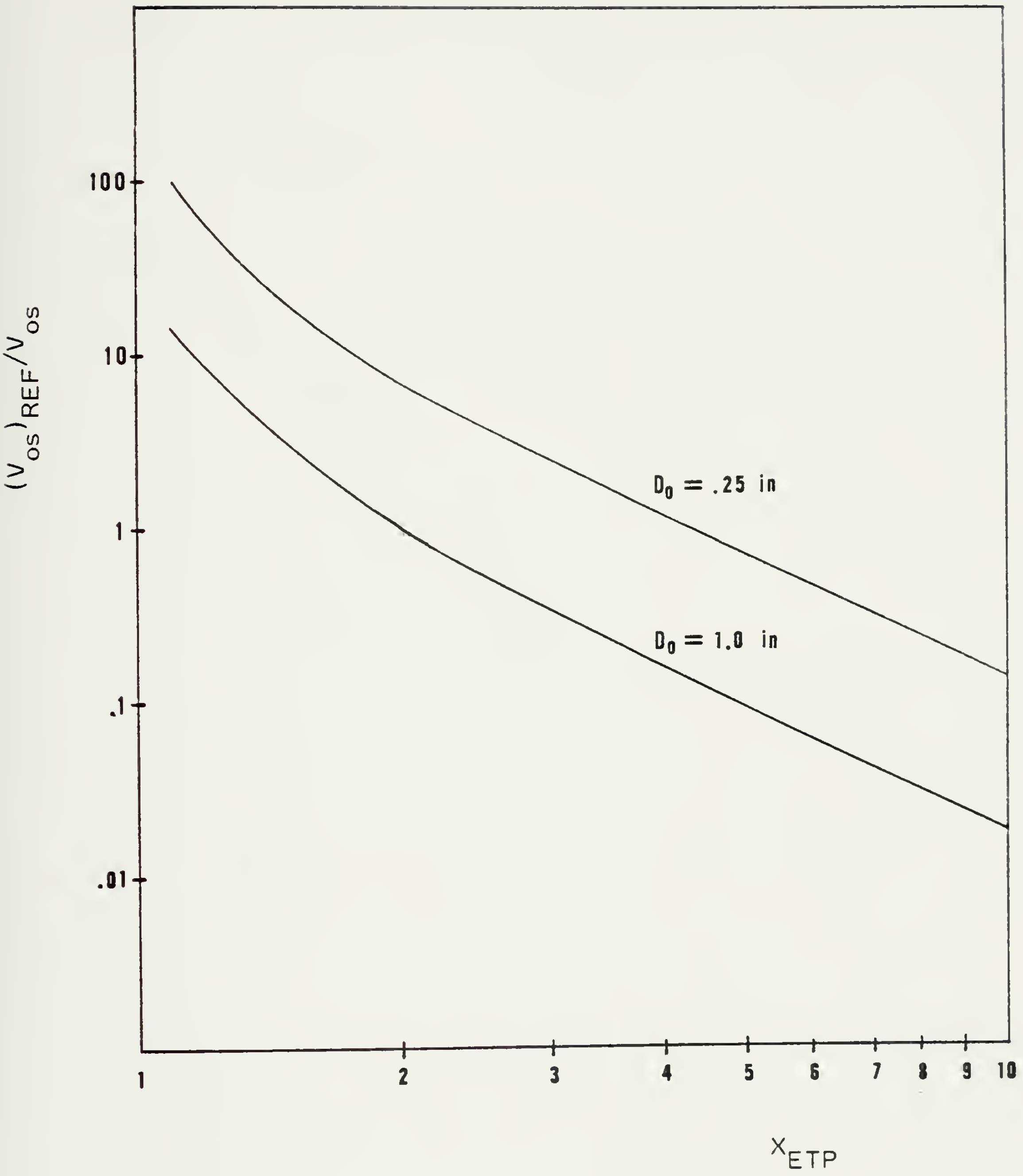

Figure 12B. $(V_{os})_{REF}/V_{os}$ versus X_{ETP} for two values of tube diameter for a bare tube surface.

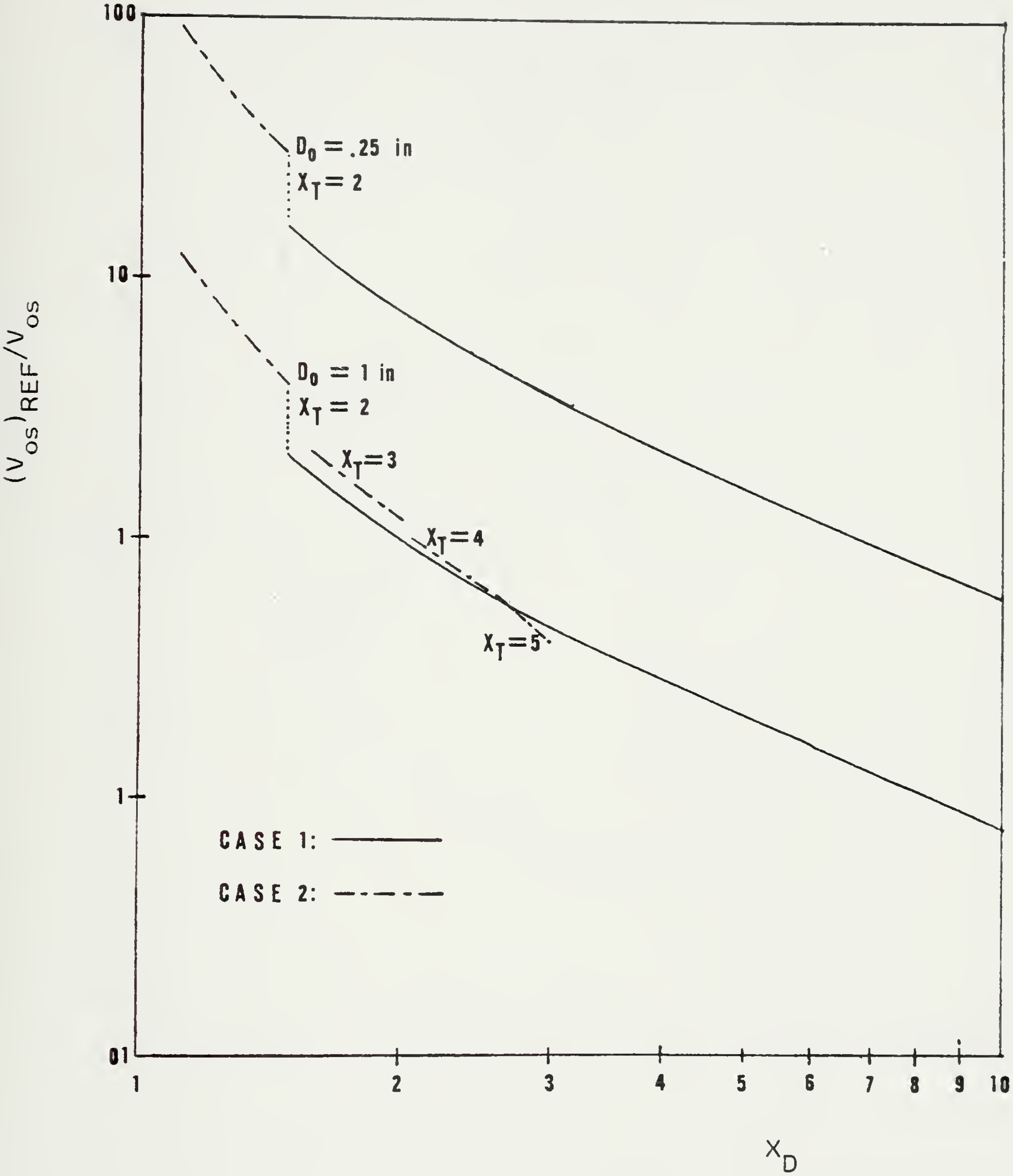

Figure 12C. $(V_{os})_{REF}/V_{os}$ versus X_D for a bare tube surface for several values of tube diameter and transverse tube pitch.

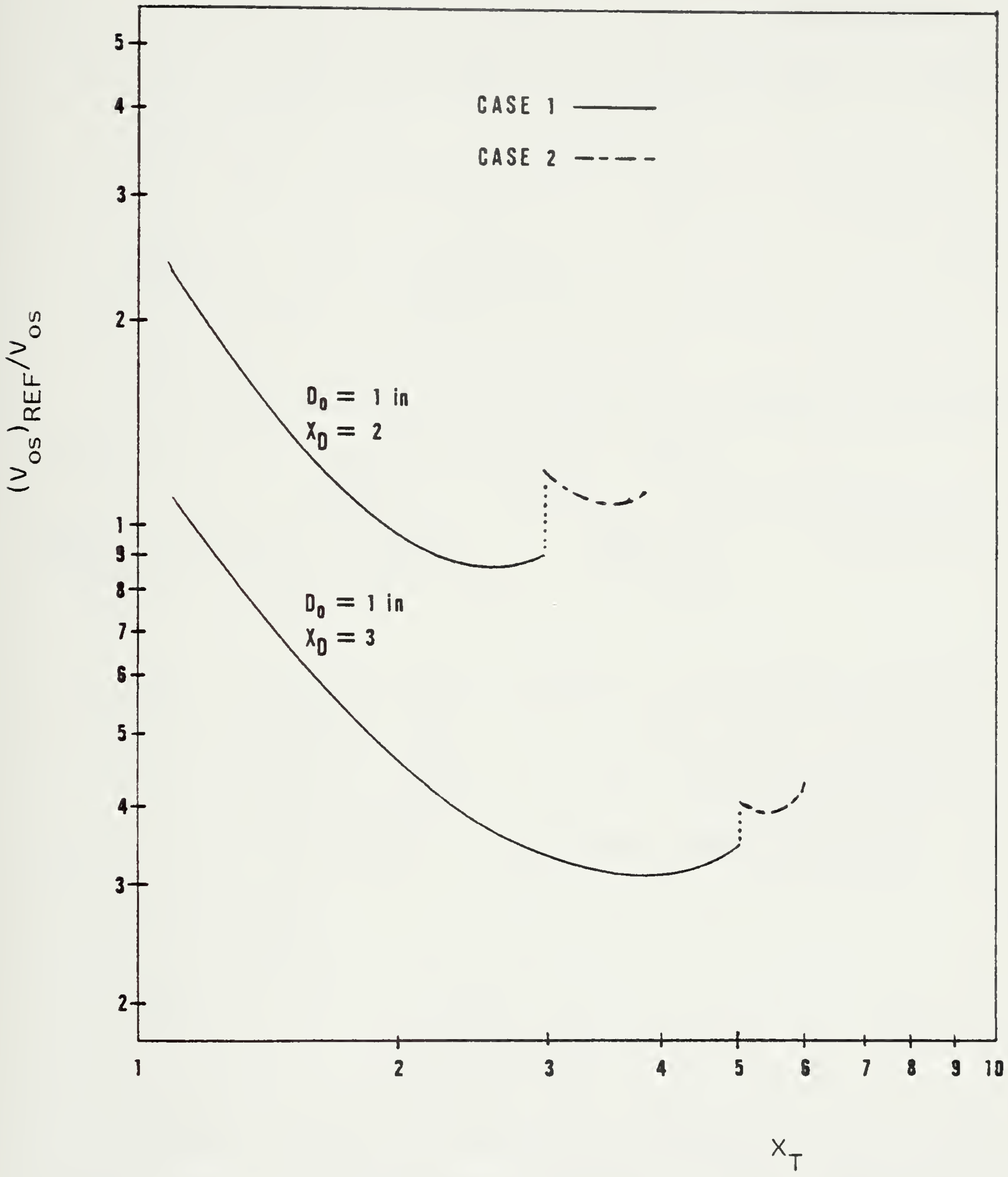

Figure 12D. $(V_{os})_{REF}/V_{os}$ versus X_T for a bare tube surface for two values of diagonal tube pitch.

Table VI and Figure 12 show the tube diameter and the tube pitch for Case I, minimum free flow area in the transverse space, to be approximately proportional to exchanger volume as follows:

$$V_{OS} \propto D_o^{1.45} \tag{34}$$

$$V_{OS} \propto X_T^{.85} \quad , \quad 1.5 \leq X_T \leq 3.0 \tag{35}$$

$$V_{OS} \propto X_D^{2.15} \quad , \quad 1.5 \leq X_D \leq 3.0 \tag{36}$$

$$V_{OS} \propto X_{ETP}^{3.0} \quad , \quad 1.5 \leq X_{ETP} \leq 3.0 \tag{37}$$

This leads to the following relation for Case I, minimum free flow area in the transverse space $(X_T \quad 2X_D-1)$

$$\frac{V_{OS}}{(V_{OS})_{REF}} \cong \left[\frac{X_T}{(X_T)_{REF}}\right]^{.85} \left[\frac{X_D}{(X_D)_{REF}}\right]^{2.15} \left[\frac{D_o}{(D_o)_{REF}}\right]^{1.45} , \quad 1.5 \leq X \leq 3.0 \tag{38}$$

Case II, minimum free flow area in the diagonal $(2D_D \leq X_T+1)$, is not as well defined. Again Table VI and Figure 12 show for Case II that the tube diameter and the diagonal tube pitch is approximately proportional to exchanger volume as follows:

$$V_{OS} \propto D_O^{1.45} \tag{39}$$

$$V_{OS} \propto X_D^{3.85} \qquad 1.1 < X_D < 1.5 \tag{40}$$

$$V_{OS} \propto X_D^{2.5} \qquad 1.5 < X_D < 3.0 \tag{41}$$

However, Figure 12 shows that exchanger volume even on a log-log scale is a non-linear function of the transverse pitch. Therefore, variation in volume versus transverse tube pitch on a log-log scale does not lend to a linear approximation even for a very limited range. However, since the change in volume is small over the possible range of transverse pitch to a first approximation

volume can be estimated to be independent of transverse tube pitch for Case II. This leads to the following approximations for Case II:

$$\frac{V_{os}}{(V_{os})_{REF}} \cong \left[\frac{X_D}{(X_D)_{REF}}\right]^{3.85} \left[\frac{D_o}{(D_o)_{REF}}\right]^{1.45}, \quad 1.1 < X_D < 1.5 \qquad (42)$$

$$\frac{V_{os}}{(V_{os})_{REF}} \cong \left[\frac{X_D}{(X_D)_{REF}}\right]^{2.5} \left[\frac{D_o}{(D_o)_{REF}}\right]^{1.45}, \quad 1.5 < X_D \leq 3.0 \qquad (43)$$

It should be recalled that Case II occurs when $2X_D < X_T+1$, but that $2X_D < X_T$ is a geometric impossibility. As the latter limit is approached the tube bank approaches an in-line tube bank. Since X_L must be at least ½ tube diameter, this further restricts the range for Case II. Since:

$$X_T^2/4 + X_L^2 = X_D^2, \qquad (44)$$

Case II is restricted to the following range:

$$(X_T^2 + 1)^{\frac{1}{2}} < 2X_D < X_T + 1 \qquad (45)$$

This range of possible values is less than a half tube diameter. Due to this limited range of geometries in which Case II may occur, the minimum free flow area usually occurs in the transverse space for most triangular pitch tube banks.

Finally, a note should be made concerning the discontinuity apparent in Figures 12C and 12D for the transition between Case I and Case II. The curves for each Case are produced by a separate set of correlations for heat transfer and pressure drop. Therefore, unless both correlations are exactly correct, a perfect match would not be expected. The amount of mismatch is in a sense a measure of the total error of the four correlations taken as a group at the point of transition between Case I and Case II.

C. Effects of Fin Geometry

The performance parameters produced by the program of Figure A5 for an enhanced surface with circular fins and equilateral triangular pitch were used to study the effects of varying fin geometry. Table VII lists the values of $(V_{os})_{REF}/V_{os}$ generated for various values of fin thickness, fin height, and fin spacing for two tube diameters (.4 inch and 1.0 inch) and two values of equilateral triangular pitch ($X_{ETP} = 2$ and $X_{ETP} = 3$). These values are plotted in Figure 13. Again, $(V_{os})_{REF}$ is taken to be a smooth tube with a one inch diameter and an equilateral triangular pitch of two. Fin spacing is given in terms of fin thickness (S_{BF}/t_f). The greater the value of $(V_{os})_{REF}/V_{os}$, the smaller is the V_{os} of the surface in question for a given number of transfer units and pumping power.

Figures 13A, 13C, 13E, and 13G show the effect of varying fin spacing with all other parameters held constant for several values of fin thicknesses. The fin height is taken to be the maximum possible value, $(H_f)_{MAX} = \frac{1}{2}(X_{ETP} - 1)$. An optional value of fin spacing, i.e., a maximum value of $(V_{os})_{REF}/V_{os}$ and, therefore, a minimum value of V_{os} for the surface in question, occurs for each case. This optional value of fin spacing ranges from .8 to 1.2 fin thicknesses. The higher values of optional fin spacing in terms of fin thicknesses corresponds to the thinner fins.

Figures 13A, 13C, 13E, and 13G show for a given fin spacing in terms of fin thicknesses the surface performance is better for thin fins than for thick fins. This is not necessarily true if fin spacing is not expressed in terms of fin thicknesses. Figure 13I

plots $(V_{os})_{REF}/V_{os}$ versus fin thickness (t_f) for two constant values of fin spacing (S_{BF}). Again optimal values are found but here thicker fins are seen to produce a surface with better performance if the fin thickness is less than the optimal fin thickness. Figure 13J plots $(V_{os})_{REF}/V_{os}$ versus F_{in} for two values of fin thickness. Again it can be seen that for low values of F_{in} the thicker fin produces the better performing surface.

The information plotted in Figures 13A, 13C, 13E, and 13G can be displayed in the form of Figure 13J, since the number of fins per inch is given by:

$$F_{in} = \frac{1}{(S_{BF}+t_f)D_o} = \frac{1}{(S_{BF}/t_f+1)t_f D_o} \tag{46}$$

There may also be other possible forms of displaying the same information.

Figures 13B, 13D, 13F, and 13H show the effect of varying fin height from the maximum possible value for values of fin spacing which were found to be optimal in Figures 13A, 13C, 13E, and 13G, respectively. An optimal value of fin height occurs ranging from 40% to 90% of the maximum possible fin height. For thinner fins the optimal value of fin height occurs at lower fin heights and is more pronounced for thinner fins.

For some optimal values displayed in Figure 13, the optimal regions are quite flat. This suggests that in the actual design of a surface great savings of fin material might be made by only slightly compromising surface performances.

TABLE VII. $(V_{os})_{REF}/V_{os}$ for various values of fin thickness, fin height, and fin spacing for two tube diameters (.4 inch and 1.0 inch) and two values of equilateral triangular pitch (X_{ETP} = 2 and X_{ETP} = 3). $(V_{os})_{REF}$ is a bare tube with a one inch tube diameter and equilateral triangular pitch of two.

A. $(V_{os})_{REF}/V_{os}$ versus fin spacing for four fin thicknesses (t_f = .005, .01, .02, .04) for an enhanced tube surface with D_o = 1", X_{ETP} = 2, and $H_f = (H_f)_{MAX}$ = .5.

	$(V_{os})_{REF}/V_{os}$ for:			
S_{BF}/t_f	t_f=.005	t_f=.01	t_f=.02	t_f=.04
.3	22.7	17.3	13.2	9.60
.4	24.6	18.5	14.1	10.19
.6	26.3	19.9	15.0	10.72
.8	26.8	20.5	15.3	10.84*
.9	27.0	20.6	15.3*	10.80
1.0	27.2*	20.7*	15.2	10.72
1.25	27.0	20.5	14.9	10.38
1.5	26.9	20.0	14.6	10.07
2.0	26.0	19.0	13.7	9.29
2.5	24.2	18.0	12.6	8.67
3.0	22.6	16.8	11.8	8.11
3.5	21.2	15.9	11.2	7.60

*Indicates Maximum Value.

TABLE VII. (Cont)

B. $(V_{os})_{REF}/V_{os}$ versus fin height for four fin thicknesses (t_f= .005, .01, .02, .04) for an enhanced tube surface with D_o = 1" and X_{ETP} = 2 and with fin spacing at the optimal value for $H_f = (H_f)_{MAX}$ = .5

$(V_{os})_{REF}/V_{os}$ for:

H_f	S_{BF}/t_f=1.0 t_f=.005	S_{BF}/t_f=1.0 t_f=.01	S_{BF}/t_f=.9 t_f=.02	S_{BF}/t_f=.8 t_f=.04
.50	27.2	20.7	15.2	10.84
.45	28.7	21.8	15.8	11.10*
.40	30.4	22.4	16.2	11.08
.35	31.7	22.9*	16.3*	10.76
.30	32.7	22.9	15.8	-
.25	32.9*	-	14.8	9.03
.20	32.0	19.9	-	-
.15	29.1	-	10.5	-
.10	23.2	12.5	-	4.23
.05	13.3	-	-	-

*Indicates maximum value.

TABLE VII. (Cont)

C. $(V_{os})_{REF}/V_{os}$ versus fin spacing for three fin thicknesses (t_f = .01, .02, .04) for an enhanced tube surface with D_o = .4", X_{ETP} = 2, and $H_f = (H_f)_{MAX}$ = .5.

	$(V_{os})_{REF}/V_{os}$ for:		
$S_{Bf}t_F$	t_f = 0.1	t_f = 0.2	t_f = 0.4
.4	35.9	27.0	20.1
.8	41.0	30.6	22.4
.95	-	-	22.4*
1.0	41.7	30.9*	-
1.15	41.8*	-	-
1.2	41.8	30.9	22.2
1.6	41.1	30.1	21.2
2.0	40.0	29.0	20.2
3.0	36.6	26.0	17.6
4.5	32.0	22.2	15.2

*Indicates maximum value.

TABLE VII. (Cont)

D. $(V_{os})_{REF}/V_{os}$ versus fin height for three fin thicknesses (t_f = .01, .02, .04) an enhanced tube surface with D_o = .4" and X_{ETP} = 2 and with fin spacing at the optimal value for H_f = $(H_f)_{MAX}$ = .5.

	$(V_{os})_{REF}/V_{os}$ for:		
	$S_{BF}t_f$=1.15	S_{BF}/t_f=1.05	S_{BF}/t_f=.95
H_f	t_f=.01	t_f=.02	t_f=.04
.50	41.8	30.9	22.4
.45	45.1	33.1	23.7
.40	48.4	35.1	24.7
.35	51.4	36.6	25.1*
.30	53.8	37.4*	24.8
.25	55.1*	36.9	23.6
.20	54.3	34.7	21.2
.15	49.8	30.1	17.7
.10	39.7	22.7	13.3

*Indicates maximum value.

TABLE VII. (Cont)

E. $(V_{os})_{REF}/V_{os}$ versus fin spacing for four fin thicknesses (t_f = .005, .01, .02, .04) for an enhanced tube surface with D_o = 1", X_{ETP} = 3 and $H_f = (H_f)_{MAX}$ = 1.0.

	$(V_{os})_{REF}/V_{os}$ for:			
S_{BF}/t_f	t_f = .005	t_f = .01	t_f = .02	t_f = .04
.40	14.75	11.71	9.11	6.92
.60	15.66	12.51	9.74	7.32
.775	-	-	-	7.38*
.80	15.88	12.75	9.90	-
.825	15.88*	12.75*	9.90*	-
.85	15.88	12.75	-	-
1.0	15.77	12.70	9.84	7.26
1.2	15.48	12.50	9.67	7.07
1.6	14.70	11.92	9.17	6.77
2.0	13.83	11.26	8.63	6.44
2.5	12.80	10.46	7.99	6.02
3.5	11.03	9.06	7.06	5.30
4.5	9.63	7.96	6.30	4.75

*Indicates maximum values.

TABLE VI. (Cont)

F. $(V_{os})_{REF}/V_{os}$ versus fin height for four fin thicknesses (t_f = .005, .01, .02, .04) for an enhanced tube surface with D_o = 1", X_{ETP} = 3 and with fin spacing at the optimal value for $H_f = (H_f)_{MAX} = 1.0$.

$(V_{os})_{REF}/V_{os}$ for:

H_f	S_{BF}/t_f=.825 t_f=.005	S_{BF}/t_f=.825 t_f=.01	S_{BF}/t_f=.825 t_f=.02	S_{BF}/t_f=.775 t_f=.04
1.0	15.88	12.75	9.90	7.38
.9	17.46	-	-	-
.85	-	-	-	7.86
.80	19.09	14.99	11.21	7.93
.775	-	-	-	7.94*
.75	-	-	-	7.94
.70	20.77	-	-	7.91
.65	-	-	11.66	-
.625	-	-	11.67*	-
.60	22.39	16.74	11.64	7.51
.55	-	16.96	11.48	-
.50	23.75	17.03*	-	-
.45	24.21	16.89	-	-
.42	24.36	-	-	-
.40	24.41*	16.48	10.04	5.70
.35	24.24	-	-	-
.30	23.52	-	-	-
.20	19.57	9.69	5.50	2.85

*Indicates maximum value.

TABLE VII. (Cont)

G. $(V_{os})_{REF}/V_{os}$ versus fin spacing for three fin thicknesses (t_f = .01, .02, .04) for an enhanced tube surface with D_o = .4", X_{ETP} = 3, and $(H_f)_{MAX}$ = 1.0.

$(V_{os})_{REF}/V_{os}$ for:

S_{BF}/t_f	t_f=0.1	t_f=.02	t_f=.04
.4	20.87	15.87	11.97
.8	23.67	17.97	13.39
.95	-	-	13.47*
1.0	23.98	18.17	13.46
1.07	-	18.18*	-
1.1	24.02*	-	-
1.2	23.98	18.14	13.35
1.6	23.51	17.71	12.88
2.0	22.77	17.07	12.28
3.0	20.71	15.35	10.78
4.5	17.99	13.14	9.43

*Indicates maximum value.

TABLE VII. (Cont)

H. $(V_{os})_{REF}/V_{os}$ versus fin height for three fin thicknesses (t_f = .01, .02, .04) for an enhanced tube surface with D_o = .4", X_{ETP} = 3, and with fin spacing at the optimal value for H_f = $(H_f)_{MAX}$ = 1.0.

	$(V_{os})_{REF}/V_{os}$ for:		
H_f	S_{BF}/t_f=1.1 t_f=.01	S_{BF}/t_f=1.07 t_f=.02	S_{BF}/t_f=.95 t_f=.04
1.0	24.02	18.18	13.47
.9	26.30	19.77	14.50
.8	28.74	21.31	15.37
.7	31.23	22.71	15.98
.6	33.66	23.77	16.13*
.5	35.68	24.13*	15.57
.4	36.57*	23.22	14.08
.3	34.87	20.33	11.54
.2	28.41	15.04	8.18

*Indicates maximum value.

TABLE VII. (Cont)

I. $(V_{os})_{REF}/V_{os}$ versus fin thickness for two values of fin spacing (S_{BF} = .04, .10) for an enhanced tube surface with D_o = 1", X_{ETP} = 2, and $H_f = (H_f)_{MAX}$ = .5.

	$(V_{os})_{REF}/V_{os}$ for:	
t_F	S_{BF} = .04	S_{BF} = .10
.005	14.13	7.96
.01	14.74*	9.15
.02	13.42	9.38*
.04	10.67	8.67
.06	8.80	7.89
.08	7.50	7.21
.10	6.56	6.65
.20	4.13	4.88
.40	2.52	3.39

TABLE VII. (Cont)

J. $(V_{os})_{REF}/V_{os}$ versus fins per inch for two values of fin thicknesses (t_F = .01, .02) for an enhanced tube surface with D_o = 1", X_{ETP} = 2, and $H_f = (H_f)_{MAX}$ = .5.

$(V_{os})_{REF}/V_{os}$ for:

F_{in}	t_f=.01	t_f=.02
2.4	4.25	4.98
4.55	-	6.71
6.25	7.11	-
8.33	-	9.79
11.8	10.89	-
13.3	-	12.30
16.7	13.24	13.65
20.0	14.79	14.62
25.0	16.79	15.21
28.6	17.99	15.31*
33.3	18.97	14.62
40.0	19.95	12.02
45.5	20.65	-
47.6	20.90*	-
50.0	20.65	-
66.7	19.28	-
80.0	15.85	-

*Indicates maximum value.

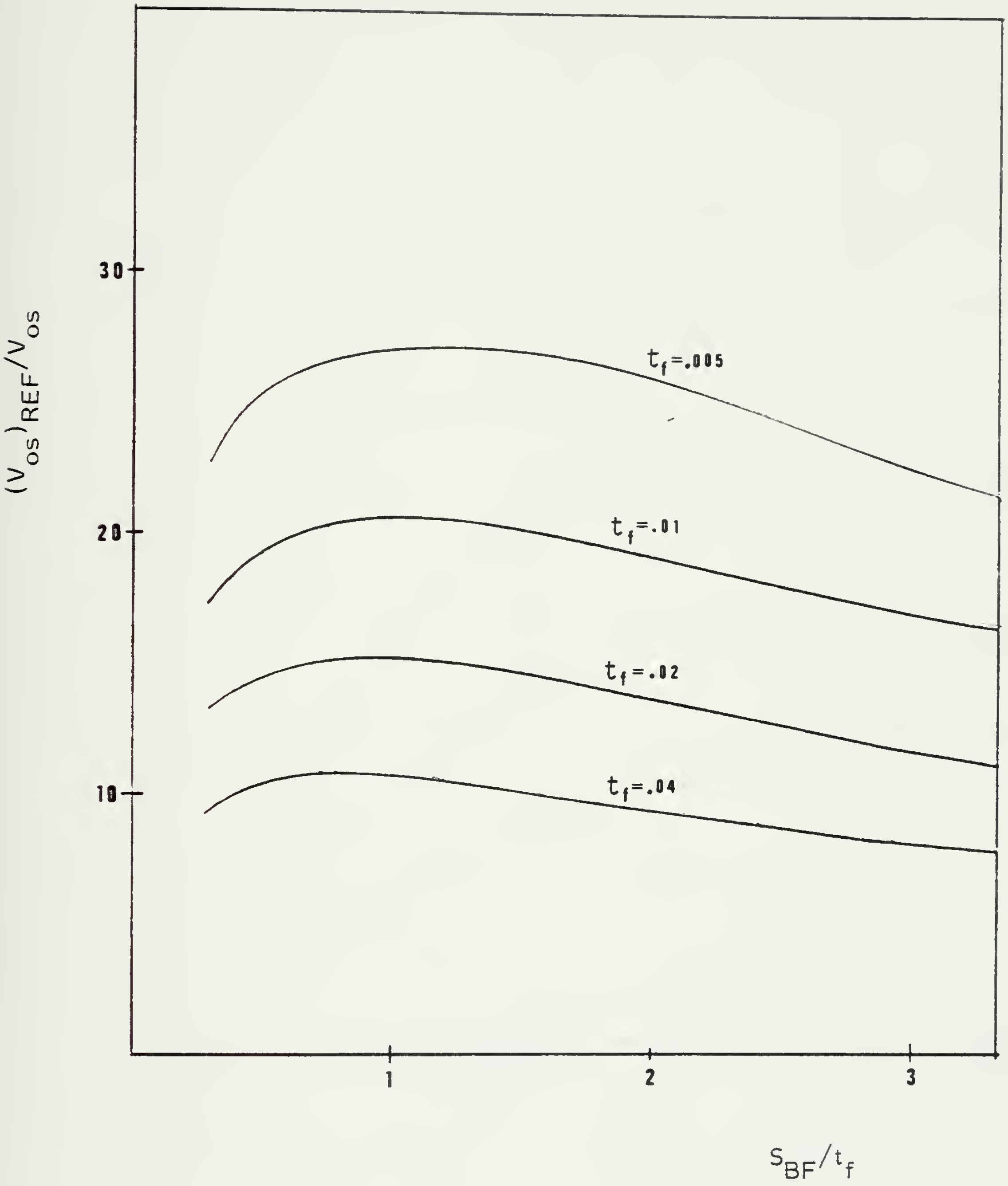

Figure 13A. $(V_{os})_{REF}/V_{os}$ versus fin spacing for four fin thicknesses (t_f = .005, .01, .02, .04) for an enhanced tube surface with D_o = 1", X_{ETP} = 2, and $H_f = (H_f)_{MAX}$ = .5

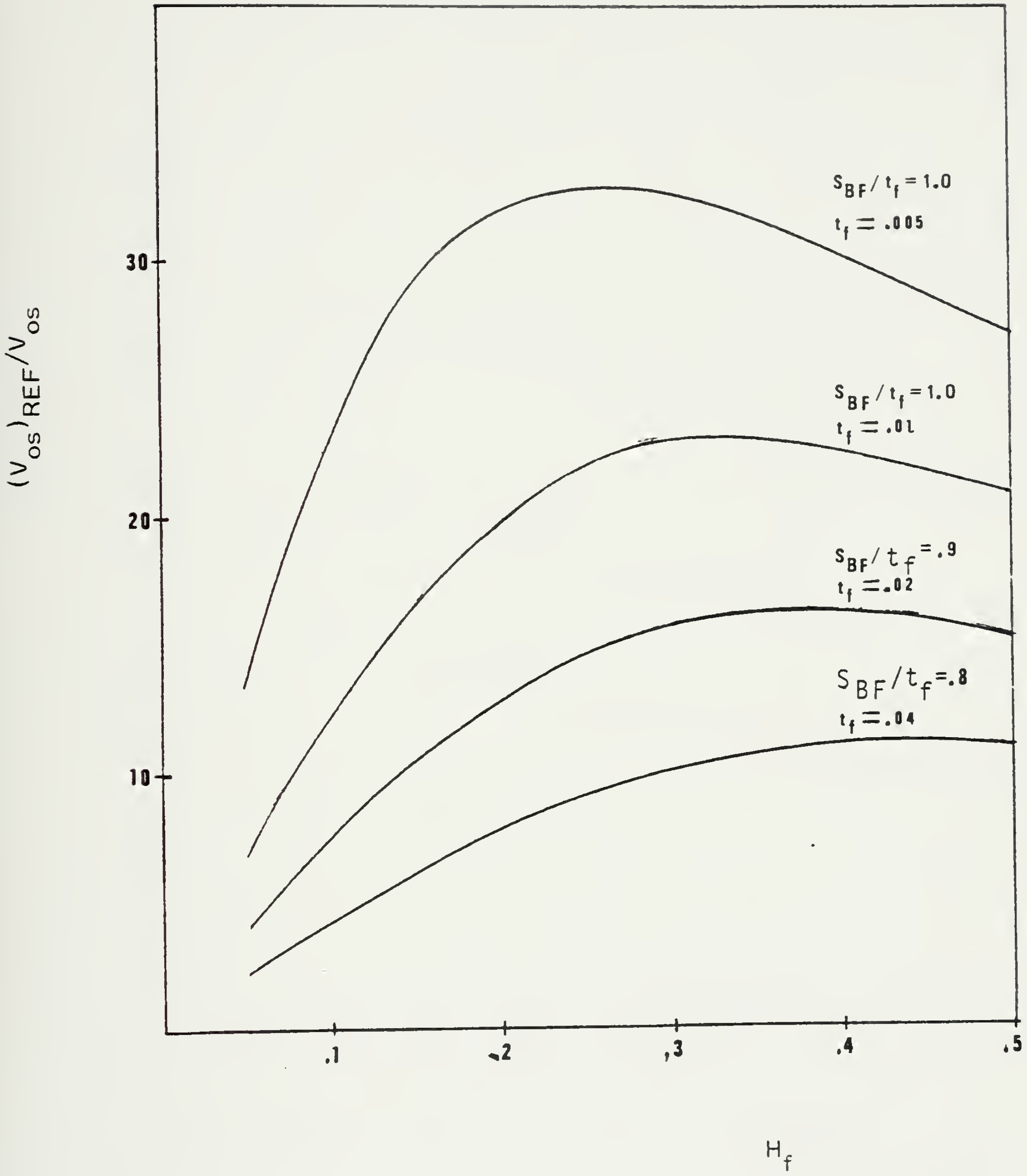

Figure 13B. $(V_{os})_{REF}/V_{os}$ versus fin height for four fin thicknesses (t_f = .005, .01, .02, .04) for an enhanced tube surface with D_o = 1" and X_{ETP} = 2 and with fin spacing at the optimal value found in Figure 13A for $H_f=(H_f)_{MAX}=.5$

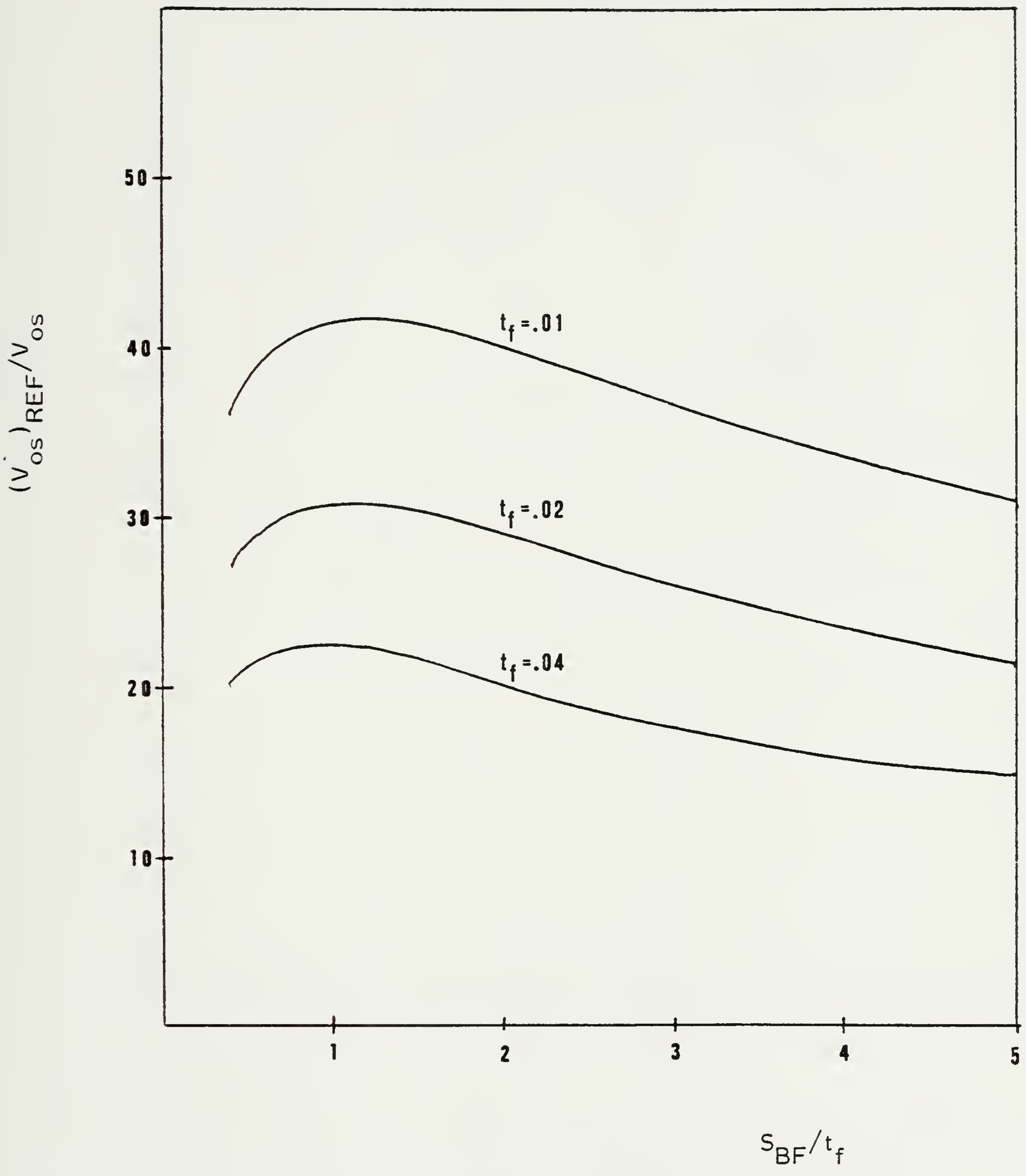

Figure 13C. $(V_{os})/_{REF}/V_{os}$ versus fin spacing for three fin thicknesses (t_f = .01, .02, .04) for an enhanced tube surface with D_o = .4", X_{ETP} = 2, and H_f=$(H_f)_{MAX}$=.5

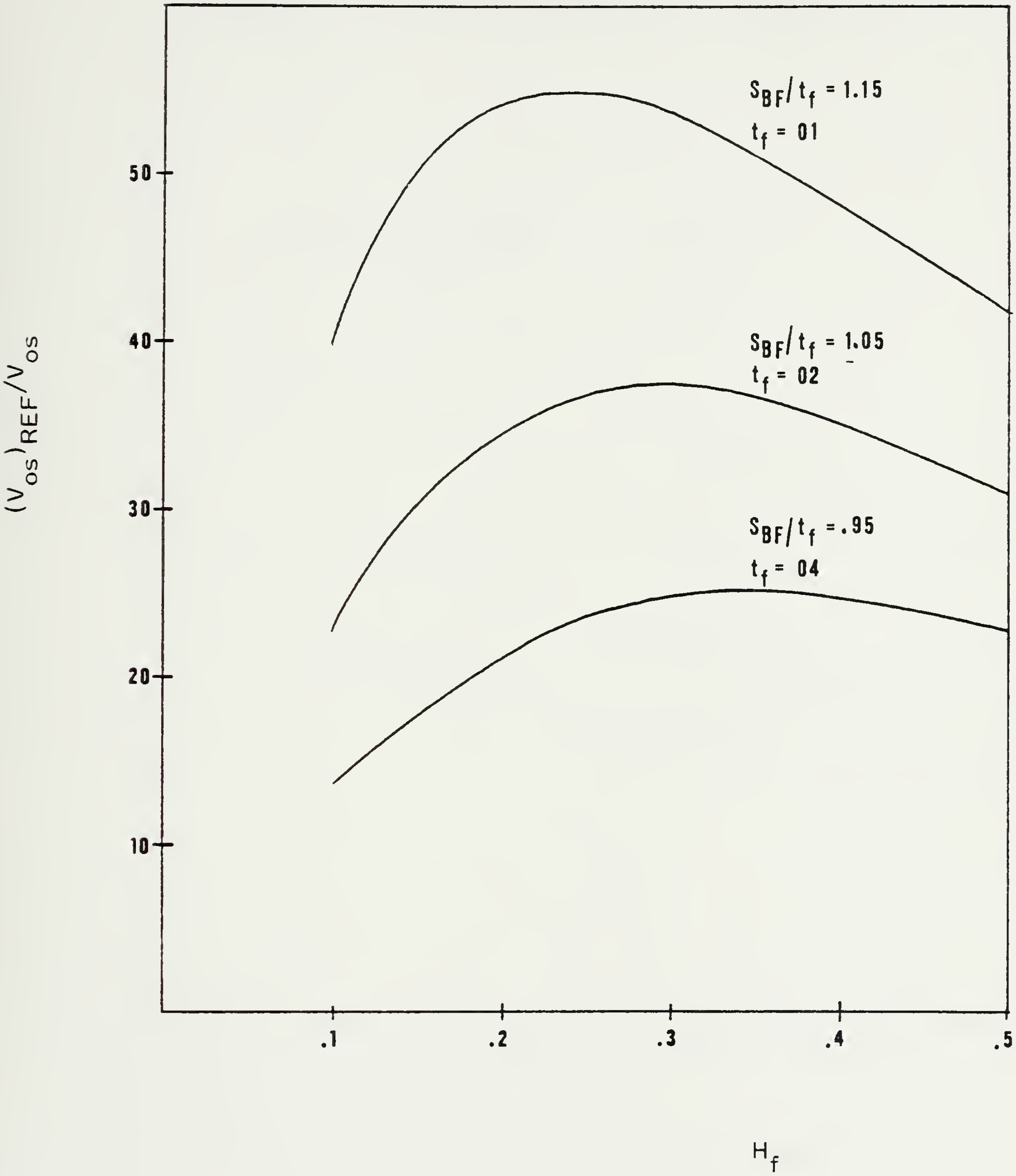

Figure 13D. $(V_{os})_{REF}/V_{os}$ versus fin height for three fin thicknesses (t_f = .01, .02, .04) for an enhanced tube surface with D_o = .4" and X_{ETP} = 2 and with fin spacing at the optimal value found in Figure 13C for $H_f=(H_f)_{MAX}=.5$

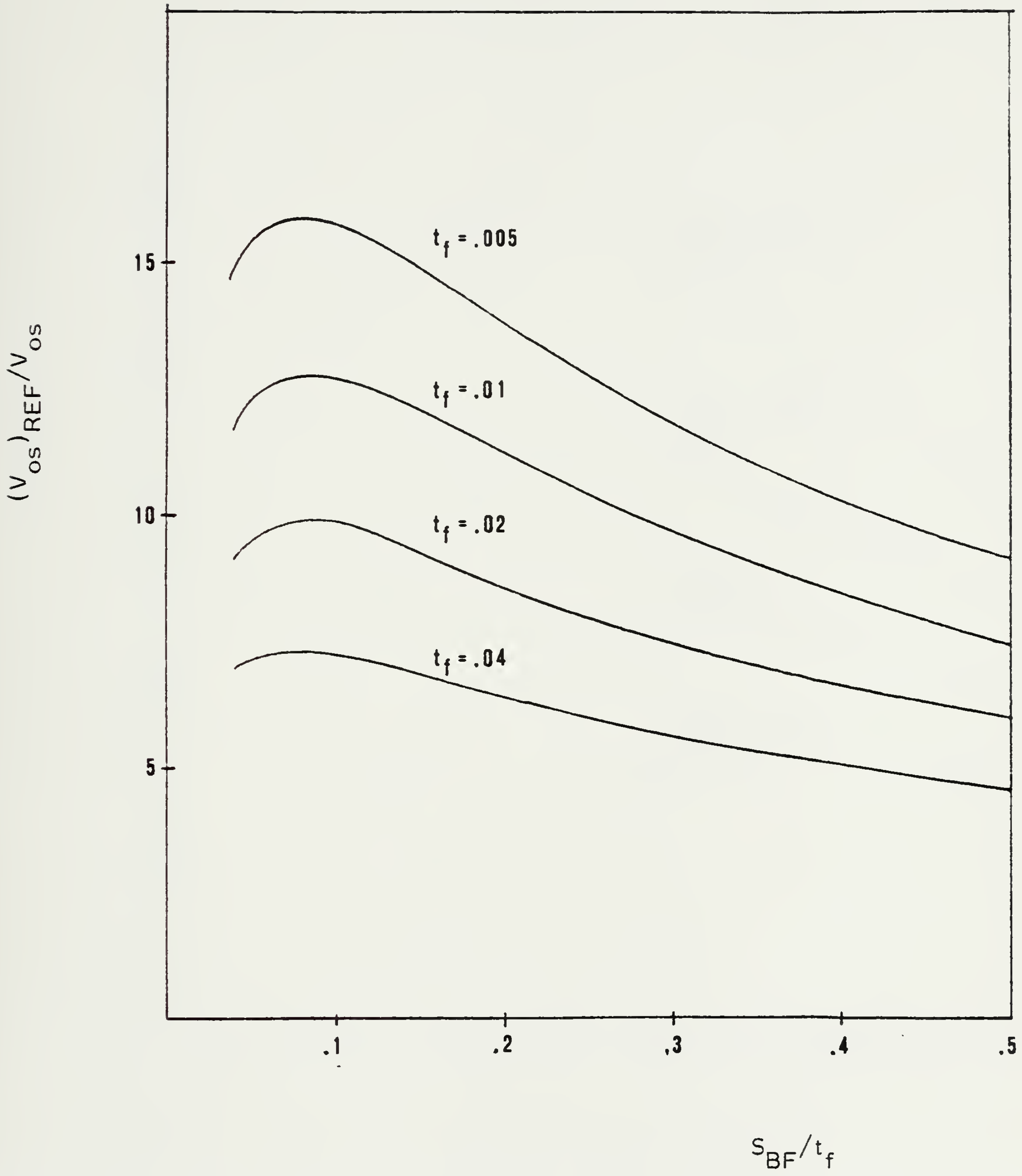

Figure: 13E. $(V_{os})_{REF}/V_{os}$ versus fin spacing for four fin thicknesses (t_f = .005, .01, .02, .04) for an enhanced tube surface with D_o = 1", X_{ETP} = 3, $H_f = (H_f)_{MAX}$ = 1.0

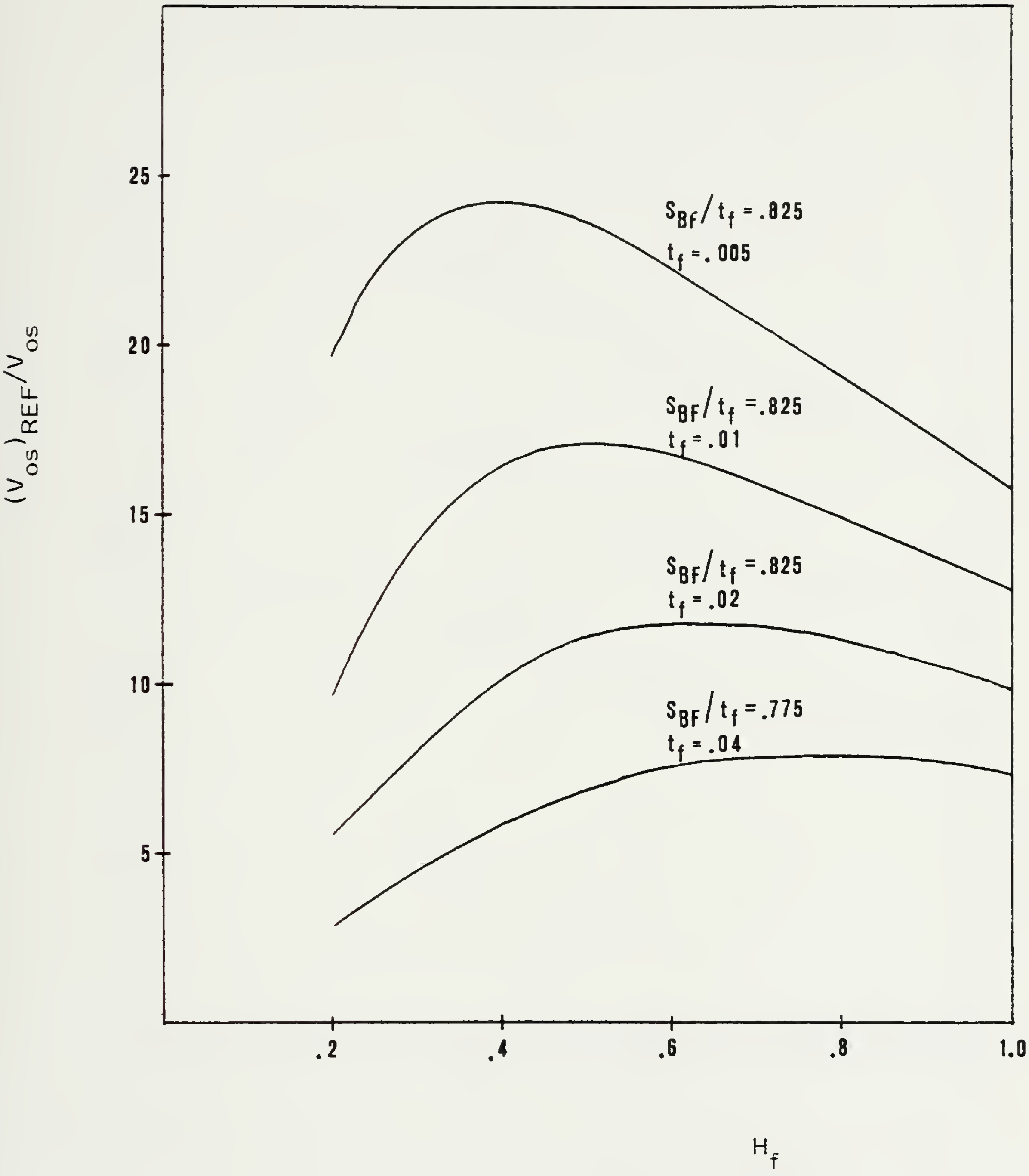

Figure 13F. $(V_{os})_{REF}/V_{os}$ versus fin height for four fin thicknesses (t_f = .005, .01, .02, .04) for an enhanced tube surface with D_o = 1", X_{ETP} = 3 and with fin spacing at the optimal value found in Figure 13E for $H_f=(H_f)_{MAX}=1.0$

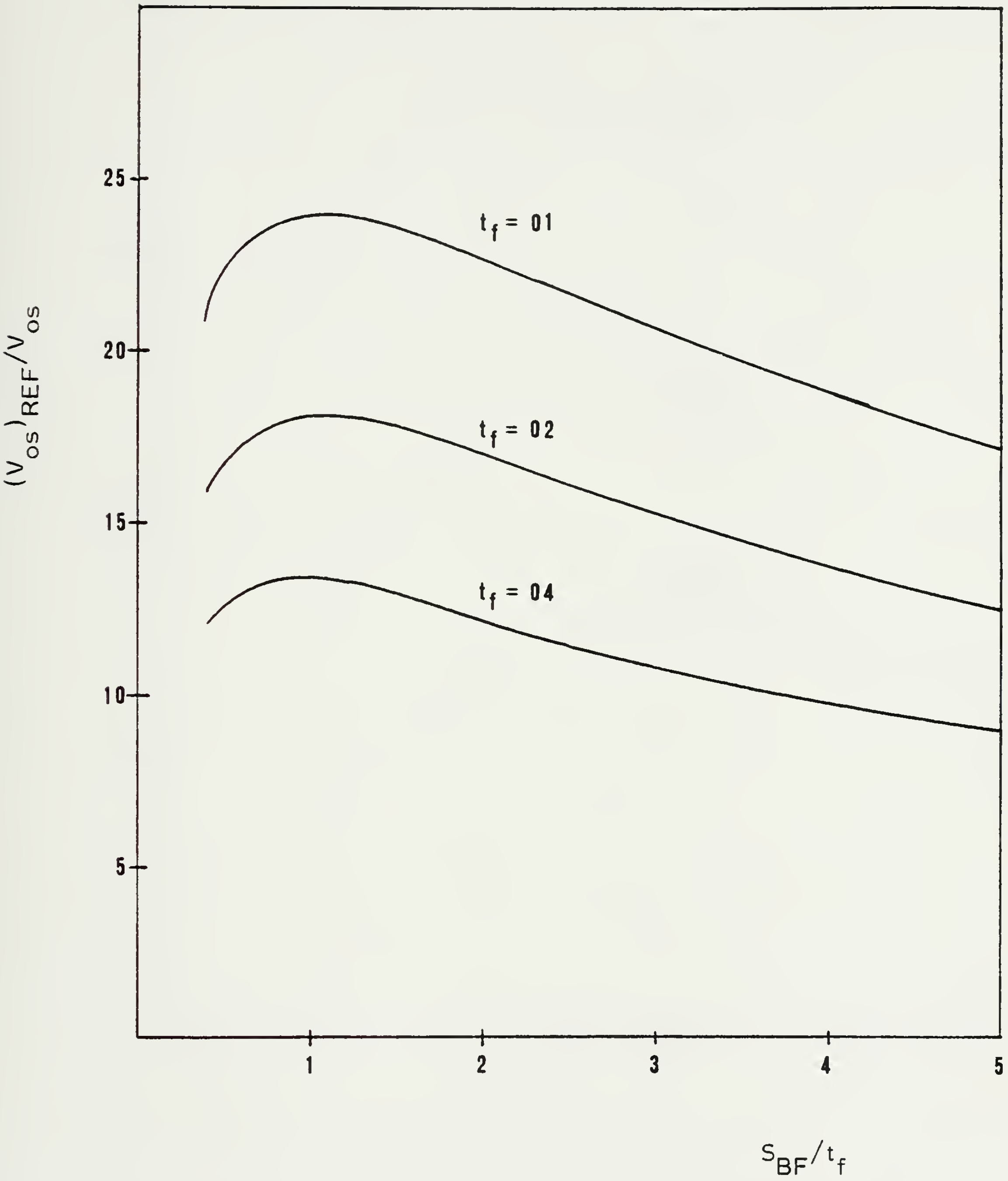

Figure 13G. $(V_{os})_{REF}/V_{os}$ versus fin spacing for three fin thicknesses (t_f = .01, .02, .04) for an enhanced tube surface with D_o = .4", X_{ETP} = 3, and $H_f=(H_f)_{MAX}=1.0$

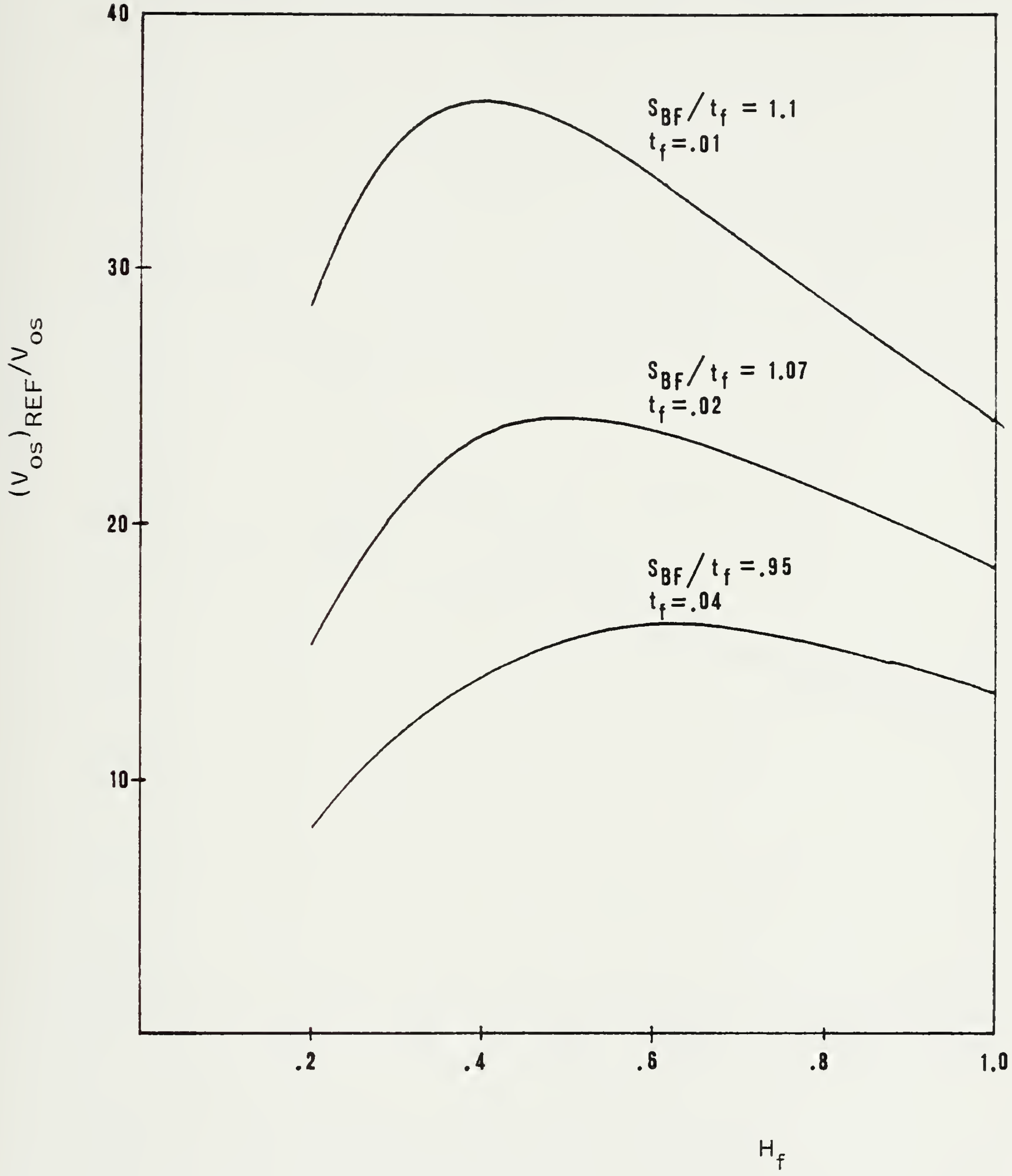

Figure 13H. $(V_{os})_{REF}/V_{os}$ versus fin height for three fin thicknesses (t_f = .01, .02, .04) for an enhanced tube surface with D_o = .4", X_{ETP} = 3, and with fin spacing at the optimal value found in Figure 13G for H_f = $(H_f)_{MAX}$ = 1.0

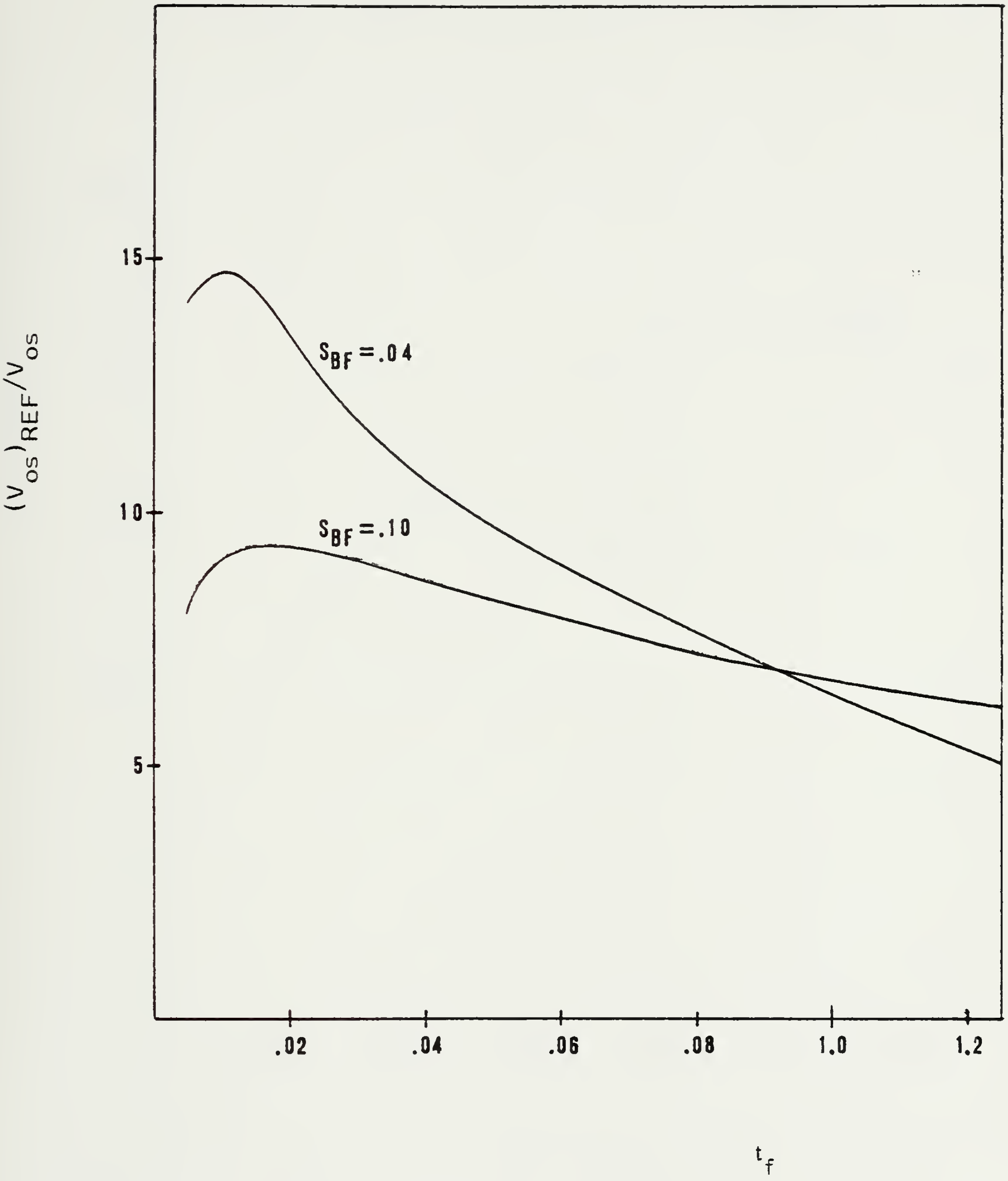

Figure 131. $(V_{os})_{REF}/V_{os}$ versus fin thickness for two values of fin spacing (S_{BF} = .04, .10) for an enhanced tube surface with D_o = 1", X_{ETP} = 2, and $H_f = (H_f)_{MAX}$ = .5

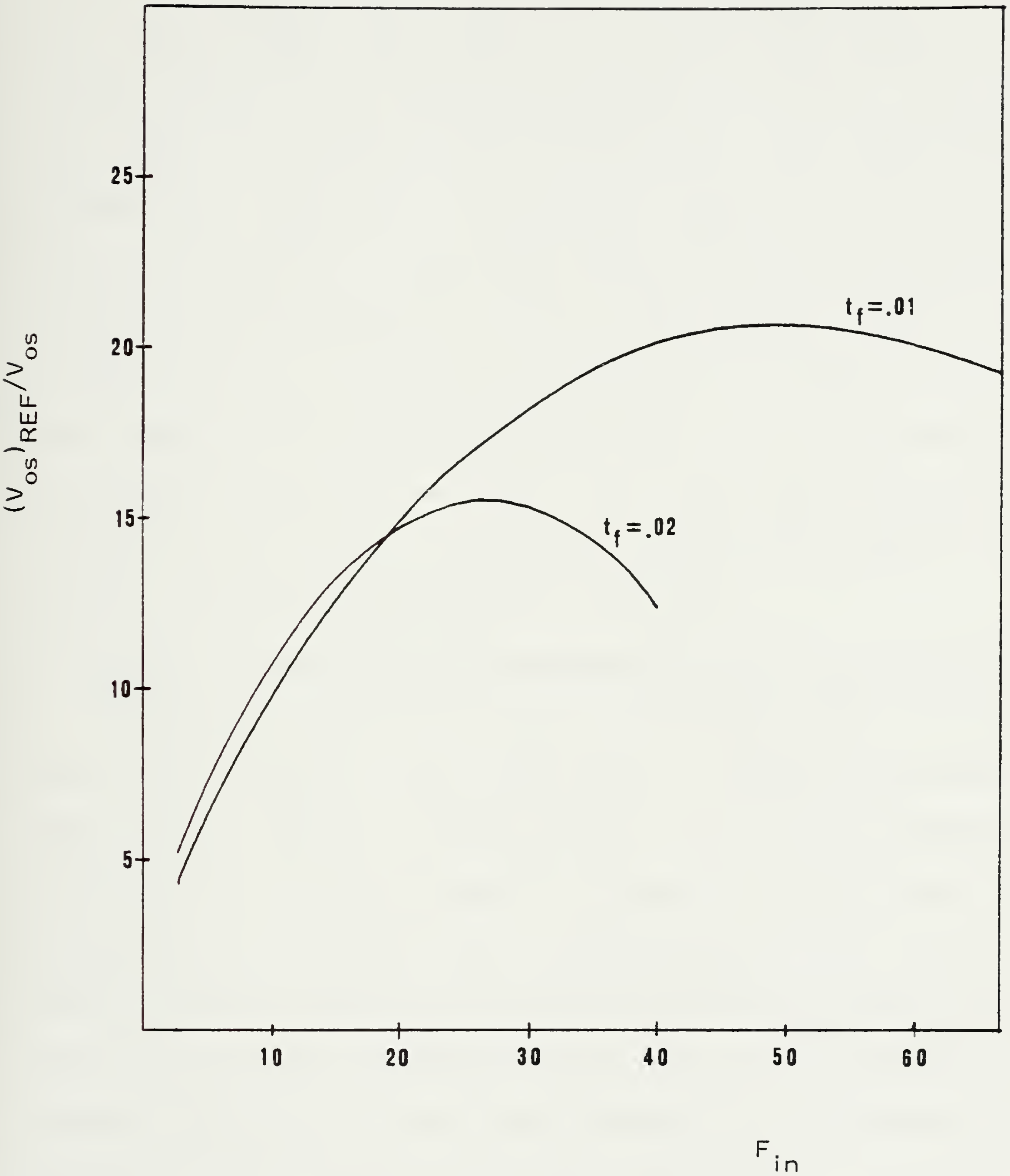

Figure 13J. $(V_{os})_{REF}/V_{os}$ versus fins per inch for two values of fin thicknesses (t_f = .01, .02,) for an enhanced tube surface with D_o = 1", X_{ETP} = 2, and $H_f = (H_f)_{MAX}$ = .5

Effect of tube diameter and pitch for enhanced tube surfaces can also be seen from Figure 13 from the two values of tube diameter and the two values of tube pitch for which $(V_{os})_{REF}/V_{os}$ was plotted for the various fin geometries. The effect of tube diameter and tube pitch on exchanger volume for an enhanced surface is less than a bare tube surface. If the optimal points in Figure 13 are compared for the two tube diameters and two tube pitches, the V_{os} is approximately doubled for a 2.5 increase in tube diameter and increased 1.5 times for a 1.5 increase in equilateral triangular tube pitch. For a bare tube surface larger changes in V_{os} would be predicted for the same change in tube diameter and equilateral triangular tube pitch.

D. Summary, Conclusions, and Recommendations for Future Studies.

Correlations for heat transfer and pressure drop for triangular pitch circular finned tube banks in crossflow developed by Biery (4) and Jameson (5) are used with a method for comparison of finned tube surfaces developed by Baskerville (3) to predict the performance of a surface with a given geometry and to study the effect of varying geometry on the performance of enhanced surfaces. There are six basic geometric parameters for a triangular pitch circular finned tube bank: tube diameter; tube transverse and diagonal pitch; fin height, thickness, and spacing.

It was found that for the same heat transfer (NTU) and pumping power, the volume of a heat exchanger decreases for smaller tube diameter and tube pitch. Optimum values of fin spacing and fin height were found for several specific fin

thicknesses, tube diameters, and pitch. Thinner fins were found to be more effective in enhancing a surface than thicker fins for the same fin spacing in terms of fin thicknesses.

This study extrapolated correlations based on experimental data for heat transfer and pressure drop beyond the range for which data exists. Experimental or theoretical work remains to be done to either prove the validity or correct any correlations that might be used in a similar parametric comparison study for the range of the geometric parameters where optimum performance appears to occur.

Future studies on the geometry effects of heat exchangers in crossflow might be extended to geometries not limited to triangular pitch tubes, circular fins, or circular tubes. With the proper correlations parametric studies, such as this one, might be performed for all the other geometries a crossflow heat exchanger might assume. Use of a high-speed computer would allow plotting families of performance curves versus the various geometric parameters.

Finally, performance might be defined in terms other than minimum volume for the same number of transfer units (NTU) and pumping power. A promising candidate might be minimum exchanger weight for the same NTU and pumping power. This would involve minimization of the volume of the material (tubes and fins) of an exchanger instead of the actual volume occupied by the exchanger for a given performance. Another dimension to this problem would be the materials from which the exchanger is constructed from. For example, although aluminum is lighter, copper has a higher heat

conductivity. However, materials are often dictated by service environment. Therefore, optimum performance for minimum volume of exchanger material would be a most useful measure to minimize the weight of an exchanger. This would insure the most efficient use of heat exchanger material on a per weight basis for a given performance.

REFERENCES

1. Soland, J.G., Mach, W.M., Jr., and Rohsenow, W.M., "Performance Ranking of Plate-Fin Heat Exchangers", ASME Journal of Heat Transfer, 100:3, pp. 514-519, August, 1978.
2. Kays, W.M. and London, A.L., Compact Heat Exchangers, McGraw-Hill Book Company, Inc., New York, 1958.
3. Baskerville, James E., "Performance Ranking of Finned Tubular Heat Exchanger Surfaces", M.I.T. Ocean Engineering Thesis, May, 1977.
4. Biery, J.D., "Prediction of Heat Transfer Coefficients in Gas Flow Normal to Finned and Smooth Tube Banks", ASME Journal of Heat Transfer, Volume 103, pp. 705-714, November, 1981.
5. Jameson, S.L., "Tube Spacing in Finned-Tube Banks", Trans. ASME, Volume 67, 1945, pp. 633-642.
6. Fraas, A.P., and Ozisik, M.N., Heat Transfer Design, Wiley, New York, 1965, pp. 326-332.
7. Mirkovic, Z., "Heat Transfer and Flow Resistance Correlation for Helically Finned and Staggered Tube Banks in Crossflow", in Heat Exchangers: Design and Theory Source Book, N.H. Afgran and E.U. Schlunder, eds., McGraw-Hill, New York, 1974, Chapter 20, pp. 559-584.
8. Grimison, E.D., "Correlation and Utilization of New Data on Flow Resistance and Heat Transfer for Crossflow Resistance and Heat Transfer for Crossflow of Gases Over Tube Banks", Trans. ASME, Volume 59, 1937, pp. 583-594.

9. Zhukaukas, A., "Heat Transfer From Tubes in Crossflow", Advances in Heat Transfer, Volume 8, pp. 93-160, 1972.

10. Briggs, D.E. and Young, E.H., "Convection Heat Transfer and Pressure Drop of Air Flow across Triangular Pitch Banks of Finned Tubes", CEP Symp. Ser. 41, Volume 59, p.1, 1963.

11. Gianolio, E. and Cuti, F., "Heat Transfer Coefficients and Pressure Drops for Air Coolers with Different Numbers of Rows Under Induced and Forced Draft", Heat Transfer Engineering, Volume 3, No. 1, pp. 38-47, July-September, 1981.

12. Ward, D.J. and Young E.H., "Convection Heat Transfer and Pressure Drop of Air in Forced Convection Across Triangular Pitched Banks of Finned Tubes", CEP Symp. Ser. 29, Volume 55, p. 37, 1959.

APPENDIX I

The purpose of this appendix is to present the derivation of several geometric relationships.

A. Derivation of total heat transfer area on one side, A_T, for circular finned tubes with fins of rectangular profile.

Figure A1 shows the layout of a circular finned tube with fins of rectangular profile.

The total heat transfer area including fin surface and edges of fins is:

$$A_T = L\left[\pi D_o + [2(\pi D_f^2/4 - \pi D_o^2/4) + \pi D_f t_f D_o - \pi D_o t_f D_o]/[(S_{BF}+t_f)D_o]\right] \quad \text{(A1)}$$

Since,

$$D_f = D_o + 2H_f D_o \quad \text{(A2)}$$

and,

$$D_f^2 - D_o^2 = (D_f - D_o)(D_f + D_o) = 4H_f^2 D_o^2 + 4H_f D_o^2 \quad \text{(A3)}$$

$$A_T = \pi L D_o \left[1 + [2H_f(H_f + t_f + 1)/(S_{BF} + t_f)]\right] \quad \text{(A4)}$$

Letting:

$$R_f = H_f/(S_{BF} + t_f) \quad \text{(A5)}$$

$$A_T = \pi L D_o[1 + 2R_f\ (H_f + t_f + 1)] \quad \text{(A6)}$$

and letting:

$$G_f = [1 + 2R_f\ (H_f + t_f + 1)] \quad \text{(A7)}$$

$$A_T = \pi L D_o G_f \quad \text{(A8)}$$

B. Derivation of minimum flow area for gas, A_c.

Figure A2 shows the triangular layout of a tube bank in crossflow.

FIGURE A1

Circular finned tube with fins of rectangular profile.

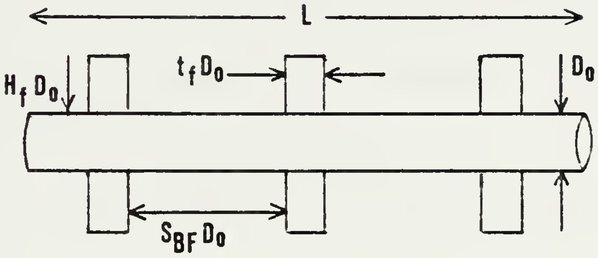

FIGURE A2

Triangular layout of a tube bank.

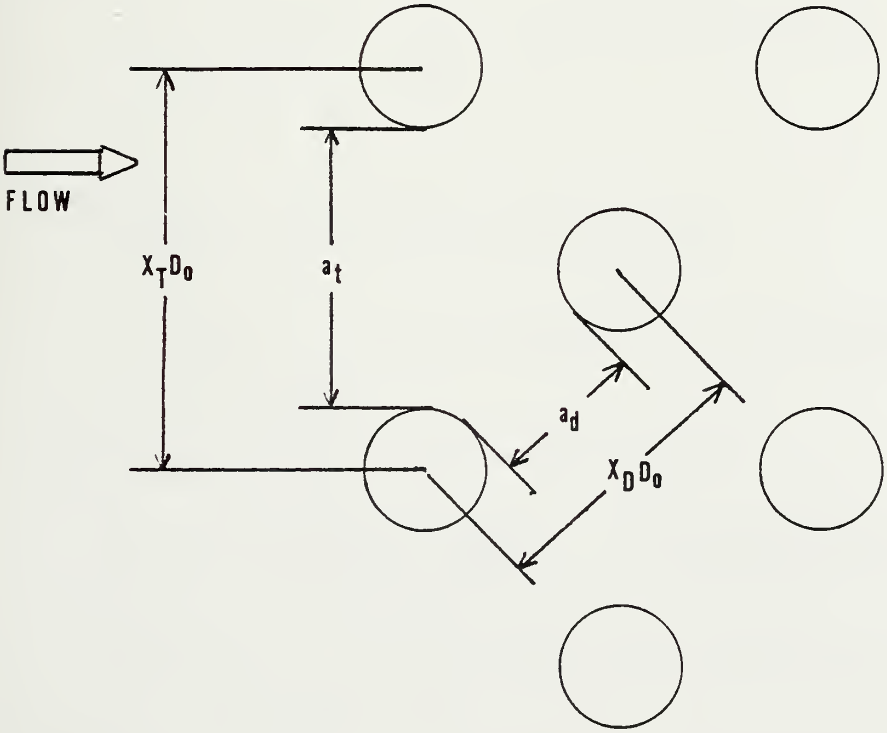

Minimum flow in the transverse space occurs when $a_t < 2a_d$, while minimum flow occurs in the diagonal space when $2a_d < a_t$. Therefore, minimum flow in the transverse space implies $X_T < 2X_D - 1$, and minimum flow in the diagonal space implies $X_D < (X_T+1)/2$. In either case, Figure A3 shows fins reduce the minimum flow area.

Therefore, in the calculation of minimum flow area, the fin cross sectional area must be subtracted.

For Case I: Minimum free flow in the transverse space:

$$X_T < 2X_D - 1$$

and,

$$\begin{aligned} A_c &= L[X_T D_o - D_o - 2t_f D_o H_f D_o/(S_{BF}+t_f)D_o] \\ &= LD_o(X_T - 2R_f t_f - 1) \qquad (A9) \end{aligned}$$

For Case II: Minimum free flow in the diagonal space:

$$X_D < (X_T+1)/2$$

and,

$$\begin{aligned} A_c &= L[2X_D D_o - 2D_o - 4t_f D_o H_f D_o/(S_{BF}+t_f)D_o] \\ &= 2LD_o[X_D - 2R_f t_f - 1] \qquad (A10) \end{aligned}$$

C. Derivation of hydraulic diameter, D_h.

For Case I: Minimum free flow in the transverse space:

$$X_T < X_D - 1$$

and, from equations (1a), (A6), and (A9)

$$D_h = \frac{4(X_T - 2R_f t_f - 1)\ X_L D_o}{\pi[1+2R_f(H_f+t_f+1)]} = \frac{4X_L D_o(X_T - 2R_f t_f - 1)}{\pi G_f} \qquad (A11)$$

For Case II: Minimum free flow in the diagonal space.

$$X_D < (X_T+1)/2$$

FIGURE A3

Layout of a tube bank with gas flow normal to paper.

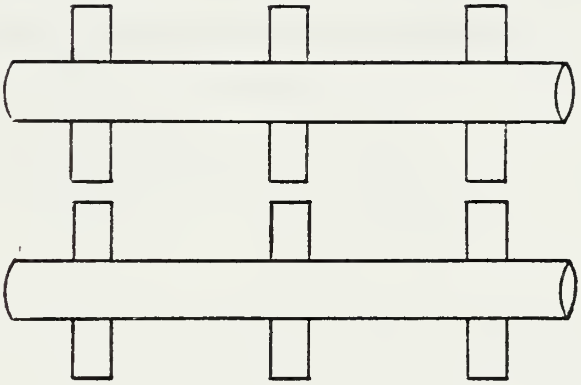

and, from equations (1a), (A6), and (A10)

$$D_h = \frac{8(X_D - 2R_f t_f - 1)X_L D_o}{\pi[1+2R_f(H_f+t_f+1)]} = \frac{8X_L D_o(X_D - 2R_f t_f - 1)}{\pi G_f} \qquad \text{(A12)}$$

D. Derivation of ratio of total heat transfer area on one side of the exchanger to total volume of the exchanger, β .

From equation (A6) and Figure 3:

$$\beta = \frac{A_T}{V_T} = \frac{\pi[1+2R_f(H_f+t_f+1)]}{X_T X_L D_o} = \frac{\pi G_f}{X_T X_L D_o} \qquad \text{(A13)}$$

E. Derivation of ratio of fin area to total transfer area, A_f/A_T:

It is seen that:

$$A_f = \frac{L[2[\ \pi(D_f^2/4) - \pi(D_o^2/4)] + \pi D_f t_f D_o]}{(S_{BF}+t_F)D_o}$$

$$= 2\pi L D_o R_f(H_f + t_f + 1 + t_f/2H_f) \qquad \text{(A14)}$$

Therefore,

$$\frac{A_f}{A_T} = \frac{2R_f(H_f + t_f + 1 + t_f/2H_f)}{[1 + 2R_f(H_f t_f + 1)]}$$

$$= 2R_f(H_f + t_f + 1 + t_f/2H_f)/G_f \qquad \text{(A15)}$$

F. Derivation of the angle define by the longitudinal centerline and the diagonal centerline, α ; see Figure 4.

$$\alpha = 2 \arctan \left[\frac{X_T D_o/2}{X_L D_o}\right] = 2 \arctan\ (X_T/2X_L) \qquad \text{(A16)}$$

G. Derivation of the equivalent diameter used by Jameson (5) and Mirkovic (7).

The projected perimeter of a finned tube, l_k, is 2π times the distance traveled axially along the tube and over the surface of the fins from one end of the tube to the other. (See Figure A1.) Therefore,

$$l_k = \frac{2\pi L(2H_f D_o + t_f D_o + S_{BF} D_o)}{t_f D_o + S_{BF} D_o} = 2\pi L(2R_f + 1) \qquad \text{(A17)}$$

The equivalent diameter of a finned tube, d_e, used by Jameson (5) and Mirkovic (7) is defined as twice the total air heat transfer surface area divided by π times the projected perimeter of a tube. Therefore,

$$d_e = \frac{2A_T}{\pi l_k} = \frac{D_o[1+2R_f(H_f+t_f+1)]}{2R_f+1} = \frac{D_o G_F}{2R_f+1} \qquad \text{(A18)}$$

APPENDIX II

The purpose of this appendix is to compare the method developed by Biery (4) as presented in Chapter III for predicting the Colburn j-modulus for gas flow normal to triangular pitch finned tube banks with the data given by Kays and London (2) and with several other correlations.

Table A1 presented the percent deviation of the Colburn j-modulus predicted by Biery's method from the experimental value given by Kays and London (2) for the corresponding surface over the given range of Reynolds numbers, where

$$\text{Percent Deviation} = \frac{j_B - j_{K\&L}}{j_{K\&L}} \times 100\% \qquad \text{(A19)}$$

Table A1 shows the Colburn j-modulus predicted by Biery's method deviates from the experimental values by approximately 40 percent for surfaces 93 and 94. However, Kays and London notes experimental uncertainty for heat transfer for surface 93 due to the necessity of estimating a contact resistance in the bi-metal tubes which were used. Another source of error for surfaces 92, 93 and 94 is, according to the values given, Kays and London calculated the hydraulic diameter without accounting for the fins as outlined in Appendix I, Section C. However, the values given for hydraulic diameter for the other surfaces, which are data taken from Jameson (5), suggest the fins were accounted for in calculating the hydraulic diameter. Therefore, due to these errors, surfaces 93 and 94 are discounted. The remaining body of data shows that Biery's

TABLE AI

Deviation of the Biery (4) method for Colburn j-modulus in predicting experimentally obtained value as presented by Kays and London (2).

Surface*	RE=1000	RE=4000	RE=7000	RE=10000
92	-27.1%	-18.5%	-14.7%	-12.2%
93	-41.7%	-40.7%	-40.3%	-40.0%
94	-37.3%	-37.1%	-37.0%	-36.9%
96	-12.0%	-18.8%	-21.4%	-23.1%
97A	-16.3%	-20.8%	-22.6%	-23.7%
97B	-11.5%	-15.5%	-17.1%	-18.0%
98A	+6.7%	-3.6%	-7.4%	-9.7%
98B	+17.8%	+6.0%	+1.6%	-1.1%
98C	+27.4%	+13.0%	+7.7%	+4.5%
98D	+6.3%	-4.0%	-7.9%	-10.2%
98E	+12.0%	+1.4%	-2.5%	-5.0%
99A	-10.1%	-13.4%	-14.7%	-15.6%
99B	-1.5%	-4.3%	-5.5%	-6.2%

*Surface designation corresponds to the Kays and London (2) figure number.

method of predicting the Colburn j-modulus agrees with the experimental values given by Kays and London (2) to within an average per surface of 20% from the mean value with a mean 7% below the Kays and London data and with a standard deviation of 8%.

The method given by Biery (4) for predicting Colburn j-modulus was also compared to correlations given by Briggs and Young (10) and Mirkovic (7). Caution should be exercised when comparing these correlations as the Reynolds number for each author is based on a different diameter. To compare these correlations a factor must be included to convert the correlations to a common diameter. The correlation given by Briggs and Young is based on the outside tube diameter while the correlation given by Mirkovic is based on an equivalent diameter, d_e, as presented in equation (A18).

The Reynolds number used by Biery (4) is based on the hydraulic diameter given by Kays and London (2) and equation (1a).

The correlation given by Mirkovic (7) when converted to a hydraulic diameter basis may be expressed as follows:

$$\begin{aligned} j_M &= N_{ST} N_{Pr}^{2/3} \\ &= .224 \left[\frac{1.1547 X_L D_o - D_o}{D_o}\right]^{.1} \left[\frac{X_L D_o - D_o}{D_o}\right]^{-.15} \left[\frac{S_{BF}}{H_f}\right]^{.25} \left[\frac{D_h}{d_e}\right]^{.338} RE^{-.338} \qquad \text{(A20)} \end{aligned}$$

It should be noted that

$$\frac{S_{BF}}{H_f} = \frac{1 - F_{in} t_f D_o}{F_{in} H_f D_o} \quad , \tag{A21}$$

which is the way Mirkovic originally included this factor in his correlation. It appears Mirkovic intended to develop a correlation which included fin thickness as a variable in this factor, although it is not. However, the Mirkovic correlation is slightly dependent upon fin thickness when expressed in terms of a hydraulic diameter due to the (D_h/d_e) term.

Biery (4) noted the Mirkovic correlation gave very fine results when used to analyze the Mirkovic (7), Kays and London (2), and Jameson (5) data. However, this should be expected since the data produced the parameters and coefficients for the correlation. Biery reported the overall result in comparing the Mirkovic correlation with these data gave an average error of +.3 percent with a standard deviation of 3.6 percent. However, since the Mirkovic correlation is not directly a function of fin thickness, its more general validity outside the narrow range of data from which it was drawn is to be suspected. Also, the Mirkovic correlation includes a term that subtracts the diameter of the tube from the longitudinal distance between tube centers. In a triangular pitch tube bank, where the transverse tube pitch is large and the longitudinal tube pitch is small, the longitudinal distance between the tube centers can approach and sometimes be smaller than the diameter of the tube.

The correlation given by Briggs and Young when converted to a hydraulic diameter basis may be expressed as follows:

$$j_{B\&Y} = N_{ST}N_{Pr}^{2/3} = .134\left[\frac{S_{BF}}{t_f}\right]^{.1134}\left[\frac{S_{BF}}{H_f}\right]^{.2}\left[\frac{D_h}{D_o}\right]^{.319} RE^{-.319} \qquad (A22)$$

Gianolio and Cuti (11) confirmed in a set of experiments that the Briggs and Young correlation predicted the air heat transfer coefficients obtained from their experiemental data for induced draft for six tube-row banks, but had to include correction factors given by Ward and Young (12) for tube banks having a number of rows less than six.

Biery's method for predicting the Colburn j-modulus agreed with the Mirkovic and Briggs and Young correlations to within plus or minus 15 percent over the range of values of tube diameter, tube pitch, fin thickness, fin height, and fin spacing from which these correlations were based. However, these correlations deviated from Biery's method by as much as 40 percent at extreme values outside the range of data. All three correlations were also in agreement by predicting an increase in the Colburn j-modulus with an increase in fin spacing or tube pitch or with a decrease in fin height or tube diameter.

However, as fin thickness was increased, Biery's method and the Mirkovic correlation predicted an increase in the Colburn j-modulus, while the Briggs and Young correlation predicted a decrease. The experimental data taken by Mirkovic (7) presents an opportunity to examine variation of the Colburn j-modulus with fin thickness. In Mirkovic's run 12 and 13 all parameters were identical except for fin thickness. Mirkovic's Figure 2 shows for run 13 (the thicker fins), the Colburn j-modulus is higher than for

run 12. Therefore, an increase in the Colburn j-modulus with increase in fin thickness seems to be the correct indication.

In conclusion, all three correlations yield general agreement, except for variation of fin thickness. For this parameter two of the three correlations (Biery and Mirkovic) are in agreement both with each other and with a particular example from the Mirkovic data. Therefore, the choice of a correlation for predicting the Colburn j-modulus of a given surface, rests between the Biery method and the Mirkovic correlation. In the final analysis, Biery's method was selected over the Mirkovic correlation. Biery's method is more general and based on a larger body of data encompassing a larger range of geometries. Further, it is not restricted to geometries in which the longitudinal distance between tube centers must be greater than one tube diameter as in the Mirkovic correlation. Therefore, the Biery method for predicting the Colburn j-modulus is used later for predicting the performance parameters of a given surface.

APPENDIX III

The purpose of this Appendix is to compare Jameson's (5) correlation for pressure drop across triangular pitch finned tube banks with the data given by Kays and London (2).

As noted in Chapter IV, to compare the friction factor used in the Jameson correlation, f_J, with the friction factor given in the data by Kays and London, a geometry factor must be included and the Reynolds number converted to a common diameter. With these changes the friction factor as defined by Kays and London (2) per equation (30) and as predicted by the Jameson correlation becomes:

$$f' = 1.532 \left[\frac{D_H}{X_L D_o}\right] \left[\frac{D_J}{D_h}\right]^{-.25} RE^{-.25} \tag{A23}$$

Table AII presents the percent deviation of the friction factor as predicted by the Jameson correlation, (f'), and the experimental value given by Kays and London (2) for the corresponding surface over the given range of Reynolds numbers, where

$$\text{Percent Deviation} = \frac{f' - f}{f} \times 100\% \tag{A24}$$

Table AII shows the friction factor predicted by the Jameson correlation (f') for surface 98D deviates from the experimental value by approximately 67%. Surface 98D is the one case of the surfaces listed in Table AII which the minimum free flow area occurs in the diagonal spaces. Jameson (5) noted that his correlation did not accurately predict the friction factor for finned tubes in which the minimum free flow area occurs in the diagonal space. This

TABLE AII

Deviation of the Jameson (5) correlation for friction factor in predicting experimentally obtained value as presented in Kays and London (2).

Surface*	RE=1000	RE=4000	RE=7000	RE=10000
92	+33.5%	+23.8%	+20.0%	+17.7%
93	+17.3%	+9.7%	+6.7%	+4.9%
94	+9.9%	+5.3%	+3.5%	+2.4%
96	+8.9%	+9.8%	+10.1%	+10.4%
97A	+0.5%	-0.1%	-0.4%	-0.5%
97B	-4.2%	-1.8%	-0.8%	-0.2%
98A	-2.1%	+0.7%	+1.9%	+2.7%
98B	-0.2%	+0.3%	+0.4%	+0.5%
98C	+10.8%	+10.3%	+10.0%	+9.9%
98D	+65.1%	+67.2%	+68.1%	+68.6%
98E	+6.2%	+7.8%	+8.4%	+8.9%
99A	+18.1%	+17.7%	+17.6%	+17.5%
99B	+9.7%	+10.6%	+11.0%	+11.3%

*Surface designation corresponds to the Kays and London (2) figure number.

conclusion appears to be supported by the results in Table AII for surface 98D. Discounting this one surface, Table AII shows the Jameson (5) correlation predicts the Kays and London (2) data to within approximately 20% of the mean value with a mean 7.8% above the Kays and London data and with a standard deviation of 7.3%. The Jameson correlation is used in Chapters V and VI to study the geometry effects of tube banks in which the minimum free flow area occurs in the spaces transverse to the air flow.

APPENDIX IV

The purpose of this Appendix is to put together the equations and correlations introduced or derived in other Chapters and Appendices in an algorithm which may be programmed into a computer or calculator for predicting the performance parameters of a triangular pitch circular finned tube bank in crossflow given the geometry and the air and fin material properties. Hence, the only inputs required are tube diameter, tube pitch, fin thickness, fin height, fin spacing, and the air and fin material properties.

The air and fin material properties are entered as a "property constant" (P_c) in the computation of fin efficiency as outlined in Figure 5.

Since:

$$m = \left[\frac{2h_2}{k_m \delta}\right]^{.5} \qquad (10)$$

and:

$$j = N_{ST} N_{Pr}^{2/3} = \frac{h_2}{G_c C_P} \quad N_{Pr}^{2/3} \qquad (A25)$$

where from (3a):

$$G_c = \frac{RE\ \mu}{D_h} \qquad (A26)$$

It can be shown:

$$ml = \left[\frac{2\ P_c\ j\ RE\ D_o}{D_h t_f}\right]^{.5} \times \left(H_f\right) \qquad (A27)$$

where:

$$P_c = \frac{\mu\, C_P}{N_{Pr}^{2/3} k_m} \qquad (A28)$$

For dry air at 90° F at atmospheric pressure $P_c = 1.17\ 10^{-4}$ for aluminum fins and $P_c = 6.23\ 10^{-5}$ for copper fins.

The algorithm for predicting the performance parameters of a surface given the geometry and property constant is introduced in Figure A4. This algorithm calculates the performance parameters for a triangular pitch smooth tube and finned tube with radial fins of rectangular profile only. An algorithm that would include tapered fins, continuous fins, in-line tubes, and other various geometries could be written employing the methods outlined in this paper, but would require the applicable correlations and geometric relationships. It should be recalled that this algorithm is not accurate for predicting enhanced surface performance parameters for minimum free flow area occuring in the diagonal due to the inaccuracy of the Jameson (5) correlation for this case. However, the program should produce accurate results for both cases of minimum free flow for bare tubes. Therefore, the effect of varying tube pitch can be studied even for the case of minimum free flow occuring in the diagonal by using the performance parameters produced for smooth tubes. The program is written to produce performance parameters for bare tube Reynolds numbers (RE_N) of 10000, 70000, and 130000. Values for only two Reynolds numbers are required to plot the performance parameters for a surface since the plot is a straight line on a log-log scale. However, a third value insures plotting accuracy. The range for RE_N of 10000 to 130000 was chosen since the typical value of RE_N/RE is 7 to 20. Therefore, performance parameters are produced for Reynolds number based on the

hydraulic diameter in the range of 500 to 18000. This is the approximate range most finned tube heat exchangers in crossflow operate and is the same range for which the Kays and London (2) data is given.

The algorithm of Figure A4 was keyed into a TI-59 calculator. This calculator program is listed in Figure A5. Due to the length of the algorithm, the calculator program is divided into two halves. The first half calculates the parameters for the equations in the algorithm up to label A (Steps 000 to 422), and stores these values in data registers for use by the second half of the program. After the first half of the program has been run, the second half of the program (Steps 000 to 632) can be read in by magnetic card and run to generate the performance parameters. Table AIII lists the data registers in which the input and calculated parameters are stored. Where more than one parameter is listed indicates the corresponding data register is used for temporary storage of the indicated parameter while the program is running.

Figure A6 shows a sample output generated by running the program of Figure A5. The program labels refer to the indicated parameter. The surface is defined in the output by a listing of the input parameters. It should be noted that the only input parameter not listed in the output is P_c. In the parametric study of Chapter VI the fin material was assumed to be copper and the fluid on the enhanced surface side was assumed to be dry air at 90° F for all cases. The property constant (P_c) for these assumptions is 6.23 10^{-5}.

The output of Figure A6 can be used to plot the performance parameters for the indicated surface. A comparison can then be made on the surface effectiveness as outlined in Chapter 2. Each surface generated in the parametric study of Chapter VI was compared on the basis of volume one side for the same pumping power and number of transfer units (Case C comparison of Chapter II). Each surface was compared to a bare tube surface where X_T = X_D = 2 and D_o = 1". To standardize this comparison the 45 degree line (slope = 1 on log-log scale) was drawn from the point on the performance parameter plot of the reference bare tube surface where log (NTU/V_{os}) = 2.0.

The 45 degree line described above and the plot of the performance parameters of a surface are straight lines. Therefore, it should be finally mentioned that as an alternative to plotting a performance parameter to make a volume comparison to another surface, linear equations may be written and solved simultaneously. This permits an analytical comparison which is faster if in the form of a program and also more accurate.

INPUT

X_T, X_D, S_{BF}, t_f, H_f, P_c, D_o (inches)

Calculation of Various Parameters for Later Use:

$X_L = (X_D{}^2 - X_T{}^2/4)^{\frac{1}{2}}$

$R_f = H_f/(S_{BF} + t_f)$

$G_f = 1 + 2R_f(t_f + H_f + 1)$

$\beta = \pi G_f/X_T X_L D_o$

$A_f/A_T = 2R_f(H_f + t_f + 1 + t_f/2H_f)/G_f$

$N_{HT} = 4D_o(X_T - 2R_f t_f - 1)X_L/\pi$

$N_{HD} = 4D_o(X_D - 2R_f t_f - 1)X_L/\pi$

$N_N = 4D_o X_L/\pi$

$N_f = 16/\beta^2 X_T{}^2$

$RE_N/RE = \beta X_T X_L D_o/\pi$

$d_e = D_o G_f/(2R_f + 1)$

$$D_J = \frac{d_e}{\left[(H_f/2S_{BF})^{.4}\left[\frac{1}{2}(X_T D_o/d_e - 1)^{-\frac{1}{2}} + \frac{1}{2}(X_D D_o/d_e - 1)^{-\frac{1}{2}}\right]\right]^4}$$

$\ln(r_o/r_e) = -\ln(1 + 2H_f)$

$C_\Delta = -.00259 - .0084 \ln(r_o/r_e)$

$D_\Delta = -.02426 - .4521 \ln(r_o/r_e)$

Figure A4: Algorithm for Prediction of Performance Parameters for Triangular Pitch Circular Finned Tube Surfaces and Bare Tube Surfaces.

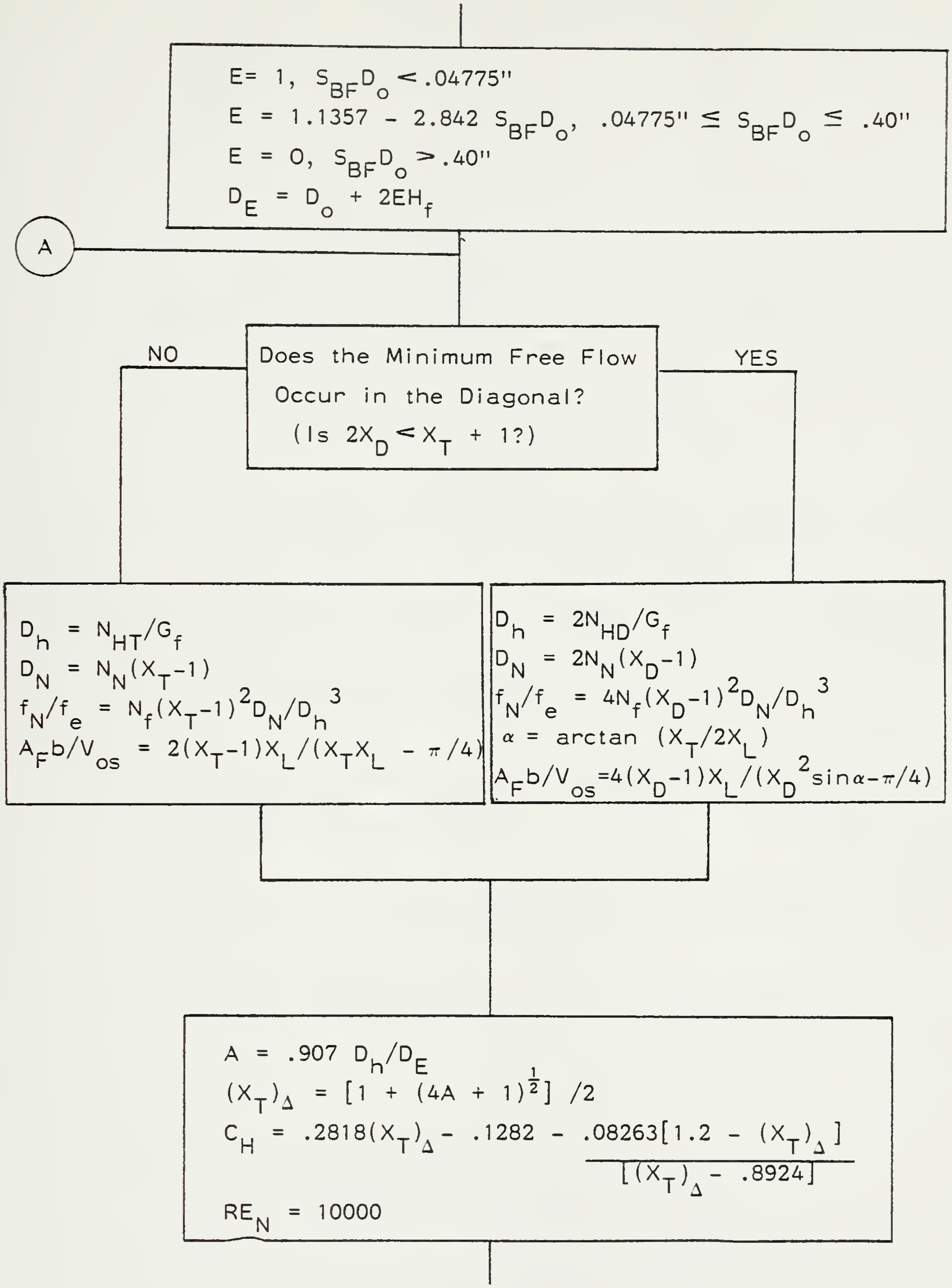
$E = 1, \ S_{BF}D_o < .04775''$
$E = 1.1357 - 2.842 \ S_{BF}D_o, \ .04775'' \leq S_{BF}D_o \leq .40''$
$E = 0, \ S_{BF}D_o > .40''$
$D_E = D_o + 2EH_f$
A
NO
Does the Minimum Free Flow Occur in the Diagonal?
(Is $2X_D < X_T + 1$?)
YES
$D_h = N_{HT}/G_f$
$D_N = N_N(X_T-1)$
$f_N/f_e = N_f(X_T-1)^2D_N/D_h^{\ 3}$
$A_Fb/V_{os} = 2(X_T-1)X_L/(X_TX_L - \pi/4)$
$D_h = 2N_{HD}/G_f$
$D_N = 2N_N(X_D-1)$
$f_N/f_e = 4N_f(X_D-1)^2D_N/D_h^{\ 3}$
$\alpha = \arctan \ (X_T/2X_L)$
$A_Fb/V_{os}=4(X_D-1)X_L/(X_D^{\ 2}\sin\alpha-\pi/4)$
$A = .907 \ D_h/D_E$
$(X_T)_\Delta = [1 + (4A + 1)^{\frac{1}{2}}] \ /2$
$C_H = .2818(X_T)_\Delta - .1282 - \dfrac{.08263[1.2 - (X_T)_\Delta]}{[(X_T)_\Delta - .8924]}$
$RE_N = 10000$

Figure A4. (Cont)

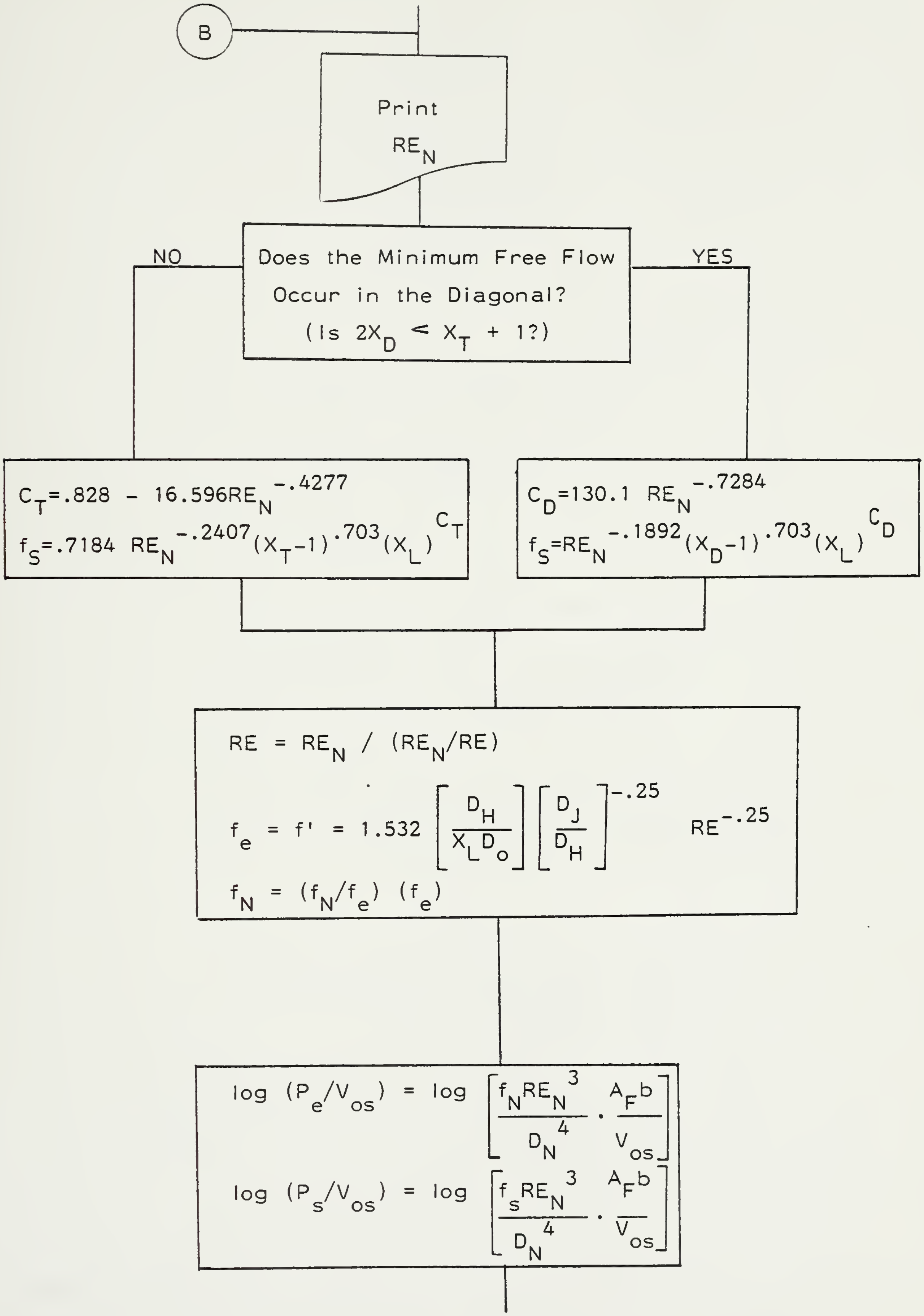
B
Print RE_N
Does the Minimum Free Flow Occur in the Diagonal? (Is $2X_D < X_T + 1$?)
NO
YES
$C_T = .828 - 16.596 RE_N^{-.4277}$
$f_S = .7184\ RE_N^{-.2407} (X_T - 1)^{.703} (X_L)^{C_T}$
$C_D = 130.1\ RE_N^{-.7284}$
$f_S = RE_N^{-.1892} (X_D - 1)^{.703} (X_L)^{C_D}$
$RE = RE_N / (RE_N/RE)$
$f_e = f' = 1.532 \left[\frac{D_H}{X_L D_o}\right] \left[\frac{D_J}{D_H}\right]^{-.25} RE^{-.25}$
$f_N = (f_N/f_e)\ (f_e)$
$\log (P_e/V_{os}) = \log \left[\frac{f_N RE_N^3}{D_N^4} \cdot \frac{A_F b}{V_{os}}\right]$
$\log (P_s/V_{os}) = \log \left[\frac{f_s RE_N^3}{D_N^4} \cdot \frac{A_F b}{V_{os}}\right]$

Figure A4. (Cont)

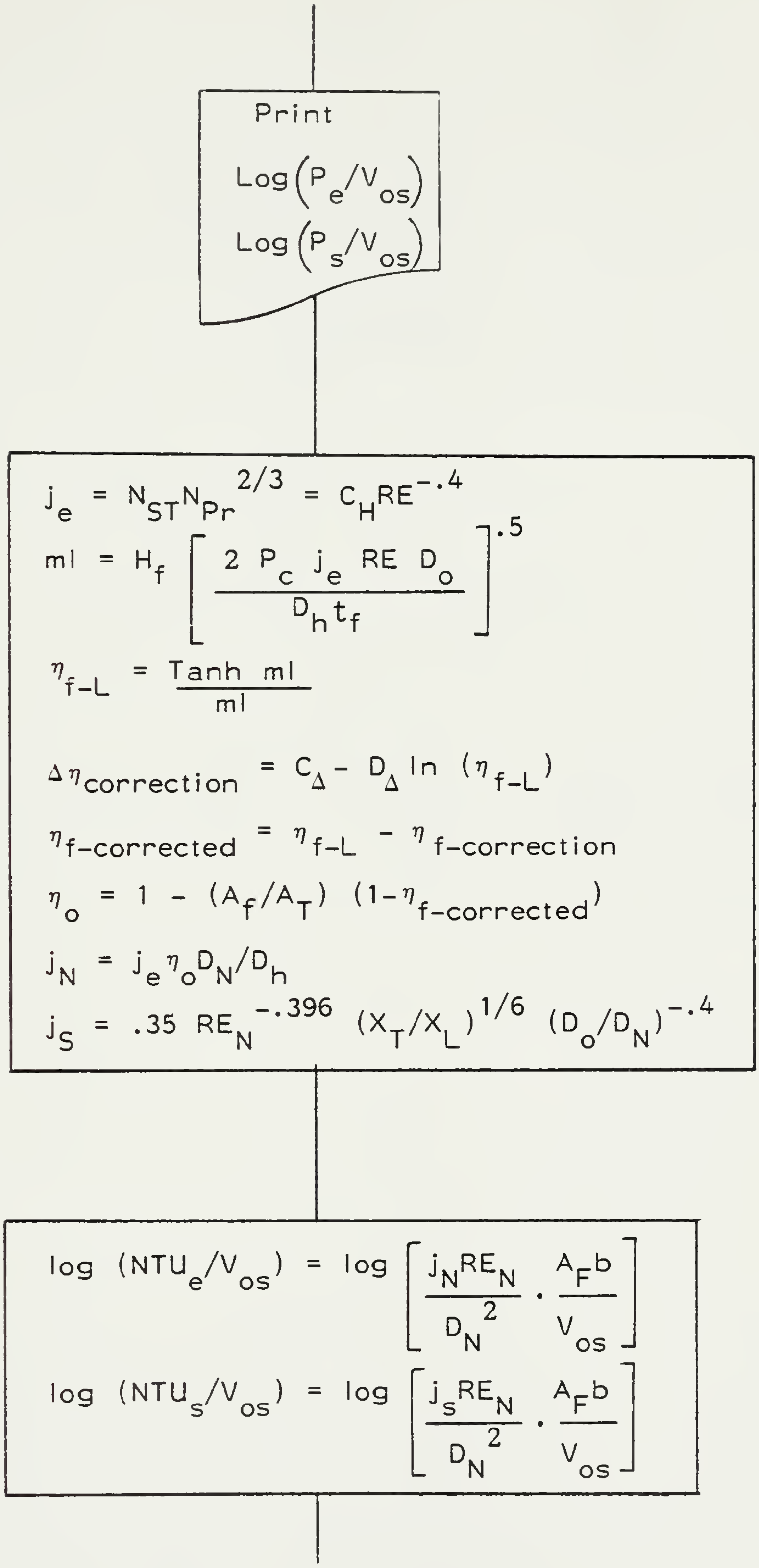

$$\text{Log}\left(P_e/V_{os}\right)$$

$$\text{Log}\left(P_s/V_{os}\right)$$

$$j_e = N_{ST}N_{Pr}^{2/3} = C_H RE^{-.4}$$

$$ml = H_f\left[\frac{2\ P_c\ j_e\ RE\ D_o}{D_h t_f}\right]^{.5}$$

$$\eta_{f-L} = \frac{\text{Tanh}\ ml}{ml}$$

$$\Delta\eta_{correction} = C_\Delta - D_\Delta \ln\left(\eta_{f-L}\right)$$

$$\eta_{f-corrected} = \eta_{f-L} - \eta_{f-correction}$$

$$\eta_o = 1 - (A_f/A_T)\ (1-\eta_{f-corrected})$$

$$j_N = j_e \eta_o D_N/D_h$$

$$j_S = .35\ RE_N^{-.396}\ (X_T/X_L)^{1/6}\ (D_o/D_N)^{-.4}$$

$$\log\ (NTU_e/V_{os}) = \log\left[\frac{j_N RE_N}{D_N^{\ 2}}\cdot\frac{A_F b}{V_{os}}\right]$$

$$\log\ (NTU_s/V_{os}) = \log\left[\frac{j_s RE_N}{D_N^{\ 2}}\cdot\frac{A_F b}{V_{os}}\right]$$

Figure A4. (Cont)

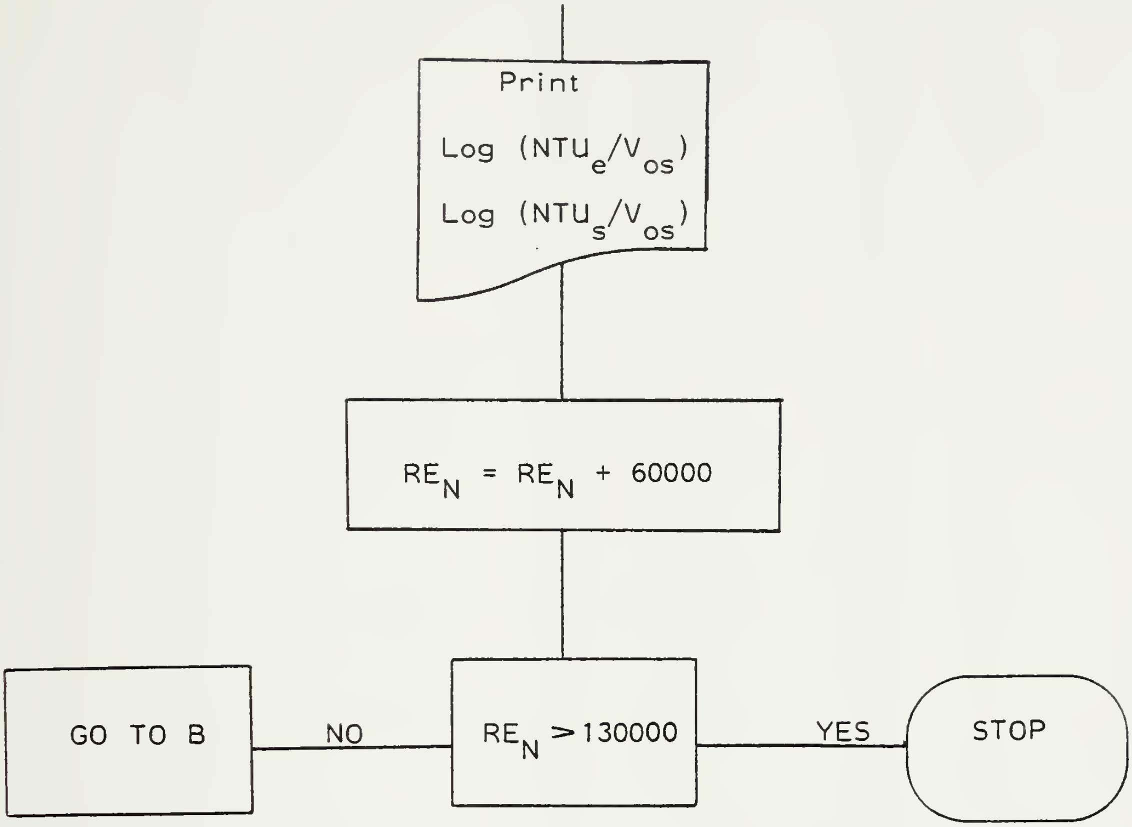

Figure A4. (Cont)

```
000  43  RCL
001  13   13
002  33  X²
003  75   -
004  43  RCL
005  11   11
006  33  X²
007  55   ÷
008  04   4
009  95   =
010  34  ΓX
011  42  STO
012  12   12
013  43  RCL
014  10   10
015  55   ÷
016  53   (
017  43  RCL
018  08   08
019  85   +
020  43  RCL
021  09   09
022  54   )
023  95   =
024  42  STO
025  15   15
026  65   ×
027  02   2
028  65   ×
029  53   (
030  43  RCL
031  09   09
032  85   +
033  43  RCL
034  10   10
035  85   +
036  01   1
037  54   )
038  85   +
039  01   1
040  95   =
041  42  STO
042  16   16
043  65   ×
044  89   π
045  55   ÷
046  43  RCL
047  11   11
048  55   ÷
049  43  RCL
050  12   12
051  55   ÷
052  43  RCL
053  00   00
054  95   =
055  42  STO
056  17   17
057  43  RCL
058  10   10
059  85   +
060  43  RCL
061  09   09
062  85   +
063  43  RCL
064  09   09
065  55   ÷
066  02   2
067  55   ÷
068  43  RCL
069  10   10
070  85   +
071  01   1
072  95   =
073  65   ×
074  02   2
075  65   ×
076  43  RCL
077  15   15
078  55   ÷
079  43  RCL
080  16   16
081  95   =
082  42  STO
083  18   18
084  43  RCL
085  11   11
086  75   -
087  02   2
088  65   ×
089  43  RCL
090  15   15
091  65   ×
092  43  RCL
093  09   09
094  75   -
095  01   1
096  95   =
097  65   ×
098  04   4
099  65   ×
100  43  RCL
101  00   00
102  95   =
103  65   ×
104  43  RCL
105  12   12
106  55   ÷
107  89   π
108  95   =
109  42  STO
110  19   19
111  04   4
112  65   ×
113  43  RCL
114  00   00
115  65   ×
116  53   (
117  43  RCL
118  13   13
119  75   -
```

Figure A5. TI-59 Calculator Program for Predicting Performance Parameters (First Half).

```
120  02   2       160  95   =       200  10  10
121  65   ×       161  42  STO      201  55   ÷
122  43  RCL      162  21  21       202  02   2
123  15  15       163  43  RCL      203  55   ÷
124  65   ×       164  17  17       204  43  RCL
125  43  RCL      165  65   ×       205  08  08
126  09  09       166  43  RCL      206  54   )
127  75   -       167  11  11       207  45  Yˣ
128  01   1       168  65   ×       208  93   .
129  54   )       169  43  RCL      209  04   4
130  65   ×       170  12  12       210  65   ×
131  43  RCL      171  65   ×       211  53   (
132  12  12       172  43  RCL      212  53   (
133  55   ÷       173  00  00       213  01   1
134  89   π       174  55   ÷       214  55   ÷
135  95   =       175  89   π       215  02   2
136  42  STO      176  95   =       216  55   ÷
137  07  07       177  42  STO      217  53   (
138  04   4       178  22  22       218  43  RCL
139  65   ×       179  43  RCL      219  11  11
140  43  RCL      180  00  00       220  65   ×
141  00  00       181  65   ×       221  43  RCL
142  65   ×       182  43  RCL      222  00  00
143  43  RCL      183  16  16       223  55   ÷
144  12  12       184  55   ÷       224  43  RCL
145  55   ÷       185  53   (       225  23  23
146  89   π       186  02   2       226  75   -
147  95   =       187  65   ×       227  01   1
148  42  STO      188  43  RCL      228  54   )
149  20  20       189  15  15       229  34  √X
150  01   1       190  85   +       230  54   )
151  06   6       191  01   1       231  85   +
152  55   ÷       192  54   )       232  53   (
153  43  RCL      193  95   =       233  01   1
154  17  17       194  42  STO      234  55   ÷
155  33  X²       195  23  23       235  02   2
156  55   ÷       196  55   ÷       236  55   ÷
157  43  RCL      197  53   (       237  53   (
158  11  11       198  53   (       238  43  RCL
159  33  X²       199  43  RCL      239  13  13
```

Figure A5. (Cont - First Half)

```
240  65   ×
241  43  RCL
242  00   00
243  55   ÷
244  43  RCL
245  23   23
246  75   -
247  01   1
248  54   )
249  34  √X
250  54   )
251  54   )
252  54   )
253  45  Yˣ
254  04   4
255  95   =
256  42  STO
257  24   24
258  93   .
259  00   0
260  04   4
261  07   7
262  07   7
263  05   5
264  32  X:T
265  43  RCL
266  08   08
267  65   ×
268  43  RCL
269  00   00
270  95   =
271  77   GE
272  12   B
273  01   1
274  42  STO
275  25   25
276  61  GTO
277  13   C
278  76  LBL
279  12   B
280  01   1
281  93   .
282  01   1
283  03   3
284  05   5
285  07   7
286  75   -
287  02   2
288  93   .
289  08   8
290  04   4
291  02   2
292  65   ×
293  43  RCL
294  08   08
295  65   ×
296  43  RCL
297  00   00
298  95   =
299  42  STO
300  25   25
301  76  LBL
302  13   C
303  02   2
304  65   ×
305  43  RCL
306  10   10
307  65   ×
308  43  RCL
309  25   25
310  85   +
311  43  RCL
312  00   00
313  95   =
314  42  STO
315  26   26
316  02   2
317  65   ×
318  43  RCL
319  10   10
320  85   +
321  01   1
322  95   =
323  35  1/X
324  23  LNX
325  42  STO
326  27   27
327  65   ×
328  93   .
329  00   0
330  00   0
331  08   8
332  04   4
333  94  +/-
334  75   -
335  93   .
336  00   0
337  00   0
338  02   2
339  05   5
340  09   9
341  95   =
342  42  STO
343  28   28
344  93   .
345  00   0
346  02   2
347  04   4
348  02   2
349  06   6
350  94  +/-
351  75   -
352  93   .
353  04   4
354  05   5
355  02   2
356  01   1
357  65   ×
358  43  RCL
359  27   27
```

Figure A5. (Cont - First Half)

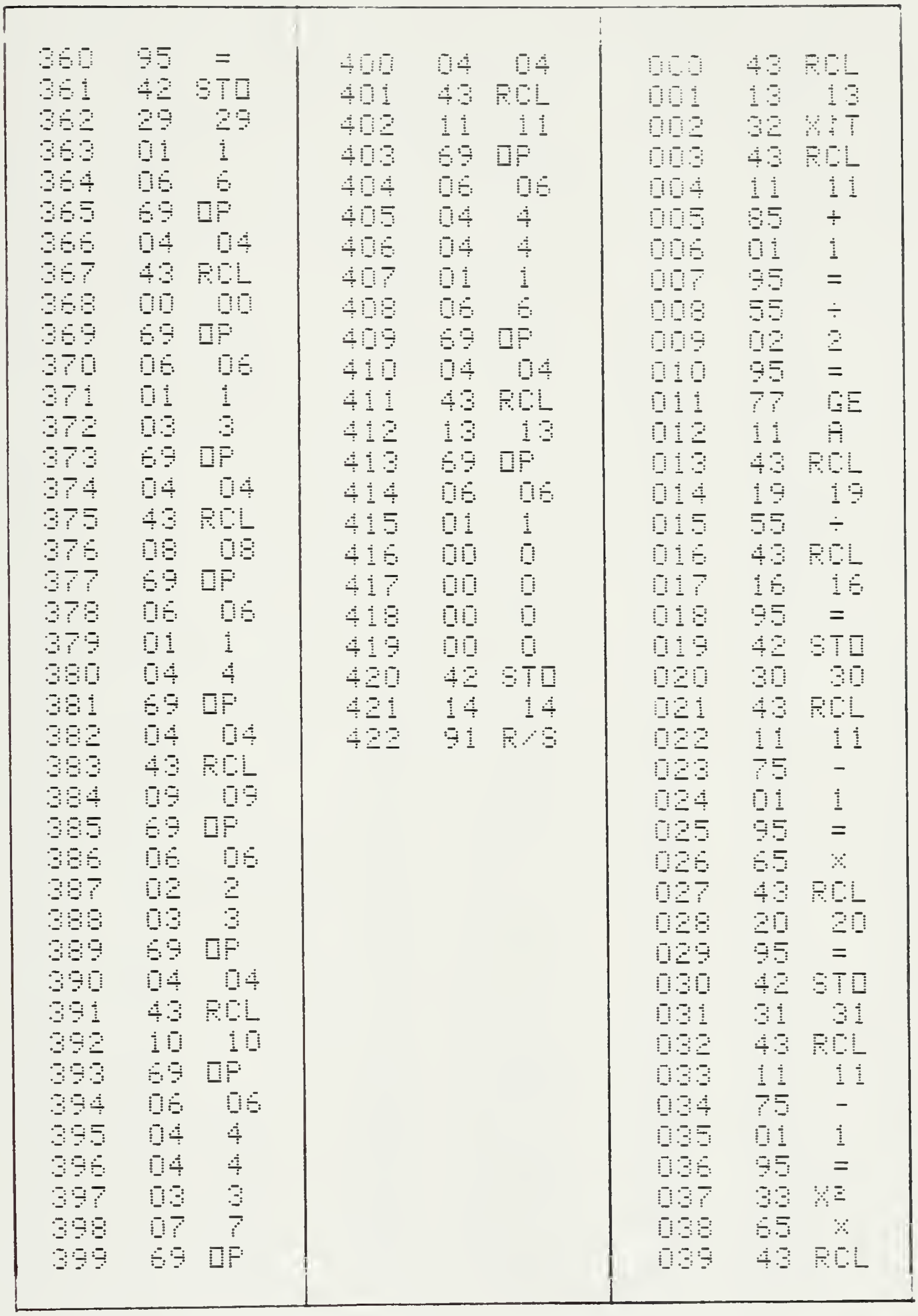

```
360   95   =
361   42  STO
362   29   29
363   01   1
364   06   6
365   69  OP
366   04   04
367   43  RCL
368   00   00
369   69  OP
370   06   06
371   01   1
372   03   3
373   69  OP
374   04   04
375   43  RCL
376   08   08
377   69  OP
378   06   06
379   01   1
380   04   4
381   69  OP
382   04   04
383   43  RCL
384   09   09
385   69  OP
386   06   06
387   02   2
388   03   3
389   69  OP
390   04   04
391   43  RCL
392   10   10
393   69  OP
394   06   06
395   04   4
396   04   4
397   03   3
398   07   7
399   69  OP
```

```
400   04   04
401   43  RCL
402   11   11
403   69  OP
404   06   06
405   04   4
406   04   4
407   01   1
408   06   6
409   69  OP
410   04   04
411   43  RCL
412   13   13
413   69  OP
414   06   06
415   01   1
416   00   0
417   00   0
418   00   0
419   00   0
420   42  STO
421   14   14
422   91  R/S
```

```
000   43  RCL
001   13   13
002   32  X↕T
003   43  RCL
004   11   11
005   85   +
006   01   1
007   95   =
008   55   ÷
009   02   2
010   95   =
011   77   GE
012   11   A
013   43  RCL
014   19   19
015   55   ÷
016   43  RCL
017   16   16
018   95   =
019   42  STO
020   30   30
021   43  RCL
022   11   11
023   75   -
024   01   1
025   95   =
026   65   ×
027   43  RCL
028   20   20
029   95   =
030   42  STO
031   31   31
032   43  RCL
033   11   11
034   75   -
035   01   1
036   95   =
037   33  X²
038   65   ×
039   43  RCL
```

Figure A5. (Cont First/Second Half)

```
040  21   21
041  65   ×
042  43  RCL
043  31   31
044  55   ÷
045  43  RCL
046  30   30
047  45  Yˣ
048  03   3
049  95   =
050  42  STO
051  32   32
052  43  RCL
053  11   11
054  75   -
055  01   1
056  95   =
057  65   ×
058  02   2
059  65   ×
060  43  RCL
061  12   12
062  55   ÷
063  53   (
064  43  RCL
065  11   11
066  65   ×
067  43  RCL
068  12   12
069  75   -
070  89   π
071  55   ÷
072  04   4
073  54   )
074  95   =
075  42  STO
076  33   33
077  61  GTO
078  12   B
079  76  LBL
080  11   A
081  43  RCL
082  07   07
083  55   ÷
084  43  RCL
085  16   16
086  65   ×
087  02   2
088  95   =
089  42  STO
090  30   30
091  43  RCL
092  13   13
093  75   -
094  01   1
095  95   =
096  65   ×
097  43  RCL
098  20   20
099  65   ×
100  02   2
101  95   =
102  42  STO
103  31   31
104  43  RCL
105  13   13
106  75   -
107  01   1
108  95   =
109  33  X²
110  65   ×
111  04   4
112  65   ×
113  43  RCL
114  21   21
115  65   ×
116  43  RCL
117  31   31
118  55   ÷
119  43  RCL
120  30   30
121  45  Yˣ
122  03   3
123  95   =
124  42  STO
125  32   32
126  43  RCL
127  11   11
128  55   ÷
129  02   2
130  55   ÷
131  43  RCL
132  12   12
133  95   =
134  22  INV
135  30  TAN
136  38  SIN
137  65   ×
138  43  RCL
139  13   13
140  33  X²
141  75   -
142  89   π
143  55   ÷
144  04   4
145  95   =
146  35  1/X
147  65   ×
148  04   4
149  65   ×
150  53   (
151  43  RCL
152  13   13
153  75   -
154  01   1
155  54   )
156  65   ×
157  43  RCL
158  12   12
159  95   =
```

Figure A5. (Cont - Second Half)

```
160  42 STD     200  02   2     240  06  06
161  33  33     201  75   -     241  43 RCL
162  91 R/S     202  93   .     242  13  13
163  76 LBL     203  00   0     243  32 X⇌T
164  12   B     204  08   8     244  43 RCL
165  93   .     205  02   2     245  11  11
166  09   9     206  06   6     246  85   +
167  00   0     207  03   3     247  01   1
168  07   7     208  65   ×     248  95   =
169  65   ×     209  53   (     249  55   ÷
170  43 RCL     210  01   1     250  02   2
171  30  30     211  93   .     251  95   =
172  55   ÷     212  02   2     252  77  GE
173  43 RCL     213  75   -     253  14   D
174  26  26     214  43 RCL     254  93   .
175  65   ×     215  20  20     255  08   8
176  04   4     216  54   )     256  02   2
177  85   +     217  55   ÷     257  08   8
178  01   1     218  53   (     258  75   -
179  95   =     219  43 RCL     259  01   1
180  34  √X     220  20  20     260  06   6
181  85   +     221  75   -     261  93   .
182  01   1     222  93   .     262  05   5
183  95   =     223  08   8     263  09   9
184  55   ÷     224  09   9     264  06   6
185  02   2     225  02   2     265  65   ×
186  95   =     226  04   4     266  43 RCL
187  42 STD     227  54   )     267  14  14
188  20  20     228  95   =     268  45  Yˣ
189  65   ×     229  42 STD     269  93   .
190  93   .     230  21  21     270  04   4
191  02   2     231  76 LBL     271  02   2
192  08   8     232  13   C     272  07   7
193  01   1     233  03   3     273  07   7
194  08   8     234  05   5     274  94 +/-
195  75   -     235  69  OP     275  95   =
196  93   .     236  04  04     276  42 STD
197  01   1     237  43 RCL     277  35  35
198  02   2     238  14  14     278  93   .
199  08   8     239  69  OP     279  07   7
```

Figure A5. (Cont - Second Half)

```
280  01   1     320  00   0     360  45  Yx
281  08   8     321  93   .     361  43  RCL
282  04   4     322  01   1     362  35   35
283  65   x     323  65   x     363  95   =
284  43  RCL    324  43  RCL    364  42  STO
285  14   14    325  14   14    365  36   36
286  45  Yx     326  45  Yx     366  76  LBL
287  93   .     327  93   .     367  15   E
288  02   2     328  07   7     368  43  RCL
289  04   4     329  02   2     369  14   14
290  00   0     330  08   8     370  55   ÷
291  07   7     331  04   4     371  43  RCL
292  94  +/-    332  94  +/-    372  22   22
293  65   x     333  95   =     373  95   =
294  53   (     334  42  STO    374  42  STO
295  43  RCL    335  35   35    375  37   37
296  11   11    336  43  RCL    376  65   x
297  75   -     337  14   14    377  43  RCL
298  01   1     338  45  Yx     378  24   24
299  54   )     339  93   .     379  55   ÷
300  45  Yx     340  01   1     380  43  RCL
301  93   .     341  08   8     381  30   30
302  07   7     342  09   9     382  95   =
303  00   0     343  02   2     383  45  Yx
304  03   3     344  94  +/-    384  93   .
305  65   x     345  65   x     385  02   2
306  43  RCL    346  53   (     386  05   5
307  12   12    347  43  RCL    387  94  +/-
308  45  Yx     348  13   13    388  65   x
309  43  RCL    349  75   -     389  01   1
310  35   35    350  01   1     390  93   .
311  95   =     351  54   )     391  05   5
312  42  STO    352  45  Yx     392  03   3
313  36   36    353  93   .     393  02   2
314  61  GTO    354  07   7     394  65   x
315  15   E     355  00   0     395  43  RCL
316  76  LBL    356  03   3     396  30   30
317  14   D     357  65   x     397  55   ÷
318  01   1     358  43  RCL    398  43  RCL
319  03   3     359  12   12    399  12   12
```

Figure A5. (Cont - Second Half)

```
400   55    ÷
401   43  RCL
402   00   00
403   95    =
404   42  STO
405   07   07
406   65    x
407   43  RCL
408   32   32
409   95    =
410   65    x
411   43  RCL
412   14   14
413   45  YX
414   03    3
415   65    x
416   43  RCL
417   33   33
418   55    ÷
419   43  RCL
420   31   31
421   45  YX
422   04    4
423   95    =
424   28  LOG
425   42  STO
426   38   38
427   03    3
428   03    3
429   69  OP
430   04   04
431   43  RCL
432   38   38
433   69  OP
434   06   06
435   43  RCL
436   36   36
437   65    x
438   43  RCL
439   14   14
440   45  YX
441   03    3
442   65    x
443   43  RCL
444   33   33
445   55    ÷
446   43  RCL
447   31   31
448   45  YX
449   04    4
450   95    =
451   28  LOG
452   42  STO
453   39   39
454   99  PRT
455   43  RCL
456   21   21
457   65    x
458   43  RCL
459   37   37
460   45  YX
461   93    .
462   04    4
463   94  +/-
464   95    =
465   42  STO
466   19   19
467   65    x
468   02    2
469   65    x
470   43  RCL
471   06   06
472   65    x
473   43  RCL
474   37   37
475   65    x
476   43  RCL
477   00   00
478   55    ÷
479   43  RCL
480   30   30
481   55    ÷
482   43  RCL
483   09   09
484   95    =
485   34  √X
486   65    x
487   43  RCL
488   10   10
489   95    =
490   42  STO
491   20   20
492   22  INV
493   23  LNX
494   42  STO
495   34   34
496   03    3
497   01    1
498   69  OP
499   04   04
500   43  RCL
501   20   20
502   94  +/-
503   22  INV
504   23  LNX
505   42  STO
506   35   35
507   85    +
508   43  RCL
509   34   34
510   95    =
511   35  1/X
512   65    x
513   53    (
514   43  RCL
515   34   34
516   75    -
517   43  RCL
518   35   35
519   54    )
```

Figure A5. (Cont - Second Half)

```
520   55   ÷
521   43  RCL
522   20   20
523   95   =
524   42  STO
525   36   36
526   23  LNX
527   65   X
528   43  RCL
529   29   29
530   94  +/-
531   85   +
532   43  RCL
533   28   28
534   95   =
535   94  +/-
536   85   +
537   43  RCL
538   36   36
539   95   =
540   94  +/-
541   85   +
542   01   1
543   95   =
544   65   X
545   43  RCL
546   18   18
547   94  +/-
548   85   +
549   01   1
550   95   =
551   65   X
552   43  RCL
553   19   19
554   65   X
555   43  RCL
556   31   31
557   55   ÷
558   43  RCL
559   30   30
560   95   =
561   65   X
562   43  RCL
563   14   14
564   65   X
565   43  RCL
566   33   33
567   55   ÷
568   43  RCL
569   31   31
570   33  X²
571   95   =
572   28  LOG
573   69  OP
574   06   06
575   93   .
576   03   3
577   05   5
578   65   X
579   43  RCL
580   14   14
581   45  Yˣ
582   93   .
583   03   3
584   09   9
585   06   6
586   94  +/-
587   65   X
588   53   (
589   43  RCL
590   11   11
591   55   ÷
592   43  RCL
593   12   12
594   54   )
595   45  Yˣ
596   06   6
597   35  1/X
598   65   X
599   53   (
600   43  RCL
601   00   00
602   55   ÷
603   43  RCL
604   31   31
605   54   )
606   45  Yˣ
607   93   .
608   04   4
609   94  +/-
610   95   =
611   65   X
612   43  RCL
613   14   14
614   65   X
615   43  RCL
616   33   33
617   55   ÷
618   43  RCL
619   31   31
620   33  X²
621   95   =
622   28  LOG
623   99  PRT
624   06   6
625   00   0
626   00   0
627   00   0
628   00   0
629   44  SUM
630   14   14
631   61  GTO
632   13   C
```

Figure A5. (Cont - Second Half)

TABLE AIII

Data Registers used for Storage of the Indicated Parameters for the Program in Figure A5.

Data Register	Parameter(s)	Data Register	Parameter(s)
00	D_o	23	d_e
06	P_c	24	D_J
07	N_{HD}	25	E
08	S_{BF}	26	D_E
09	t_f	27	$\ln(r_o/r_e)$
10	H_f	28	C_Δ
11	X_T	29	D_Δ
12	X_L	30	D_h
13	X_D	31	D_N
14	RE_N	32	f_N/f_e
15	R_f	33	$A_F b/V_{os}$
16	G_f	34	e^{ml}, $\eta_{f\text{-Corr}}$
17	β	35	C_T, C_D, e^{-ml}
18	A_f/A_T		$\log(NTU_e/V_{os})$
19	N_{HT}, j_e	36	f_s, $\eta_{f\text{-}L}$
20	N_N, $(X_T)_\Delta$, ml,	37	RE
	$\log(NTU_s/V_{os})$	38	$\log(P_e/V_{os})$
21	N_f, C_H	39	$\log(P_s/V_{os})$
22	RE_N/RE		

```
          1.         D
       0.02          A
       0.02          B
        0.5          H
         2.         XT
         2.         XD
     10000.          R
11.27392388          P
9.751822282
2.797923241          N
1.532592398
     70000.          R
13.59794349          P
12.12723271
3.287570581          N
2.043031614
    130000.          R
 14.3372681          P
12.87685563
3.437757844          N
2.205414183
```

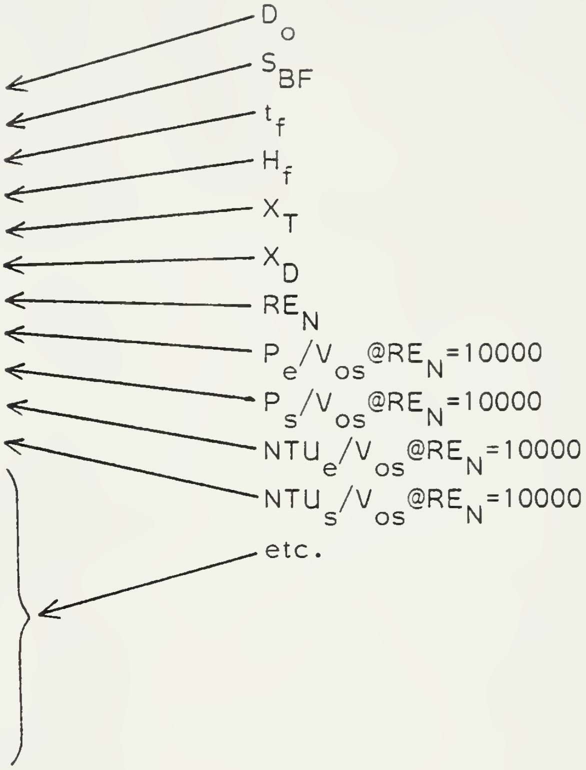
D_o
S_{BF}
t_f
H_f
X_T
X_D
RE_N
P_e/V_{os}@RE_N=10000
P_s/V_{os}@RE_N=10000
NTU_e/V_{os}@RE_N=10000
NTU_s/V_{os}@RE_N=10000
etc.

Figure A6. Sample Output Generated by Program listed in Figure A5.

199468

Thesis
R6429 Robinson
c.1 Geometry effects on triangular pitch circular finned heat exchangers in crossflow.

199468

Thesis
R6429 Robinson
c.1 Geometry effects on triangular pitch circular finned heat exchangers in crossflow.

Geometry effects on triangular pitch cur
3 2768 001 94913 4
DUDLEY KNOX LIBRARY